Design Coefficients of Friction for MoDOT PTFE Bearings

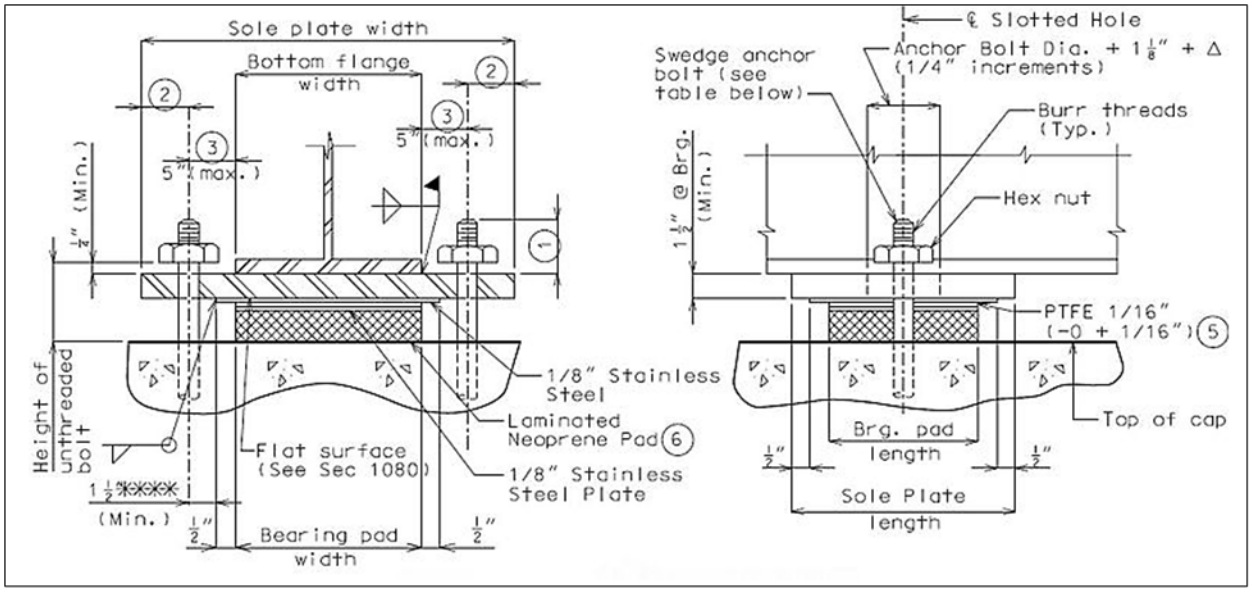

June 2024	Project number TR202204
Final Report	MoDOT Research Report number cmr 24-005

PREPARED BY:

Saeed Nejad

Jonathan C. McGormley

Wiss, Janney, Elstner Associates, Inc. (WJE)

PREPARED FOR:

Missouri Department of Transportation

Construction and Materials Division, Research Section

Technical Report Documentation Page

1. Report No. cmr 24-005	2. Government Accession No.	3. Recipient's Catalog No.
4. Title and Subtitle Design Coefficients of Friction for MoDOT PTFE Bearings		5. Report Date May 2024 Published: June 2024
		6. Performing Organization Code
7. Author(s) Saeed Nejad Jonathan C. McGormley		8. Performing Organization Report No.
9. Performing Organization Name and Address Wiss, Janney, Elstner Associates, Inc. (WJE) 330 Pfingsten Road Northbrook, IL 60062		10. Work Unit No. (TRAIS)
		11. Contract or Grant No. MoDOT project # TR202204
12. Sponsoring Agency Name and Address Missouri Department of Transportation (SPR-B) Construction & Materials Division P. O. Box 270 Jefferson City, MO 65102		13. Type of Report and Period Covered Final Report (November 2022-May 2024)
		14. Sponsoring Agency Code
15. Supplementary Notes Conducted in cooperation with the U.S. Department of Transportation, Federal Highway Administration. MoDOT research reports are available in the Innovation Library at https://www.modot.org/research-publications.		

16. Abstract

This report evaluates the design coefficients of friction for polytetrafluoroethylene (PTFE) bearings, identifying key influencing parameters through a literature review and a detailed test program. Seven parameters were studied: PTFE material and surface types, size, contact pressure, temperature, sliding speed, and surface contamination. The analysis presented in the report showed that unfilled dimpled lubricated PTFE and filled flat PTFE exhibited the lowest and highest coefficients of friction, respectively. The coefficients of friction for unfilled flat and filled dimpled PTFE fell in between.

The study found that coefficients of friction increased with higher sliding speeds and surface contamination but decreased with increased contact pressure. No consistent changes in the coefficients were observed with variations in specimen size or at low temperatures. Notably, surface contamination drastically increased friction coefficients—light dust levels increased friction tenfold, while heavier contamination prevented sliding altogether.

Based on these findings, updated design coefficients of friction are proposed for the four main PTFE bearing types: flat (both unfilled and filled) and dimpled lubricated (both unfilled and filled). The report also discusses various preventative measures and underscores the importance of regular maintenance and the adoption of protective strategies to enhance bearing longevity and functionality.

17. Key Words PTFE Bearings, Bearing bad, Coefficient of friction, Surface contamination, Dimpled lubricated PTFE, Flat PTFE	18. Distribution Statement No restrictions. This document is available through the National Technical Information Service, Springfield, VA 22161.

19. Security Classification (of this report) Unclassified	20. Security Classification (of this page) Unclassified	21. No. of Pages 98	22. Price

Form DOT F 1700.7 (8-72) Reproduction of completed page authorized

TR202204 - Design Coefficients of Friction for MoDOT PTFE Bearings

By
Saeed Nejad, Ph.D.
Jonathan C. McGormley, P.E., S.E.
Wiss, Janney, Elstner Associates, Inc.

Prepared for
Ms. Jennifer Harper, P.E.
Research Director
Missouri Department of Transportation

April 2024

Final Report

Disclaimer

The opinions, findings, and conclusions expressed in this document are those of the investigators. They are not necessarily those of the Missouri Department of Transportation, U.S. Department of Transportation, or Federal Highway Administration. This information does not constitute a standard or specification.

Acknowledgments

Financial support from the Missouri Department of Transportation, which made this research possible, is gratefully acknowledged. Technical assistance and access to laboratory facilities provided by Mr. Adam Wellington and Mr. Richard Lewis from D.S. Brown are also acknowledged.

Executive Summary

Wiss, Janney, Elstner Associates, Inc. (WJE) was engaged to conduct an experimental program to investigate and validate essential Polytetrafluoroethylene (PTFE) bearing performance criteria, allowing for potential adjustments in bearing design procedures to improve the efficiency in designing substructure elements. This experimental program was designed and implemented, examining seven parameters from the literature review: PTFE material and surface types, size, contact pressure, temperature, sliding speed, and surface contamination. Seven standard Type N PTFE bearing specimens used by Missouri Department of transportation (MoDOT) were tested, including four PTFE types: unfilled flat, filled flat, unfilled dimpled, and filled dimpled. A matrix of thirteen tests, each comprising sixteen to over a hundred cycles, was executed using a testing apparatus that facilitated the simultaneous application of vertical and horizontal loads to a test pad. High precision sensors were employed to document the behavior of the testing assembly throughout each test.

The report's analysis indicated that unfilled dimpled lubricated PTFE and filled flat PTFE showed the lowest and highest coefficients of friction, respectively. The coefficients for unfilled flat and filled dimpled PTFE fell in between. It was determined that coefficients of friction increased with increased sliding speeds and surface contamination but decreased with increased contact pressure. No consistent changes were noted with variations in specimen size or at low temperatures.

Surface contamination significantly raised friction coefficients—light dust levels caused a tenfold increase in friction, while heavier contamination halted sliding. Both flat and dimpled PTFE specimens displayed increased friction with higher loading rates. Once elevated, friction values did not decrease even when loading rates decreased, suggesting irreversible changes to the PTFE surfaces due to thermal and mechanical stresses encountered during testing.

A review of twenty-five states showed no specific mandate by departments of transportation requiring protection of PTFE elastomeric bearing pads from surface contamination. Although past studies recommended various shrouding methods, these were not verified through long-term studies. Despite preventive measures, real-world conditions show that dust accumulation occurs, emphasizing the need for regular maintenance and protective strategies, potentially verified by laboratory or field tests, to maintain the longevity and functionality of PTFE bearings.

The experimental results for the coefficient of friction were compared with those from NCHRP Project 10-20 (Report 432), which were adopted as the PTFE bearing design coefficients in the AASHTO LRFD Bridge Design Specifications (BDS). Although the experimental results generally aligned with NCHRP Report 432, discrepancies suggested that material type and preloading might explain differences between the findings. Additional laboratory experiments using a setup similar to that of NCHRP Report 432 are recommended to eliminate the effects of

preloading and elastomeric flexibility, thus isolating and accurately comparing the effects of PTFE material types.

Ultimately, updated coefficients of friction were proposed in this study for the PTFE types tested. A comparison of test results with the NCHRP Report 432 findings and referenced to AASHTO LRFD BDS and MoDOT design values, led to proposed updated design coefficients of friction for four primary PTFE bearing types: flat (both unfilled and filled) and dimpled lubricated (both unfilled and filled).

Key parameters for future studies were outlined, including extended testing and microscopic examination of PTFE surfaces to better understand the dependencies of friction coefficients on load cycles, sliding speeds, and surface contamination. Additionally, unexplored factors such as eccentric loading and surface roughness were identified, necessitating further experimental investigation.

Table of Contents

List of Tables

List of Figures

List of Equations

List of Abbreviations and Acronyms

AASHTO ..... American Association of State Highway and Transportation Officials

DIC ..... Digital Image Correlation

FHWA ..... Federal Highway Administration

LRFD BCS ..... LRFD Bridge Construction Specifications

LRFD BDS ..... LRFD Bridge Design Specifications

MoDOT ..... Missouri Department of Transportation

MoDOT EPG ..... MoDOT Engineering Policy Guide

NCHRP ..... National Cooperative Highway Research Program

PTFE ..... Polytetrafluoroethylene

LRFD ..... Load and Resistance Factor Design

Chapter 1. Introduction

Polytetrafluoroethylene (PTFE) bearing pads play a critical role in Missouri Department of Transportation (MoDOT) bridge designs, especially when elastomeric expansion bearings prove insufficient for the required expansion length. These bearings serve as essential components in accommodating expansion and facilitating the rotation of beam ends in bridge structures. MoDOT specifies the use of either filled or unfilled flat PTFE bridge bearings, and their application involves a proper analysis of vertical forces and multiple lateral forces including seismic, temperature, wind, and braking forces. For lateral loads, designers employ a pre-slip analysis treating the substructure as a fixed bent, and a post-slip analysis where zero force is applied. The design coefficient of friction is a crucial parameter, with MoDOT specifying specific values—0.12 for first breakaway and 0.06 for subsequent breakaways. These values are less than those used in the AASHTO Load and Resistance Factor Design (LRFD) Bridge Design Specifications (BDS). This report examines the challenges and design considerations associated with PTFE bearings, exploring the implications of friction coefficients, temperature variations, and design specifications outlined in MoDOT guidelines (MoDOT EPG 2024) and the AASHTO LRFD BDS (AASHTO LRFD BDS 2020). The seismic performance of PTFE bearings was not a focus of this research.

Chapter 2. Background

Bearings are important bridge elements that, in addition to supporting vertical loads, also transmit lateral forces due to seismic forces, thermal changes, wind effects, and vehicle braking forces from the superstructure to the substructure. Historically, elastomeric bearing pads have been successfully used by many states for this purpose. In cases where elastomeric expansion bearings are not capable of handling the required expansion length due to limitations of the elastomer or bearing height stability restrictions, such elastomeric bearing pads are supplemented with an external PTFE sheet. When properly mated to a contact surface, PTFE has an exceptionally low coefficient of friction and provides a sliding surface for expansion while the elastomeric pad allows for some pre-slip deformation and rotation of the beam end. The coefficient of friction of the contact surface between PTFE and the mating surface can be further reduced by introducing a lubricant, such as silicone grease, in recesses (dimples) on the PTFE surface.

MoDOT routinely evaluates its bridge design procedures to improve the design efficiency and performance of its bridge assets. Currently, designers following MoDOT provisions can limit the forces applied to a substructure element by specifying maximum friction coefficients at first breakaway and subsequent slips; however, the achievement of these limits has been questioned by manufacturers (Request for Proposal TR202204). Instead, if designers were to evaluate the lateral load effects on substructures using AASHTO LRFD BDS PTFE slip values for either filled or unfilled PTFE bearings, the larger friction values and ensuing larger reactions will greatly increase the demands on substructures. Use of dimpled PTFE pads offers one solution to reduce the design slip coefficient; however, there have been concerns about the durability and practicality of a dimpled pad because of possible dirt accumulation and the need to confine the PTFE within the bearing.

Chapter 3. Literature Review

The State of Missouri operates and maintains a total of 24,617 bridges. From a total of 3,670 bridges in the state that had reported elemental data in 2023 and are within the National Highway System (NHS), over 19 percent were built using elastomeric bearings (see Figure 1). Out of this group of bridges with elastomeric bearings, 68, 22, 8, and 1 percent of the bearings were reported in Condition States 1 (good), 2, 3, and 4 (poor), respectively (see Figure 2). Most of the in-service NHS bridges with elastomeric bearings in Missouri were built between the 1960s and 2010s.

When laminated elastomeric bearings cannot accommodate the required superstructure movements at the service limit state, the application of PTFE sheets creates a sliding interface that allows increased movement capacity. The PTFE sheets are fabricated as an unfilled sheet, filled sheet, or fabric woven from PTFE and other fibers. According to the AASHTO LRFD BDS, unfilled sheets shall be made from PTFE resin alone while filled sheets shall be made from PTFE resin uniformly blended with glass fibers, carbon fibers, or other chemically inert fillers. The primary reason behind the application of such blended fibers is to reduce creep, i.e., cold flow, and wear. In addition, PTFE sheets may contain dimples to act as reservoirs for lubricant. Unfilled dimples can act as reservoirs for contaminants (dust, etc.) which can help to keep these contaminants from the contact surface (AASHTO LRFD BDS 2020).

The application of PTFE in bearing pads makes it attractive due to its low frictional characteristics, chemical inertness, and resistance to weathering and water absorption (Ala et al. 2015). The friction coefficient of PTFE depends on many factors, such as sliding speed, contact pressure, lubrication, temperature, and properties such as the finish of the mating surface (AASHTO LRFD BDS 2020; Campbell and Kong 1987). Plain PTFE wears under certain service conditions, particularly when subjected to combinations of high contact pressure, high rates of movement, and low temperatures. The continuous sliding of PTFE over the mating surface creates wear in the PTFE with time and is exacerbated by deteriorated or rough surfaces (Campbell and Kong 1987). Even in the presence of lubricated PTFE, this gradual wear results in higher friction and reduces the thickness of the remaining PTFE (AASHTO LRFD BDS 2020).

Unfilled PTFE has a lower friction coefficient when compared to filled PTFE. Virgin (unfilled) PTFE resin is typically utilized to create a vertical load-carrying sliding surface over the bearing, however, filled PTFE is typically used for the guide bars to induce lateral restraints. In turn, the addition of fillers to PTFE enhances its resistance against wear and creep (Campbell and Kong 1989).

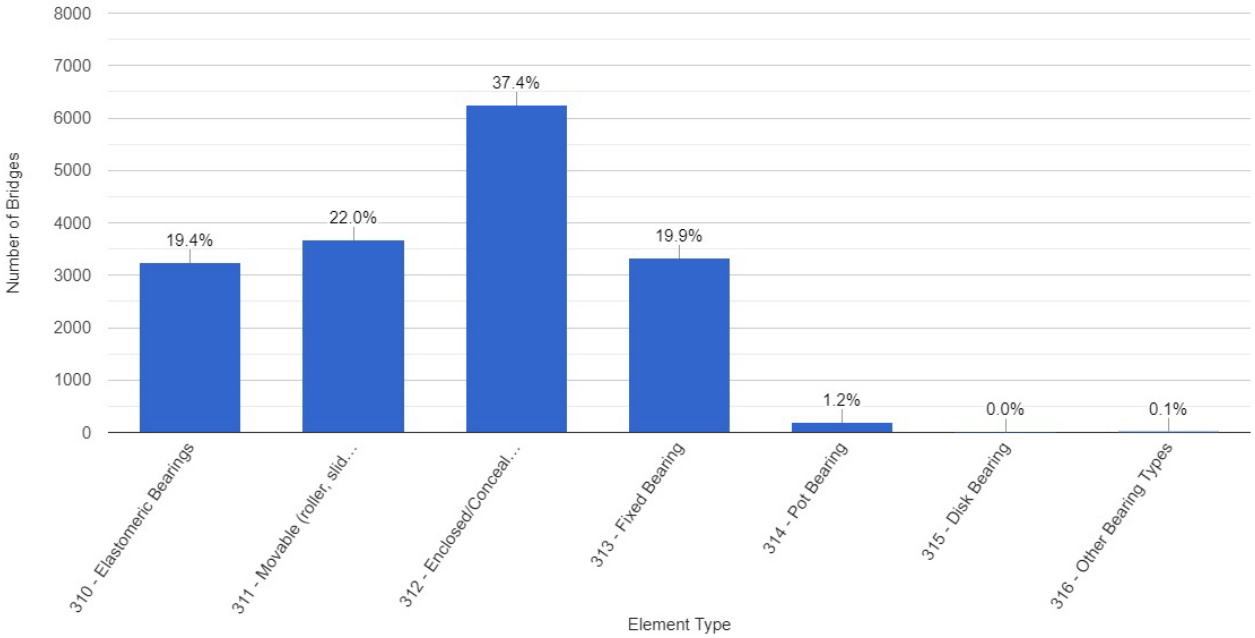

Figure 1. Bar chart showing distribution of bearing types for Missouri (bridges on the NHS with available element-level info) [Plots are taken from FHWA's InfoBridge portal].

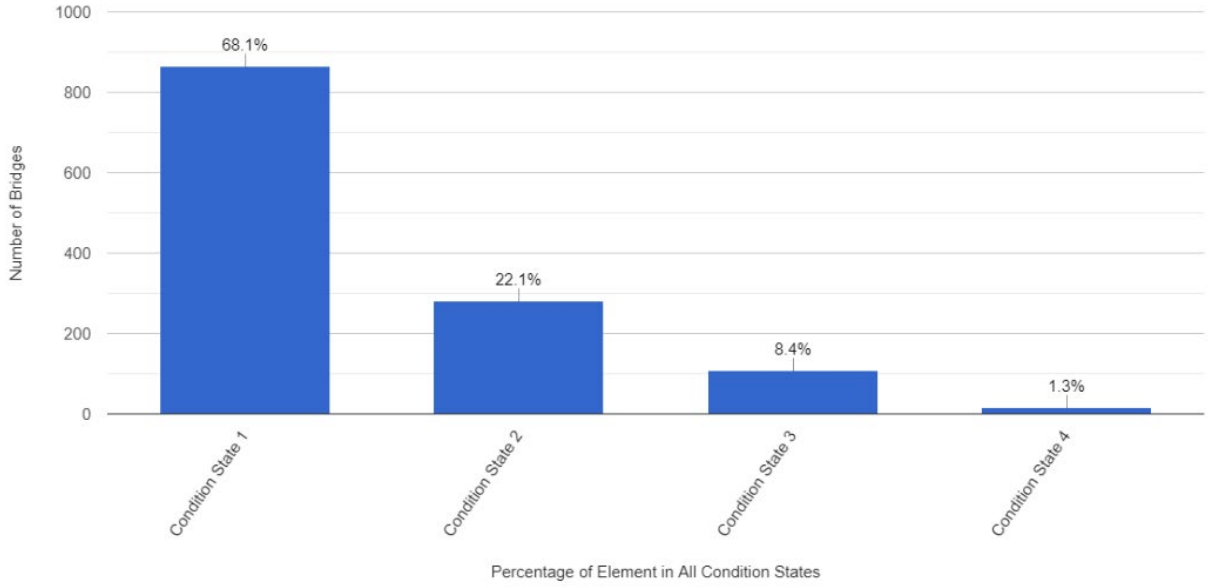

Figure 2. Bar chart showing distribution of element-level condition states of elastomeric bearing pads in Missouri (bridges on the NHS with available element-level info) [Plots are taken from FHWA's InfoBridge portal].

With the invention of neoprene (polychloroprene) and PTFE, several laboratory and field tests have been conducted to better understand the performance of PTFE elastomeric bearing types. A summary of the studies relevant to this research follows:

Campbell and Kong (1987; 1989)

Campbell et al. (1987; 1989) developed a comprehensive series of test programs to investigate the influence of four parameters, namely, contact pressure, temperature, sliding speed, and stainless-steel surface roughness. It was found that lubrication, contact pressure, temperature, speed, and length of travel had the greatest effects on the friction coefficients. To a lesser degree, steel surface roughness, type of PTFE, and surface contamination also affected the friction values.

In particular, the results showed that both the static and dynamic coefficients of friction increased with an increase in sliding speed and stainless-steel surface roughness, and with a decrease in contact pressure and temperature. The initial coefficient of friction was as high as five times the coefficient of friction after fifty cycles of movement. The difference between the static and dynamic coefficients of friction became less as the total movement accumulated. Overall, the coefficient of friction for PTFE increased with the total accumulated bearing movement. It was also found that both contact pressure and sliding velocity contributed to PTFE wear, but that the relationship of the combined pressure and velocity (P×V) had a dominant influence.

Campbell et al. (1987; 1989) also noted that unfilled PTFE is comparatively soft and absorbs contamination with no considerable effect on the friction coefficient and bearing life. However, this could be dramatically changed with the presence of heavy contamination such as dry cement or dust. The increase in the friction coefficient was reported as being ten times greater due to the effects of contamination. Complete PTFE seizure occurred in tests using an unlubricated surface contaminated with cement dust.

Mokha et al. (1990)

In this study, more than 160 tests were conducted to evaluate the impact of PTFE sheets on sliding velocity, sliding acceleration, bearing pressure, type of PTFE, and surface finish of PTFE bearings assemblies. Testing was performed on both unfilled and glass-filled PTFE sheets that were cut into circular shapes of 5-inch and 10-inch diameters. A bearing pressure of 1.0 ksi, 2.0 ksi, and 3.0 ksi was imposed on the 10-inch diameter PTFE sheet and 6.5 ksi was placed on the 5-inch diameter PTFE sheet. Tests were conducted with a constant sliding velocity of 0.120 in/sec. The direction of sliding was either parallel or perpendicular to the lay; however, the glass-filled PTFE tests were only performed with the direction of sliding parallel to the lay. This study determined that the coefficient of friction is not impacted significantly by sliding acceleration but is sensitive to bearing pressure and sliding velocity. The author concluded that the coefficients of friction increased with increased sliding speeds but decreased with increased contact pressure.

Stanton and Campbell (1999)

In one of the most comprehensive studies to date, researchers reported properties and wear behavior of PTFE in the National Cooperative Highway Research Program (NCHRP) Report 432. A total of ninety-nine tests of 3-inch diameter PTFE sliding surface specimens were completed. Different types of PTFE including flat dry, dimpled lubricated, filled, and woven specimens were tested. This study reported that low temperatures, fast sliding speeds, low contact pressures, rough mating surfaces, and contamination of the sliding interface all contributed to the increased wear rate of PTFE. However, fast sliding speed was shown to be a dominant parameter. Movement due to temperature change is a low-cycle, high-amplitude movement and produced little wear. However, movement due to truck inertial and braking load effects resulted in high-cycle, low-amplitude movement and produced more wear due to faster sliding speeds. Additional discussion regarding NCHRP Report 432 and the results of this study are provided later in this report.

Taylor and Stanton (2010)

In a comprehensive exploration of frictional properties of stainless steel-PTFE surfaces conducted by Taylor and Stanton in 2010 for the Wisconsin Highway Research Program (WHRP), the report stands out as a significant contribution to the understanding of PTFE bearings with two different surface finishes: #8 mirror, 2B, and a rough, hot-rolled finish, to provide an initial evaluation of the effects of higher friction on the forces transmitted to the substructure. The research conducted a variety of experiments to analyze the friction coefficients associated with stainless steel bearings coated with PTFE. The study encompassed various factors, including load, speed, and lubrication conditions, shedding light on the interplay of these elements. The outcomes of the test exhibited similarities to findings from past research. The initial friction at rest, known as static or breakaway friction, exceeded that of friction during movement. The friction coefficient demonstrated a dependence on the contact pressure, showing a rise at lower pressures, in contrast to cases like steel-on-steel where it remained largely unaffected by such pressure. Furthermore, the friction coefficient increased with an increase in sliding velocity. However, within the spectrum of velocities anticipated in non-seismic contexts, this dependency was relatively minor. In addition, the 2B surface finish stainless steel demonstrated consistent and comparatively low friction qualities, leading to its consideration as an appropriate substitute for the #8 mirror finish, with the understanding that its behavior at low temperatures remains to be determined.

LaFave et al. (2013)

In this research project funded by the Illinois Department of Transportation (IDOT) in 2013, the use of elastomeric bearings to act in a manner comparable to seismic isolation bearings instead of just accommodating thermal movements was investigated. Among multiple types of elastomeric bearings, three PTFE bearing pads with different configurations were tested under multiple testing orientations. Tests were conducted to simulate transverse bridge motion using monotonic and cyclic displacement protocols, at compression loads corresponding to a range of elastomer compression stresses from 200 to 800 psi. The PTFE bearings were found to tolerate

large displacements (over 400 percent of the total elastomer thickness), prior to unseating at the sliding interface. That being said, localized damage or unusual mechanical responses tended to emerge at displacements larger than about 200 percent of the elastomer thickness. The PTFE was likely to incur damage and delaminate for relatively short elastomer heights while the sliding response did not transition smoothly upon loading reversal for relatively tall elastomer heights.

Ala et al. (2015)

In a different study in 2015, as part of SHRP2, Project R19A, the feasibility of achieving increased service life of sliding bearings subject to high sliding speeds through the use of alternative high-performing materials with greater wear resistance than conventional plain PTFE was studied. Two potential high-performance sliding materials were investigated: ultrahigh-molecular-weight polyethylene (UMWP) and glass-filled reinforced PTFE (GFR-PTFE). Tests confirmed that both UMWP and GFR-PTFE can provide considerably greater wear resistance compared with conventional plain PTFE, and can be used to increase service life when sliding surfaces are subject to high movement speed and high contact pressure.

Dorafshan et al. (2019)

In this 2018 joint work by AASHTO and the Federal Highway Administration (FHWA), a number of PTFE bearing pads were experimentally investigated to determine the friction coefficients of different PTFE samples with variable surface roughness, lubrication type, sliding speed, and contact pressure. Among three tested surfaces, the rough-rolled stainless steel and the carbon steel produced higher friction coefficients than those of stainless steel with a #2B surface. Unlubricated and graphite-lubricated surfaces resulted in very high friction values, whereas the values for soap, grease, and oil were comparably lower. The use of lubricants on the dimpled PTFE pads reduced the friction values significantly, except for graphite. Unlubricated sliding surfaces were not recommended due to the large scatter in published comparable data.

Nejad and McGormley (2022)

In response to problems encountered by the Louisiana Department of Transportation and Development (LADOTD) and Indiana Department of Transportation (INDOT) in regard to the unexpected performance of elastomeric bearing pads (with and without PTFE) in the field, two laboratory testing programs were developed and executed by WJE between 2020 to 2022 (Nejad and McGormley 2022; Nejad et al. 2022). In tests for LADOTD, elastomeric bearing pads with no PTFE sheets were slid against concrete and steel surfaces. The INDOT tests utilized elastomeric bearing pads bonded with dimpled PTFE sheet against a mating steel plate.

The primary objective of the INDOT test was to assess different variables to determine the root cause of an unexpected field performance of similar bearing pads and to verify key bearing performance criteria for elastomeric PTFE bearing pads. The laboratory tests indicated that the PTFE bearing pads followed an expected normal behavior and the observed issue in the field was unrelated to the performance of these pads.

Implementation of Dimpled PTFE Sheets by DOTs

Dimpled lubricated PTFE bearing pads offer the lowest design coefficients of friction, which may be desirable by bridge designers to reduce forces acting on the substructure. The coefficient of friction of the dimpled lubricated PTFE bearing pad, however, increases when the sliding surface becomes contaminated. To prevent contamination of the PTFE, it is generally recommended that the stainless-steel plate be on top and longer than the PTFE sheet and its maximum travel length (AASHTO LRFD BDS 2020). This will prevent debris from collecting on the steel plate and mixing with the lubrication.

Figure 3 through Figure 6 show the respective elastomeric bearing pads standard drawings for the Illinois, Indiana, and Maryland Departments of Transportation (MDOT). The IDOT Elastomeric Bearing Assembly Type II, as shown in Figure 3, utilizes the large stainless-steel top plate to protect the bearing from contamination. The details include side retainers, which are primarily used for wind/earthquake load transfer, but could add some protection from accumulating dust. MoDOT uses the same details for its PTFE bearing design (Figure 4). Alternatively, Figure 5 shows a similar detail of a PTFE bearing used by INDOT; however, that detail shows a top plate with a length and width matching the PTFE sheet. Figure 6 similarly shows the details of PTFE bearing used by MDOT. The Pennsylvania Department of Transportation (PennDOT) also specifies the use of PTFE in contact with a stainless-steel plate; however, their standard drawings specify the bearing assembly requirements in notes and does not issue a standard drawing with a schematic of the bearing assembly. A cursory review of available departments of transportation (DOTs) standard specifications, bridge design manuals, and standard drawings was performed on states adjacent to Missouri as well as for other selected states as shown in Table 1.

Table 1 shows the twenty-five different state DOTs selected for review, including MoDOT, and which states have available standards drawings. Four out of the twenty-five states selected had their own standard drawing or schematic details for dimpled and lubricated elastomeric bearing pad assemblies. In three out of those four states with standard drawings, a stainless-steel plate, the most common protection for PTFE bearings against contamination, was placed on top and larger than the PTFE sheet. No other method of protection against contamination was identified.

In summary, there is very little information provided in state DOTs specifications regarding the characteristics and performance of PTFE bearing pads. In most cases, those specifications simply refer to the AASHTO LRFD BDS.

Regarding the maintenance of PTFE dimpled lubricated bearings, a review of current practices of twenty-five state DOTs (through their published online documents) revealed almost no information. That being said, some states may have internal documents or instructions for the maintenance of such bearings to protect them from dirt and debris.

Table 1. State DOTs reviewed for PTFE bearing specifications

State DOT	Standard drawings with dimpled lubricated bearing pads	Larger stainless steel top plate
Arkansas	-	-
California	-	-
Colorado	-	-
Florida	-	-
Illinois	✓	✓
Indiana	✓	-
Iowa	-	-
Kansas	-	-
Kentucky	-	-
Louisiana	-	-
Maryland	✓	✓
Minnesota	-	-
Mississippi	-	-
Missouri	-	-
Nebraska	-	-
New York	-	-
Ohio	-	-
Oklahoma	-	-
Oregon	-	-
Pennsylvania	✓	✓
Tennessee	-	-
Texas	-	-
Virginia	-	-
Washington	-	-
Wisconsin	-	-

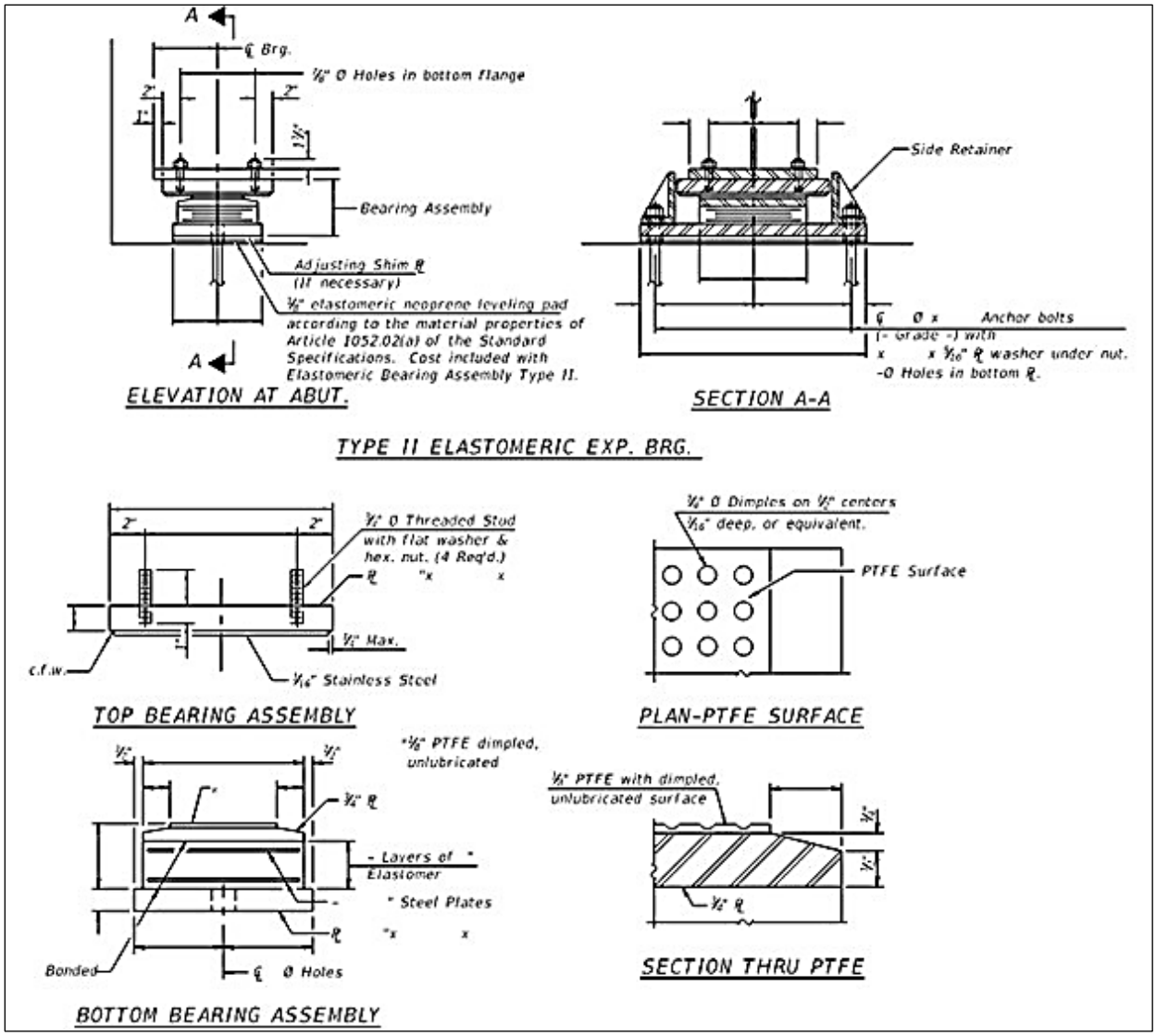

Figure 3. Engineering drawing image showing IDOT's Elastomeric Bearing Type II Standard Drawing with a larger stainless-steel plate on top of the PTFE.

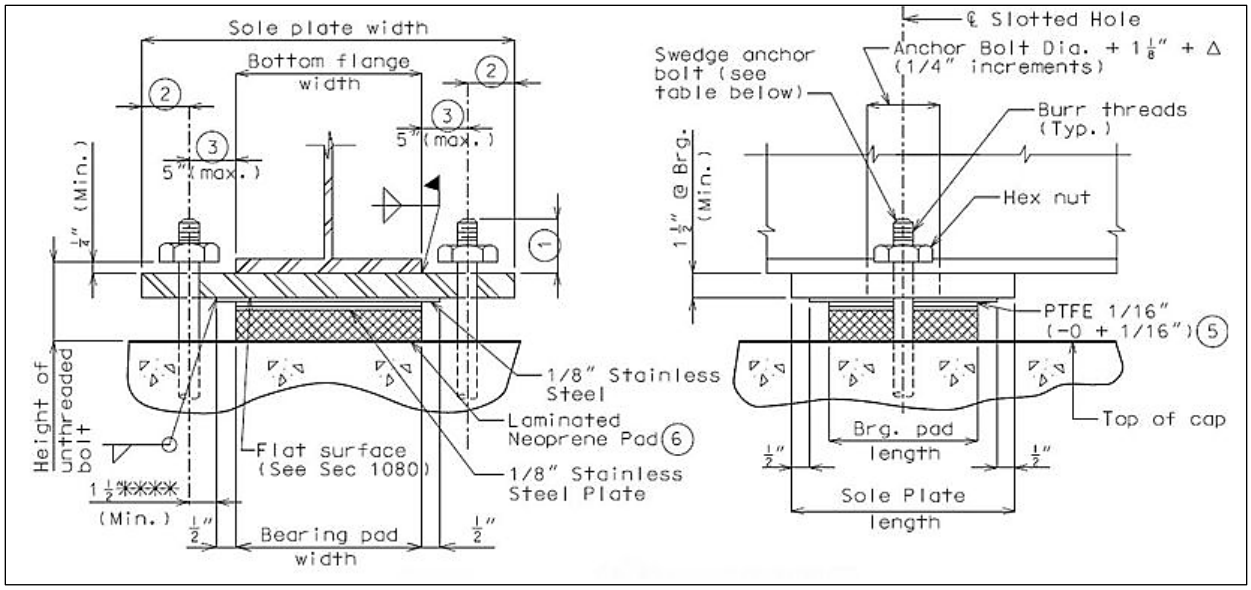

Figure 4. Engineering drawing image showing MoDOT's PTFE elastomeric bearing assembly detail (MoDOT EPG 2024).

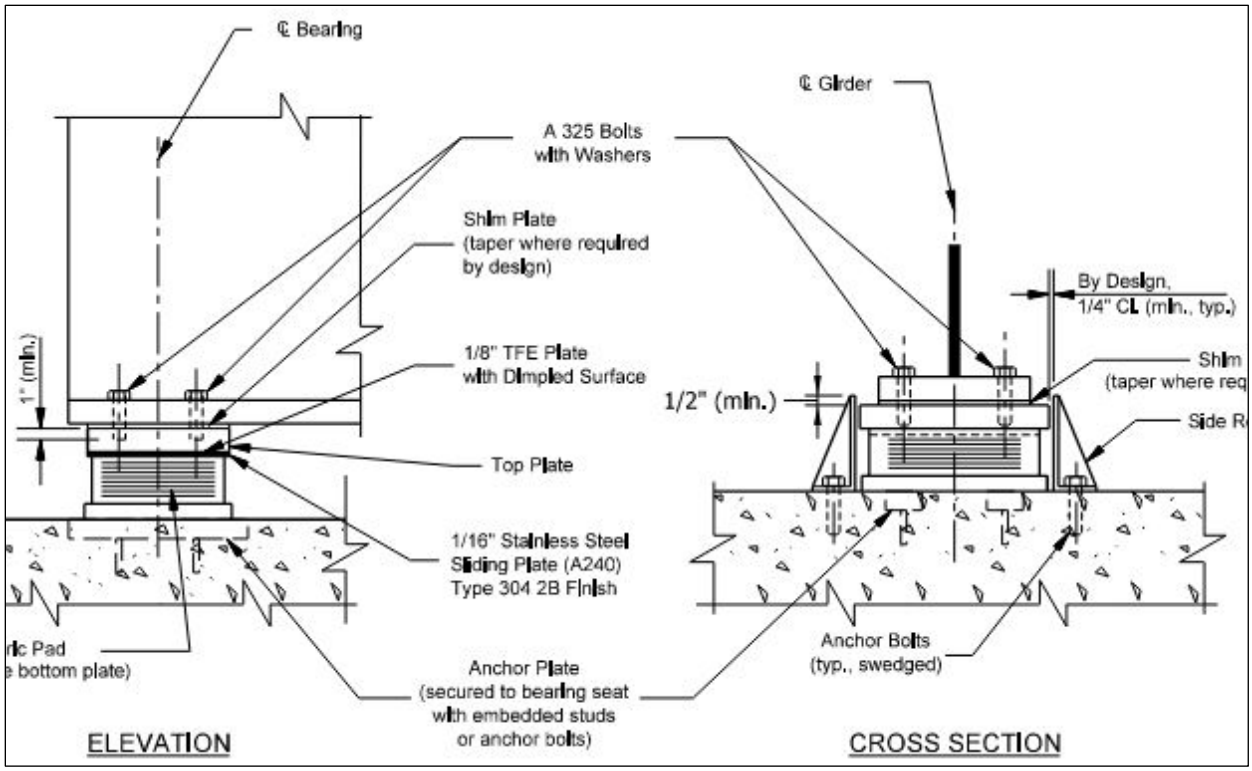

Figure 5. Engineering drawing image showing INDOT's PTFE elastomeric bearing assembly detail (INDOT – *2013 Design Manual, Chapter 409: Abutment, Bent, Pier, and Bearing*).

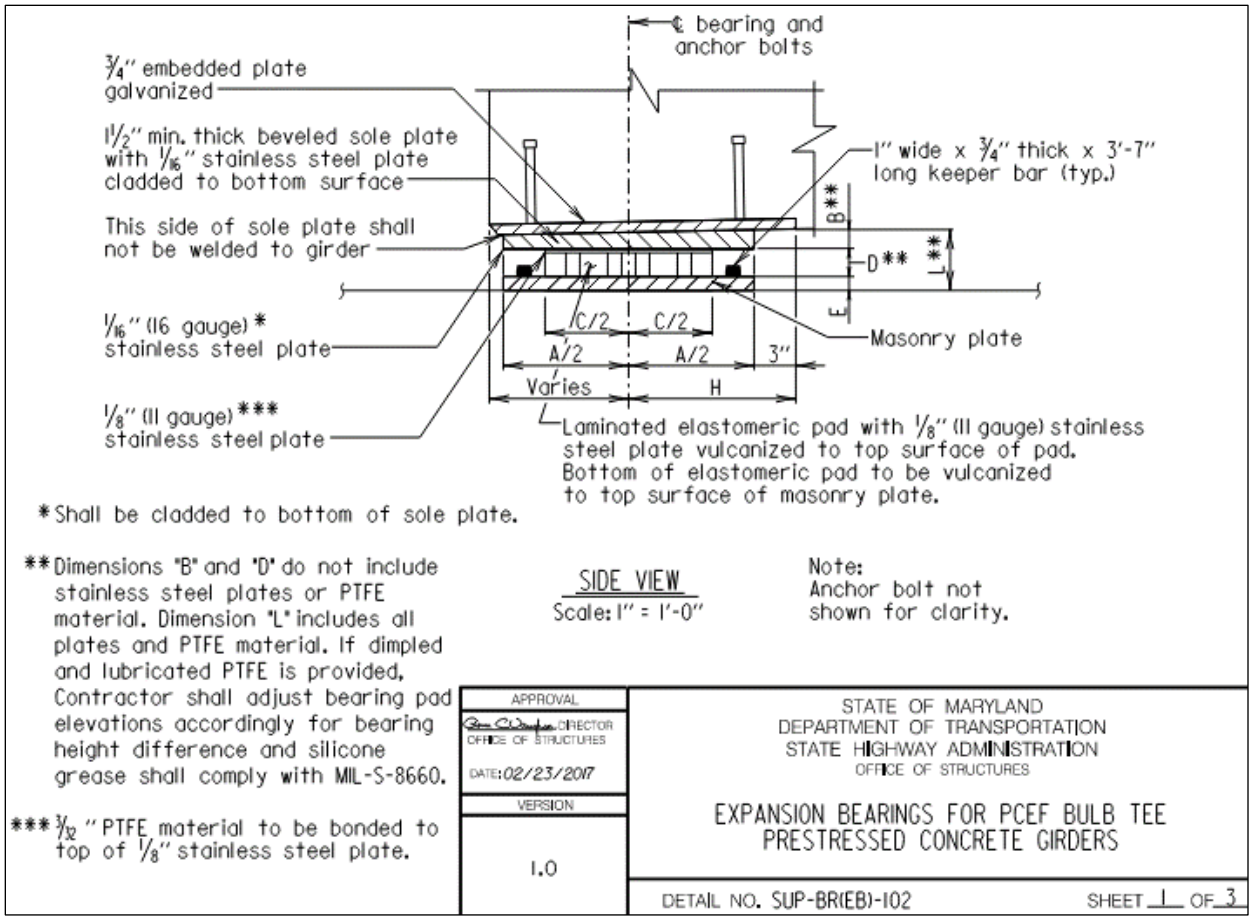

Figure 6. Engineering drawing image of MDOT's PTFE elastomeric bearing assembly detail. (MDOT – Structural Detail Manual, Chapter 03 - Superstructure: Section 09 Bearings).

Chapter 4. Description of Experimental Program

An experimental program was developed to establish the design coefficients for filled and unfilled flat and dimpled PTFE bearings. The experimental tests followed the generalized experimental program process depicted in Figure 7. The test plan attempted to optimize the number of experimental tests needed to evaluate the test parameters. The bearings were manufactured by D.S. Brown and tested by WJE engineers at the D.S. Brown laboratory in North Baltimore, Ohio.

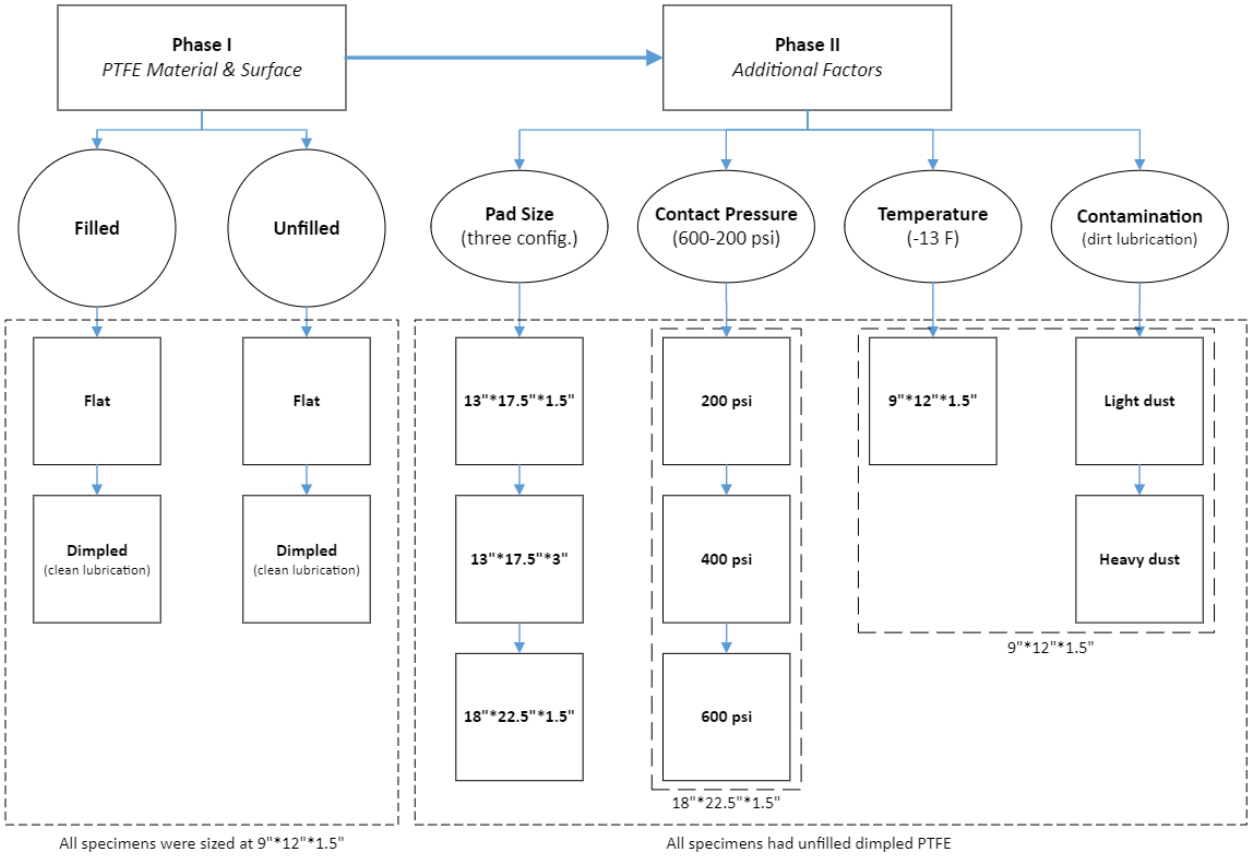

Figure 7. Process chart showing organization of the PTFE bearings experimental program. Tests completed at 800 psi unless noted otherwise.

Experimental Program Matrix

The experimental program was completed in two primary phases. In the first phase, the main objective was to decouple the effects of PTFE material type (filled or unfilled) and PTFE contact surface type (flat, dimpled). To study the behavior of these two parameters, six series of

experiments were conducted. Other influencing parameters such as bearing size and thickness, bearing temperature, contamination, and contact pressure were kept unchanged during the Phase I test plan to eliminate their effects from the results and to optimize the number of experimental tests. These tests were conducted at slow (1 in./min.), intermediate (2.5 in./min.), and fast (6 in./min.) horizontal load application rates.

At the conclusion of Phase I experimental tests, the different PTFE bearing specimen results were reviewed and representative bearing specimen(s) was selected for further investigation. In Phase II, thereafter, the effects of additional parameters of interest were studied using the specimens (some of which were carried over from Phase I).

Phase I Experiments

Four PTFE-Type N bearing pads with 9 inch x 12 inch x 1.5 inch neoprene elastomer, 1/8 inch stainless plate, and a top PTFE sheet were fabricated and used for testing with the only difference between the four specimens being the material (filled or unfilled) and surface (flat or dimpled) types.

Phase II Experiments

At the conclusion of Phase I, additional investigations were conducted to measure the effects of bearing size, temperature, contamination, and contact pressure. To isolate the effect of each of these factors, a single type of PTFE material with an unfilled dimpled surface was selected for use in Phase II experiments.

To study temperature effects, the primary PTFE-Type N bearing pad specimen with 9 inch x 12 inch x 1.5 inch neoprene elastomer was tested at a temperature of -13 deg. F. The bearing pad was subjected to the specified thermal environment for 24 hours before being immediately placed in the test apparatus.

To further evaluate the impact of contamination on the performance of dimpled lubricated PTFEs, the lubricant was mixed with fine dirt and tested. Initially, the dimpled specimen was tested without contamination (Phase I), and subsequently, it was contaminated and retested (Phase II). Two levels of contamination, light and heavy, were applied to the dimpled PTFE specimen.

In addition to the standard PTFE-Type N bearing pad measuring 9 inch x 12 inch x 1.5 inch with a neoprene elastomer, three additional specimens of varying sizes were tested, including bearings sized at 13 inch x 17.5 inch x 1.5 inch and 18 inch x 22.5 inch x 1.5 inch. These were selected from MoDOT's standard laminated expansion bearing pad sizes to explore the impact of different elastomeric areas, covering the lower, intermediate, and upper ranges of PTFE bearing sizes (MoDOT EPG 2024). The original bearing measuring 9 inch x 12 inch x 1.5 inch, along with the additional sizes of 13 inch x 17.5 inch x 1.5 inch and 18 inch x 22.5 inch x 1.5 inch, had shape factors of 5.1, 7.5, and 10, with length/width ratios of 1.33, 1.35, and 1.25,

respectively. Additionally, a third bearing size of 13 inch x 17.5 inch x 3 inch was tested to assess the effects of elastomeric thickness. All neoprene elastomers were laminated with internal steel sheets spaced at 1/2 inch intervals and featured the same PTFE configuration.

To understand the general behavior of the tested PTFE bearing pads under vertical contact pressure, a series of representative tests were conducted on the PTFE-Type N bearing pad specimen with 18 inch x 22.5 inch x 1.5 inch neoprene elastomer. Using the same bearing pad, a reduced vertical load equal to 75 percent of the maximum value (0.75 x 800=600 psi) was applied and the test repeated. Additional tests were performed at 50 and 25 percent of maximum pressure (400 psi and 200 psi) to evaluate the effect of vertical load on the friction coefficient.

Test Apparatus

A bearing pad test fixture at the D.S. Brown laboratory was utilized to simultaneously apply horizontal and vertical loads to the test specimen. Figure 8 shows a schematic of the test apparatus, identifying the horizontal and vertical rams. The apparatus can exert a maximum horizontal load of 40,000 pounds and a maximum vertical load of 1,000,000 pounds. The vertical and horizontal hydraulic rams applied the loads using load and deflection control, respectively. The vertical load was exerted by a single hydraulic ram between the fixed top and bottom platens, as illustrated in yellow boxes in Figure 8. In a similar fashion, the horizontal load was applied by a single hydraulic ram connected to a load plate positioned between the upper and lower portions of the bearing assembly. The hydraulic ram and connected load plate are enclosed in the white box in Figure 8. The upper half of the test assembly comprised a stainless-steel sheet (No. 8 mirror plate) and PTFE, while the lower half included the stainless-steel sheet, PTFE, elastomeric pad, and a masonry plate. WJE further calibrated the vertical ram using a high-precision load cell to address potential measurement errors caused by its high loading capacity. A correction factor was then applied to adjust the vertical load measurements, ensuring greater accuracy at lower loads.

As schematically illustrated in Figure 9, the test apparatus consists of the following components, listed from top to bottom: a fixed top platen that provides lateral and vertical support for the bearing assembly; a PTFE sheet designed to slide over the stainless steel sheet (i.e., No. 8 mirror plate) below it; a horizontal load plate connected to the horizontal hydraulic ram; a second stainless steel sheet (i.e., No. 8 mirror plate); and the bearing specimen, which included a PTFE sheet bonded to a 1/8-inch thick stainless steel sheet and the reinforced elastomer vulcanized to the masonry plate; a bottom platen applying vertical pressure while being restrained laterally.

The PTFE sheet in the bearing specimen was bonded to the 1/8-inch thick stainless steel using an epoxy designated by the manufacturer as compatible with both PTFE and stainless steel and capable of withstanding vulcanization temperatures. According to AASHTO standards, a silicone grease lubricant meeting the Society of Automotive Engineers Specification SAE-AS8660 was

used for the dimpled PTFE specimens. The 1/8-inch thick stainless steel plate was vulcanized to the neoprene elastomer to ensure a homogeneous bond free of air and moisture pockets. The elastomer was reinforced internally with 1/8-inch thick steel sheets spaced at 1/2 inch. The bottom of the neoprene elastomer was fitted with a steel masonry plate vulcanized to the pad for placement in the test fixture. The opposing mating surfaces to the PTFE were stainless-steel sheets with a No. 8 mirror finish, as specified by the American Iron and Steel Institute (AISI). The bearings were fabricated following MoDOT Standards and Specifications.

The direction of horizontal loading is indicated in Figure 9 by a white arrow and was applied perpendicular to the long dimension of the bearing. As denoted by green and white arrows in the figure, multiple parts within the assembly were capable of movement during testing. Notably, there were two design slip planes, highlighted by blue arrows: between the PTFE and mirror plate at the top and the lower half of the test assembly, respectively. To capture any movement at those and other potential slip locations, comprehensive sensing instrumentation was employed and will be discussed later in the report.

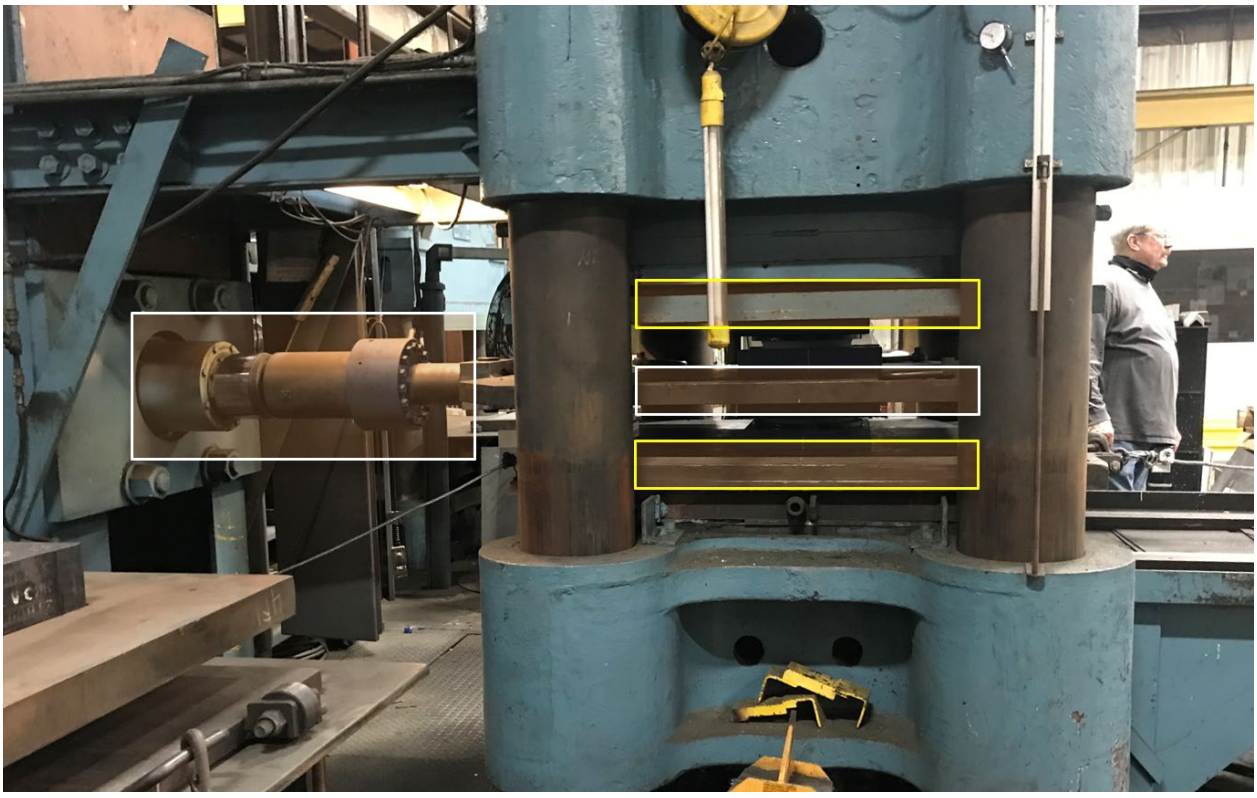

Figure 8. Photo of a test setup assembly (horizontal and vertical loading components are enclosed in white and yellow boxes, respectively).

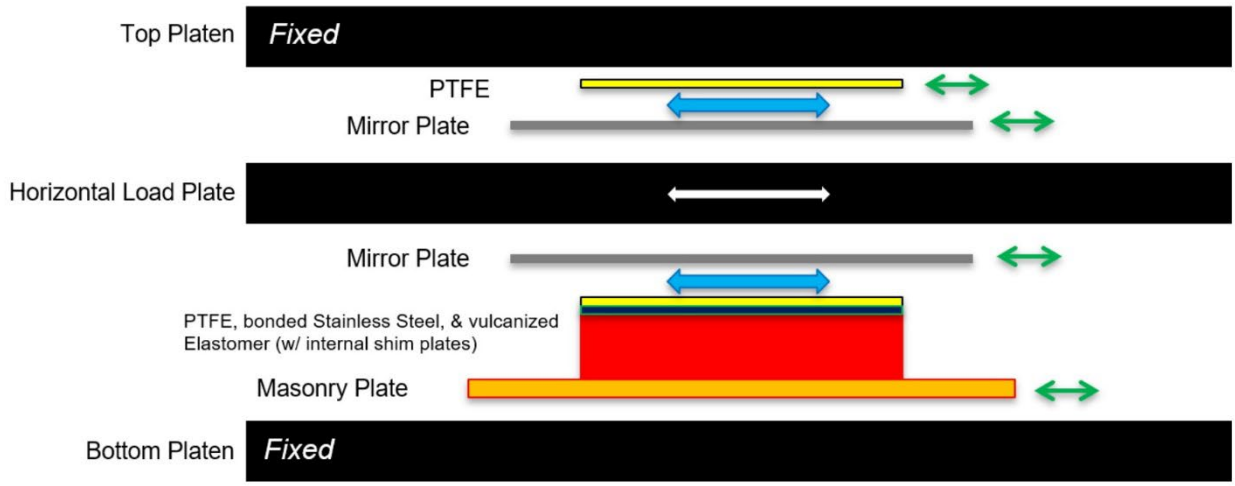

Figure 9. Simplified sketch of bearing assembly test setup.

Bearing Pad Types

The MoDOT PTFE Type "N" bearing pads were fabricated by D.S. Brown (a Gibraltar Industries Company) for all tests bearings used in Phase I and Phase II. The bearing pad products of this manufacturer were listed in MoDOT's Approved Materials List. The purchased bearing pads were manufactured to meet the requirements of the MoDOT Standard Specifications Section 716, Section 1038.3, and Section 1038.4. Each ordered bearing pad was composed of Grade 3 elastomer (neoprene), 100 percent virgin chloroprene, appropriate for Temperature Zone C and had a hardness of 70 durometer. The internal laminates were 1/8-inch thick, hot rolled steel sheets in accordance with ASTM A 1011 with steel grade meeting at least ASTM A36. There was a total of 1.5 inches of elastomer equally spaced at 1/2 inch around two internal 1/8-inch-thick steel plates for Phase I specimens. Figure 10 schematically shows the geometry of the bearing pad specimen. For one of the specimens tested in Phase II with thick elastomer, there was a total of 3 inches of elastomer equally spaced at 1/2 inch around five internal 1/8-inch thick steel plates.

Four types of PTFE sheets were used in the preparation of bearing specimens with the only difference between the four specimens being the material (filled or unfilled) and surface types (flat or dimpled). The PTFE material was 100 percent virgin PTFE fluorocarbon resin, unfilled or filled with fiberglass reinforcement. The amount of filler by weight of filled PTFE sheet was 15 percent.

For flat and dimpled PTFE, thicknesses of 1/8 inch and 3/16 inch were used, respectively. Figure 11 represents two types of flat and dimpled PTFE bearings. The diameter of the dimples was 0.313 inch at the surface of the PTFE, and their depth was 0.094 inch. The reservoirs were uniformly distributed over the surface area and covered around 25 percent of the contact surface. Dimples were not placed to intersect the edge of the contact area. PTFE surfaces were fabricated as a single piece and not spliced.

Table 2 lists the procured bearing pad test specimens along with their dimensions for Phase I. The geometry of each bearing pad used in Phase I was 9-inches long (parallel to load) by 12-inches wide with 1.5-inches of elastomer equally spaced at 1/2 inch around two internal 1/8-inch thick steel plates. The PTFE type was selected to evaluate the PTFE material and surface used by MoDOT in its routine bridge projects.

Table 3 lists the procured bearing pad test specimens along with their dimensions for Phase II. The size and type selected was intended to represent the full range of elastomeric bearings used by MoDOT in its routine bridge projects (MoDOT EPG 2024).

Table 2. PTFE elastomeric bearings (Phase I)

No.	L* (in.)	W (in.)	TB** (in.)	Neoprene Thickness (in.)	No. of Internal 1/8-in. Laminated Steel Plates	PTFE Type	PTFE Surface	PTFE Thickness (in.)
PF1	9	12	1 3/4	1 1/2	2	Unfilled	Flat	1/8
PF2	9	12	1 3/4	1 1/2	2	Filled	Flat	1/8
PF3	9	12	1 3/4	1 1/2	2	Unfilled	Dimpled	3/16
PF4	9	12	1 3/4	1 1/2	2	Filled	Dimpled	3/16

** L and W denote direction parallel and perpendicular to horizontal loading, respectively.*

*** TB = Total elastomeric bearing thickness (excluding the PTFE and bonded 1/8 in. stainless steel plate)*

Table 3. Additional PTFE elastomeric bearings (Phase II)

No.	L* (in.)	W (in.)	TB** (in.)	Neoprene Thickness (in.)	No. of Internal 1/8-in. Laminated Steel Plates	PTFE Type	PTFE Surface	PTFE Thickness (in.)
PF5	13	17.5	1 3/4	1 1/2	2	Unfilled	Dimpled	3/16
PF6	13	17.5	3 5/8	3	5	Unfilled	Dimpled	3/16
PF7	18	22.5	1 3/4	1 1/2	2	Unfilled	Dimpled	3/16

** L and W denote direction parallel and perpendicular to horizontal loading, respectively.*

*** TB = Total elastomeric bearing thickness (excluding the PTFE and bonded 1/8 in. stainless steel plate)*

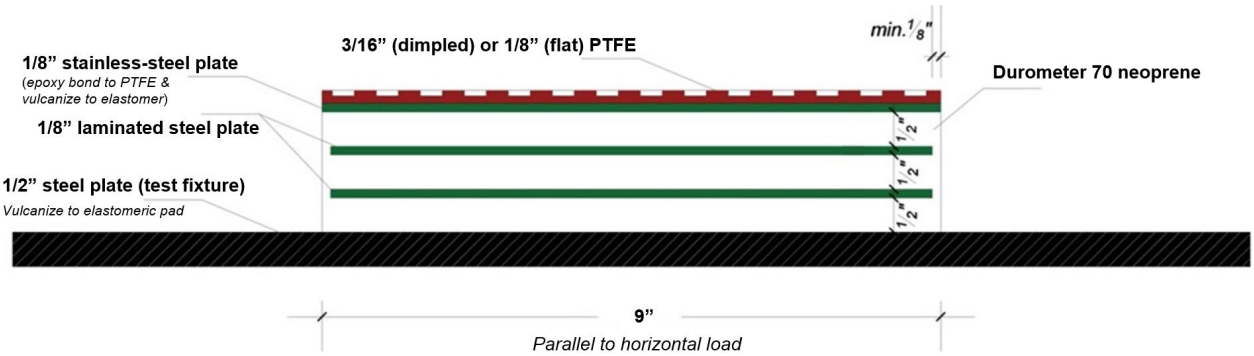

Figure 10. Schematic of bearing pad specimen.

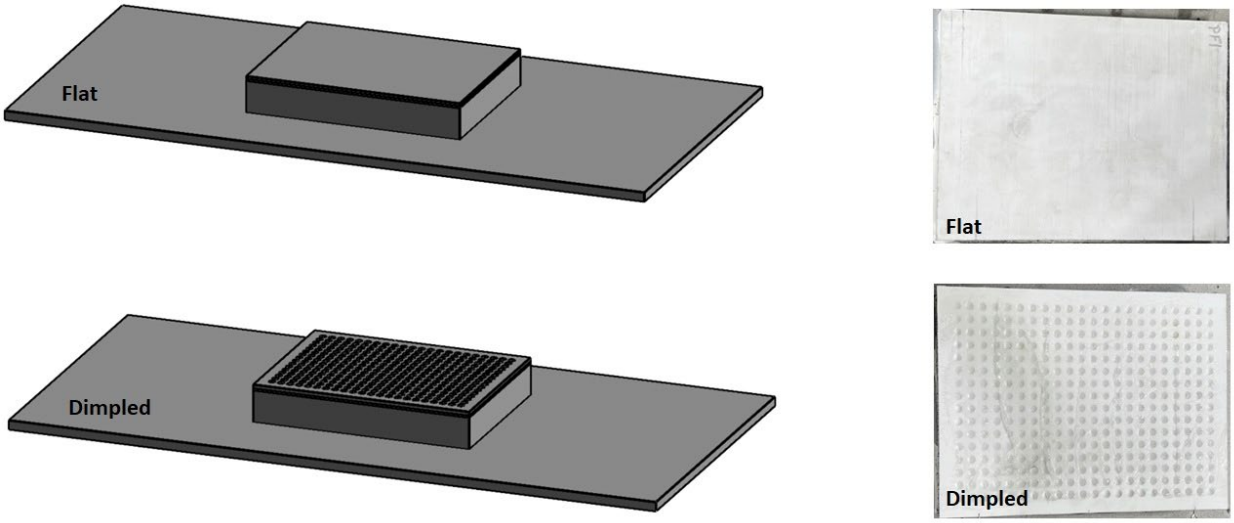

Figure 11. Images of flat and dimpled PTFE specimens.

Test Setup and Instrumentation

To measure the movements within the test assembly as depicted in Figure 12, multiple sensors were installed to comprehensively monitor the behavior of the bearing pad throughout each test. The measurements were recorded using cable extension transducers (string pots) designed to track the displacement of moving parts during testing. Due to the limited space between the PTFE and mirror plate in both the upper and lower halves of the test apparatus, an instrumentation tree was constructed to house all the string pots outside the apparatus. Consequently, wire extensions were employed to connect the components of the bearing assembly to the sensors mounted on the instrumentation tree. Figure 13 provides both a schematic and actual photograph of the instrumentation tree.

Figure 14 illustrates the setup of the bearing testing assembly. Figure 14-1 shows the main bearing specimen, consisting of a bottom masonry plate, an elastomer, and a top PTFE sheet. The two corners along the width of the PTFE sheet were connected to the instrumentation tree (indicated as sensors WP1 and WP2 in Figure 12) via two wire extensions. Although not depicted in Figure 14-1, a mounted magnet linked the bottom masonry plate to the instrumentation tree. Figure 14-2 reveals the mirror plate in the lower half of the bearing assembly, positioned upside down on the PTFE sheet. This plate was also connected to the instrumentation tree. Figure 14-3 displays the upper portion of the assembly, where the second PTFE sheet rested on the mirror plate, both stacked atop the large horizontal load plate. The mirror plate and PTFE sheet were oriented to slip against each other and were linked to the instrumentation tree for monitoring. Finally, Figure 14-4 shows the entire assembly sandwiched between the fixed top and bottom plates. For enhanced clarity, Figure 15 distinguishes the instrumentation extension wires using different colored lines. Figure 15-1 highlights the two wire extensions connected to the edges of the PTFE sheets and the wire connected to the masonry plate. Figure 15-2 displays the wire extensions connected to the second PTFE and mirror plate in the upper half of the bearing assembly. Figure 15-3 shows the wire extensions from Figure 15-2 emerging from the assembly. Lastly, Figure 15-4 depicts the entire assembled structure with all wire extensions connected to the instrumentation tree.

A Campbell Scientific CR9000X high-speed data acquisition system was employed to continuously sample and record data from the string pot sensors at a frequency of 10 Hz. In addition to this setup, high-resolution digital video cameras were utilized across all tests to visually capture the behavior of the bearing pad. Measurements were conducted using either individual sensors or a combination of various conventional sensors, which monitored the following components:

- The absolute horizontal movement of the PTFEs, mirror plates, horizontal load plate, elastomeric pad, and masonry plate.
- The slip of the bearing pad at the contact of PTFE sheets and mirror steel plates (in both upper and lower portions of the bearing assembly).

Both vertical and horizontal loads were applied to the test assembly using hydraulic rams and measured with integrated load cells.

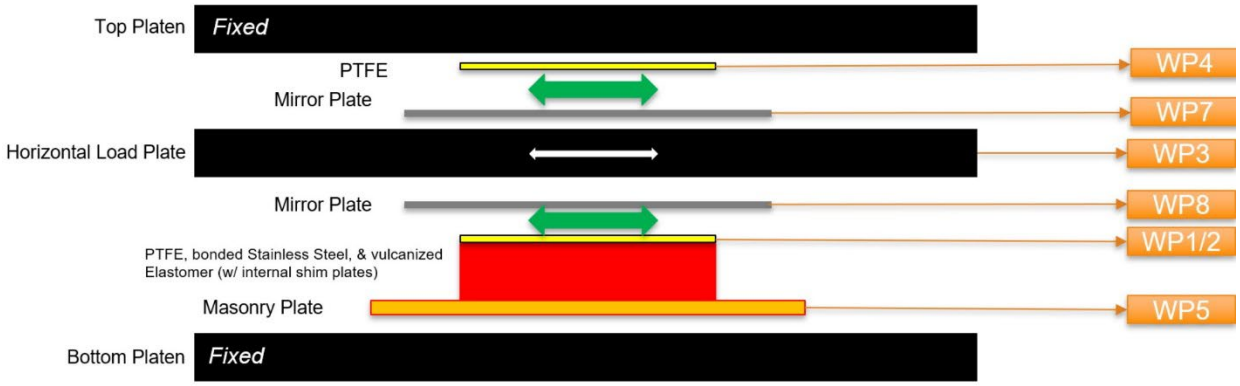

Figure 12. Simplified sketch of bearing assembly test setup with instrumentation.

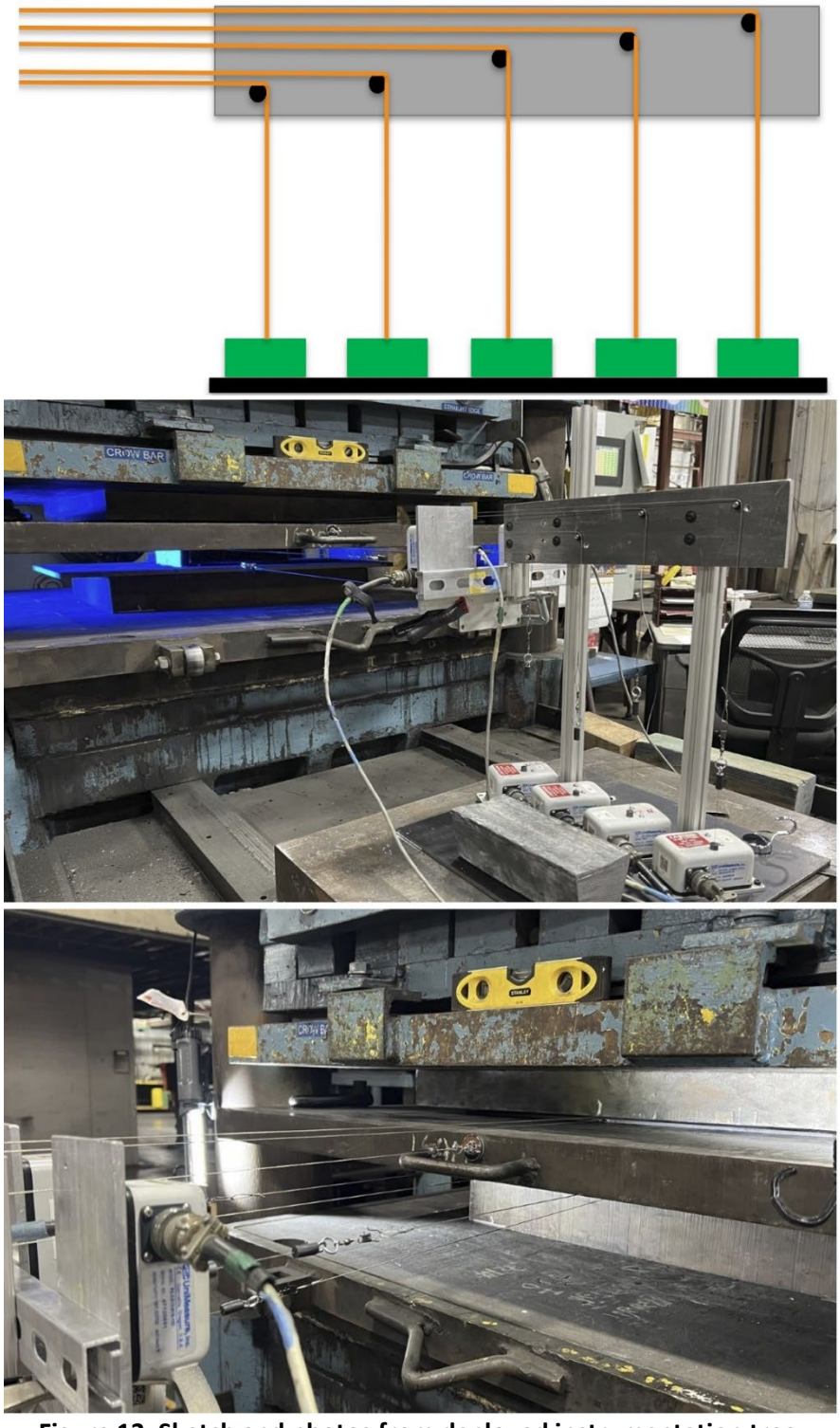

Figure 13. Sketch and photos from deployed instrumentation tree.

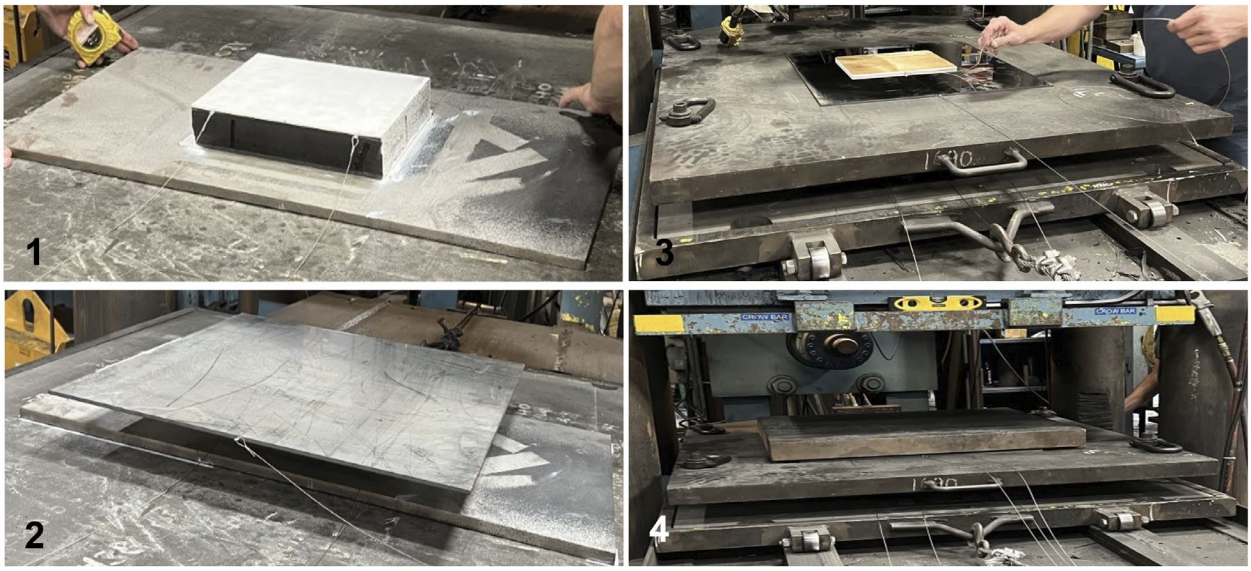

Figure 14. Photos of staged setup of bearing assembly.

Figure 15. Photos taken of bearing assembly setup ready for testing.

Friction Testing Matrix

The friction tests were conducted to determine the coefficient of friction between the lower PTFE sheet and the mirror plate. A total of thirteen individual tests were completed as part of the experimental friction testing program. Prior to each test, the test apparatus and system configuration were restored to their original settings. Table 4 provides a summary of the various friction test configurations.

Table 4. Friction test matrix for the experimental test program

Test No.	Specimen No.	PTFE Type	PTFE Surface	Contaminant	Elastomer Area (in^2)	Elastomer Thick. (in)	Contact Pressure (psi) [kips]	Temp. (°F)
1	PF1	Unfilled	Flat	-	108	1.5	800 [86]	68
2	PF2	Filled	Flat	-	108	1.5	800 [86]	68
3	PF3	Unfilled	Dimpled	-	108	1.5	800 [86]	68
4	PF4	Filled	Dimpled	-	108	1.5	800 [86]	68
5	PF5	Unfilled	Dimpled	-	228	1.5	800 [182]	68
6	PF6	Unfilled	Dimpled	-	228	3.0	800 [182]	68
7	PF7	Unfilled	Dimpled	-	405	1.5	800 [324]	68
8	PF3	Unfilled	Dimpled	Light	108	1.5	800 [86]	68
9	PF3	Unfilled	Dimpled	High	108	1.5	800 [86]	68
10	PF3	Unfilled	Dimpled	-	108	1.5	800 [86]	-13
11	PF7	Unfilled	Dimpled	-	405	1.5	200 [81]	68
12	PF7	Unfilled	Dimpled	-	405	1.5	400 [162]	68
13	PF7	Unfilled	Dimpled	-	405	1.5	600 [243]	68

Bearing Pad Testing Procedure

To align with the AASHTO LRFD Bridge Construction Specifications (BCS) [LRFD BCS 2017] and MoDOT's Standard Specification for Type "N" PTFE bearings, the following steps were implemented on new specimens (Phases I and II) to conduct the friction tests:

1) The test apparatus was set at its original condition and all the connected sensors were offset to zero.
2) The specimen was preloaded for one hour under a vertical load to achieve 800 psi.
3) The vertical pressure was held constant at 800 psi during the test, i.e., during the application of the horizontal load. The horizontal load was applied cyclically as outlined below:
4) The load was first applied in the positive direction until 1 inch of displacement.
5) The load was reversed in a negative direction until 2 inches of displacement.

6) The load was applied in a positive direction until 1 inch of displacement.
7) The cyclic loading at 1 in./min. (12 cycles), 6 in./min. (85 cycles), 2.5 in./min. (3-6 cycles), 1 in./min. (3-6 cycles) was repeated.
8) The horizontal load was removed followed by removal of the vertical load.

The 1-inch displacement of the load plate mentioned above was nominal and varied between 0.8 inch and 1 inch during the tests. The actual displacement was accurately measured by the instrumentation. As outlined by the AASHTO LRFD BCS, one of the key objectives was conditioning the bearing specimens through one-hour of preloading and repeated loading cycles (over 100 cycles). Once conditioning was complete, there was no requirement to continue one-hour or repeated 100-cycle loading on the same specimen for any additional testing in Phase II. For Phase II, except for new specimens being tested for the first time, a shortened version of the friction testing protocol was implemented as follows:

1) The test apparatus was set at its original condition and all the connected sensors were offset to zero.
2) The specimen was preloaded for five to ten minutes under the designated maximum vertical contact pressure.
3) The vertical load at the designated contact pressure was held constant during the test, i.e., during the application of the horizontal load. The horizontal load was applied cyclically as outlined below:
4) The load was first applied in the positive direction until 1 inch of displacement.
5) The load was reversed in a negative direction until 2 inches of displacement.
6) The load was applied in a positive direction until 1 inch of displacement.
7) The cyclic loading of 1 in./min. (12 cycles), 2.5 in./min. (3-6 cycles), and 1 in./min. (3 cycles) was repeated.
8) The horizontal load was removed followed by removal of the vertical load.

A review of literature as well as LRFD BCS for friction testing of PTFE specimens revealed that loading rates of 1 in./min and 2.5 in./min. are loading rates that a bridge bearing typically experiences throughout its life. An additional speed of 6 in./min. was also used to shorten the duration of testing as well as study the effect of higher loading rates, which is primarily applicable to seismic regions.

Chapter 5. Summary of Friction Test Results

Thirteen friction tests were conducted using seven different types of bearing pads, varying in PTFE material and surface characteristics, along with additional variables such as bearing size, temperature, contamination, loading rate, and contact pressure. Each test encompassed multiple repeated cycles, resulting in over 1,700 individually calculated friction values. Depending on the specific test, test durations ranged from one to four hours. Throughout each testing session, continuous data were collected at a 10 Hz sampling frequency from seven displacement sensors and two load cells. Given the extensive volume of datasets, numerous scripts were developed using Python software to efficiently process, analyze, validate, visualize, and report the results.

Figure 16 depicts the horizontal load data collected from testing Specimen PF7 (unfilled dimpled PTFE). This example included 105 cycles of horizontal loading while being vertically loaded at a contact pressure of 800 psi. Multiple friction tests were conducted using the loading speeds and cycle counts illustrated in Figure 16. Each test cycle involved two instances of friction breakaway. The first occurred when the horizontal load plate exerted the load in the positive direction and moved approximately one inch. The second breakaway occurred as the load plate returned in the negative direction. Figure 17 shows a single load cycle. Each half cycle typically includes three sequential loading stages: pre-slip, post-slip of top PTFE, and post-slip of bottom PTFE, all of which are highlighted in the figure. Figure 17 features two vertical axes, where the primary (left) axis represents the horizontal load, and the secondary (right) axis displays the movement of the horizontal load plate (indicated by WP3 in Figure 12).

In Stage I, the horizontal load plate moved in the positive direction under displacement control, where it displaced at a set rate regardless of the load. While the vertical load remained constant in force-control mode, the gradual application of the horizontal load commenced. As the horizontal load increased, initially there was no relative movement between the PTFE and the mirror plate in both the upper (indicated by the difference of WP7-WP5 in Figure 12) and lower (indicated by the difference of WP8-WP1/2 in Figure 12) halves of the test assembly. Some minor deformation of the elastomeric pad occurred during this initial loading. Figure 18 and Figure 19 provide close-up views of this phenomenon, with Figure 19 specifically depicting the load-displacement plot of the same test. The displacement remained constant with continued application of horizontal load during Stage I referred to as “pre-slip”. However, when slip occurred in Stage II, the relative displacement between the PTFE and the mirror plate at the top of the test assembly changed. Following the slip of the top PTFE, the static friction transitioned to dynamic friction, resulting in a drop in the horizontal load. Meanwhile, the bottom PTFE remained in place via static friction during Stage II. The top PTFE slid before the bottom PTFE, primarily due to the reduced stiffness caused by the flexibility of the bottom PTFE adhered to the elastomer. However, sometimes, they slipped simultaneously. It is notable that the duration of Stage II could be brief if a harder (stiffer) elastomer is used.

During quality control tests, manufacturers sometimes use a different type of PTFE with a very low friction coefficient in the top portion of the test assembly to facilitate earlier slip. For instance, if testing an elastomer bearing with bonded flat PTFE in the lower portion, a lubricated dimpled PTFE might be used in the upper half. This could make the duration of Stage II considerably longer and make the two instances of slip more distinct.

For Stage II, the horizontal load continued to increase with the top PTFE continuing to slip relative to the top mirror plate while the bottom PTFE moved with the elastomer deformation but did not slip relative to the bottom mirror plate. However, once the bottom PTFE slipped at the end of Stage II, the load briefly dropped and then continued to increase while the relative displacements of the top and bottom PTFE and their corresponding mirror plates increased at a constant rate. After the horizontal load plate had traveled one inch, the half cycle was finished, the horizontal load dropped to zero, and the process was restarted in the opposite direction, repeating the three loading stages. Two friction coefficient values were captured from each testing cycle.

Figure 20 shows various PTFE surfaces after undergoing over a hundred cycles of friction testing. Figure 21 shows the surface of a mirror plate after more than a hundred cycles using a clean lubricant. The photo on the left displays the surface immediately after removal from the assembly, still bearing the lubricant imprint, while the figure on the right depicts the same mirror plate after cleaning. There are visible scratches that cannot be detected by touch.

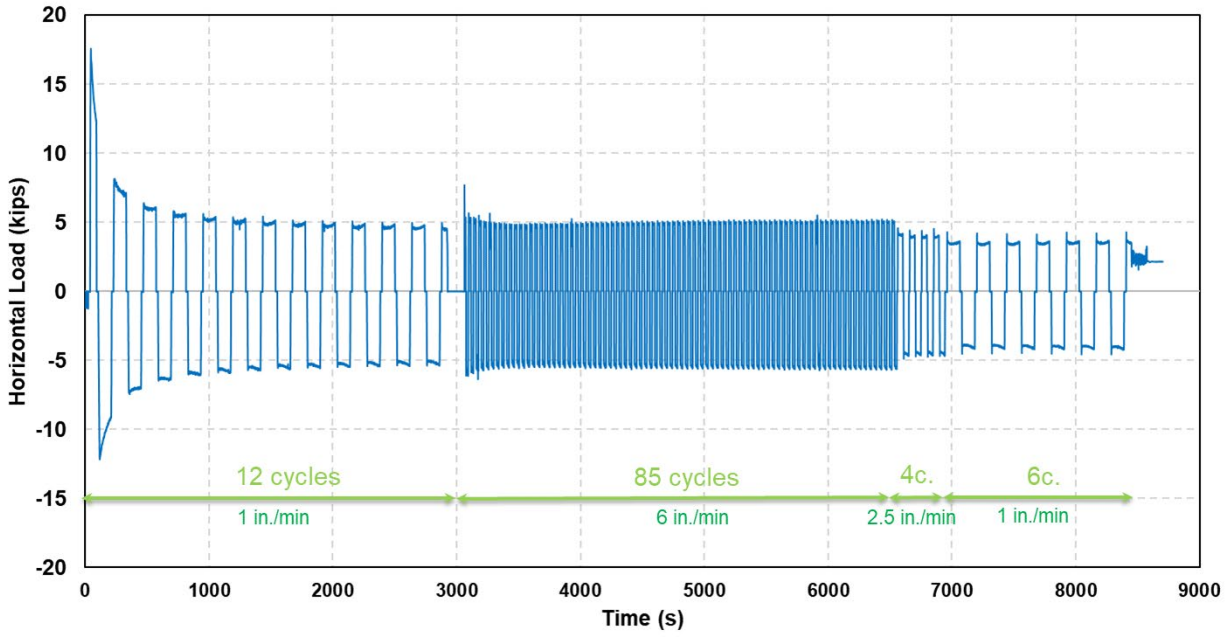

Figure 16. Line chart showing time history plot of horizontal load on PF7 specimen under 800 psi vertical pressure.

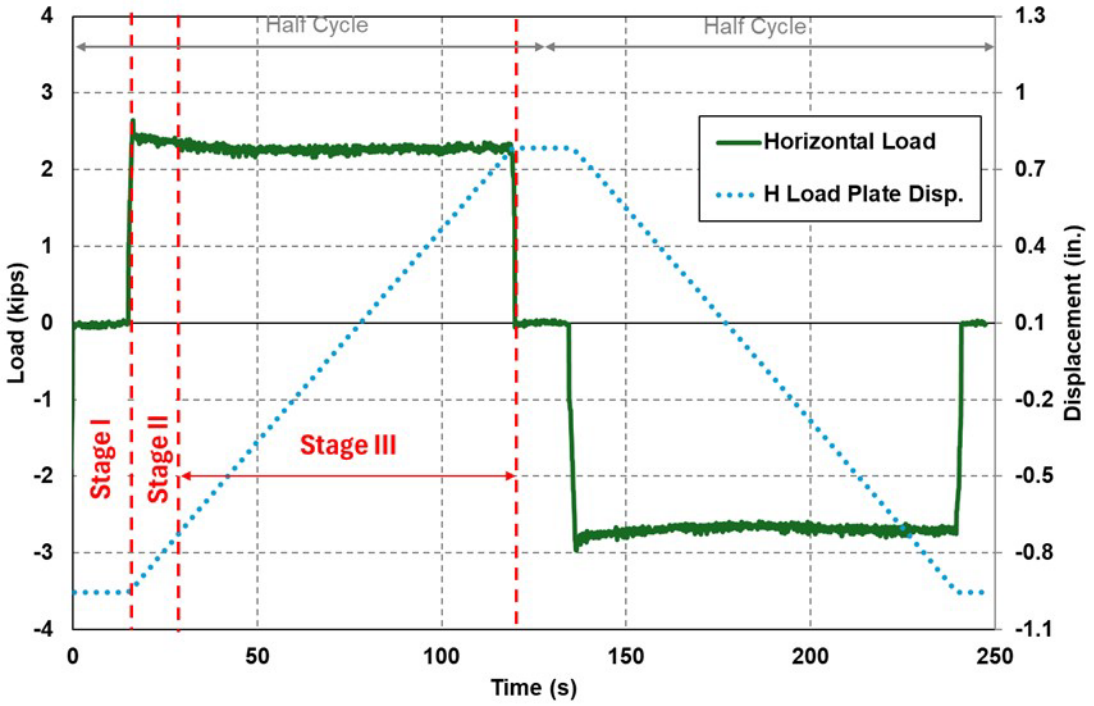

Figure 17. Line chart showing time history plot of horizontal load and load plate movement on PF7 specimen under 200 psi vertical pressure during one cycle testing.

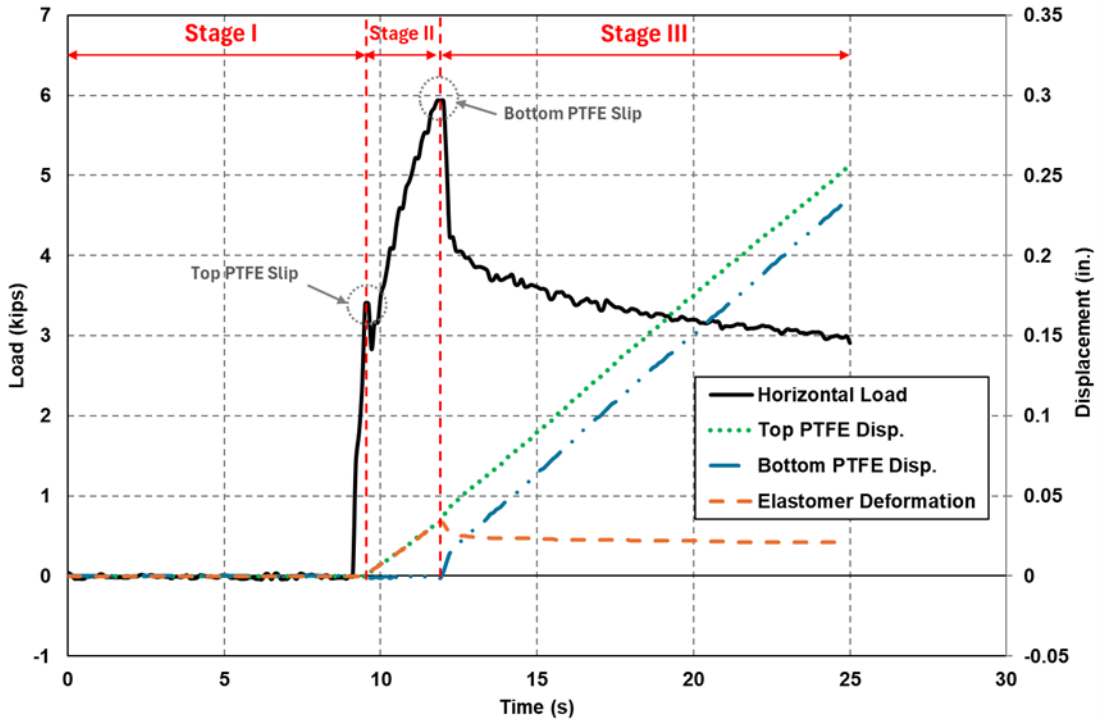

Figure 18. Line chart showing time history plot of horizontal load and relative movements of top and bottom PTFEs and elastomer for Specimen PF7 under 200 psi vertical pressure.

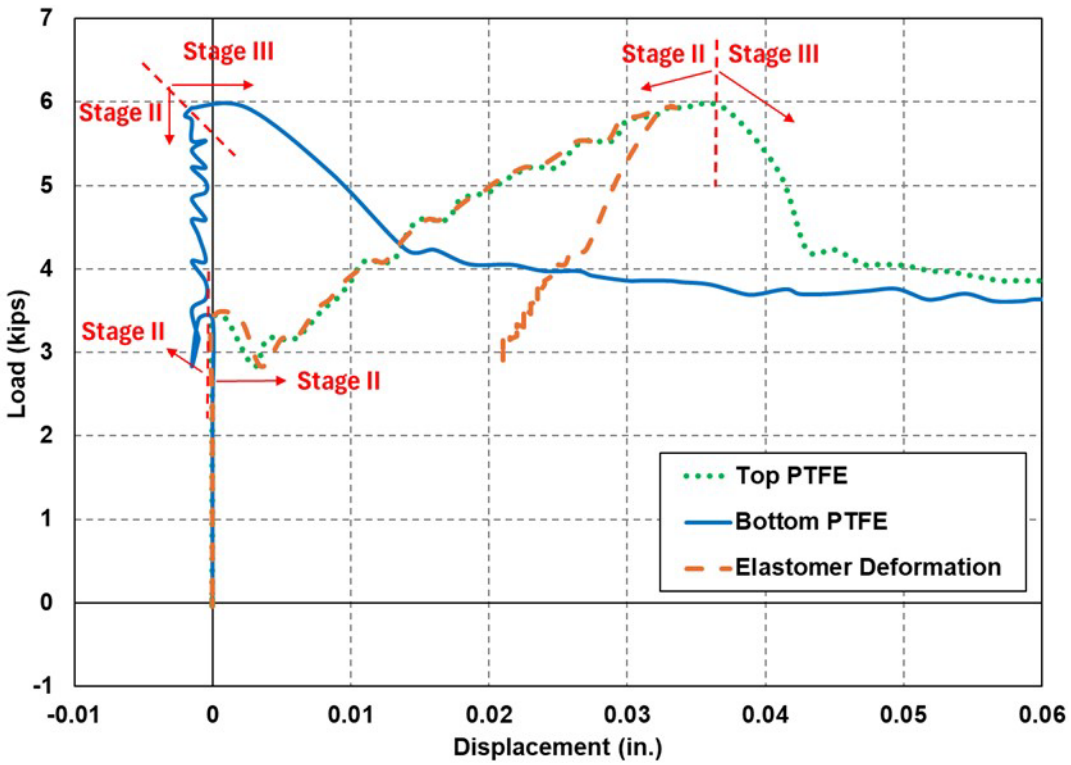

Figure 19. Line chart of load-displacement plot of horizontal load and relative movements of top and bottom PTFEs and elastomer for Specimen PF7 under 200 psi vertical pressure.

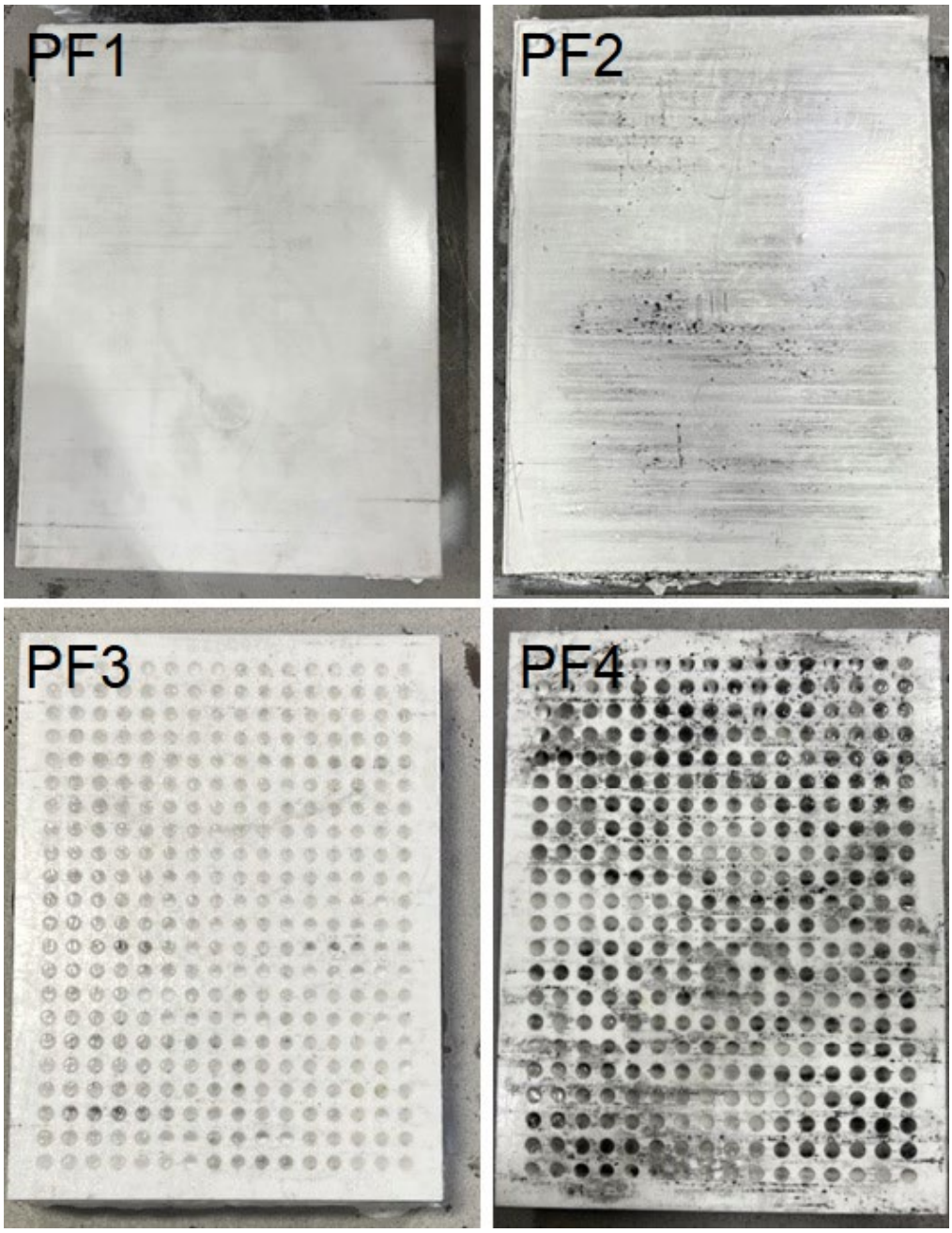

Figure 20. Photos of the PTFE specimens after Phase I testing.

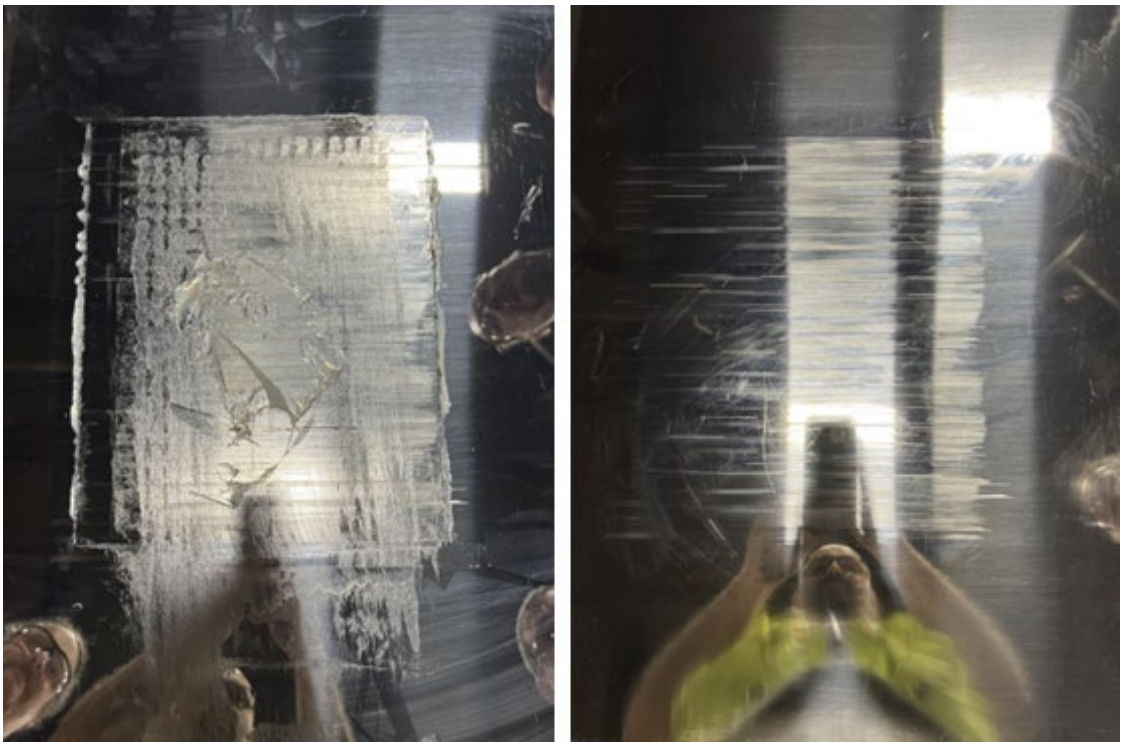

Figure 21. Photos of the lubricant imprint (left) and visible scratches (right) of PTFE on the mirror plate.

Slip Verification Tests

During the friction tests, the observed slip regularly occurred at values lower than those measured in NCHRP Report 432. Therefore, in order to confirm these results, additional verification testing was performed that included the use of a stereo vision digital image correlation (DIC) system to measure displacements of the specimens during testing. The measurements from the DIC were then compared to the measurements obtained from the sensor set up mounted on the instrumentation tree.

The DIC was set up along the side of the bearing assembly to measure movements of the test assembly during the application of the horizontal load providing full field strain and displacement images to better understand the behavior of the specimens during testing. The DIC non-contact measurement method captures a series of digital photos over the duration of testing, which can be compared against a “reference” (zero displacements and strains) photo to give relative deformations and strains. For this testing, the DIC system was used to measure relative displacements between slip planes and to identify where and when this slip occurred. Prior to testing, the bearing specimen surfaces were sprayed with a contrasting black and white stochastic speckle pattern. These speckles can be tracked over time using the stereo-DIC system to provide information on identified surfaces or points of interest. A GOM ARAMIS DIC system,

as shown in Figure 22, was used. Due to length of tests, images were collected at certain times (such as first breakaway) at a frequency of 25 Hz during the test. Figure 23 displays a photo of the DIC system positioned adjacent to the side of the testing apparatus. The DIC system consisted of a pair of 2.3 megapixel CMOS sensors on an 800 mm adjustable base manufactured by GOM. The calibration was completed with a CP40/200 calibration object supplied by GOM. This calibration had a field of view of (12.8 inch, 8.27 inch, 8.27 inch). The calibration deviation was 0.0122 pixels, which is less than the acceptance criterion of 0.1 pixels.

The horizontal measurements from the DIC system were overlain on an image of the bearing specimen to better visualize the slip at the contact surface. Due to the size and configuration of the test setup, only the lower bearing assembly could be captured. Figure 24 presents contour plots from the verification test conducted for Specimen PF6. The top figure shows the horizontal displacement of the PTFE just before it slips while the bottom image shows the condition when the horizontal load was stopped.

Figure 25 illustrates the relative displacement measurement (slip) of the bottom PTFE as it slides under the top mirror plate, focusing on the portion where slip occurred. Additionally, Figure 25 includes another slip measurement taken by the primary string pot, demonstrating that the timing of the slip recorded by the string pot was consistent with that recorded by the DIC system. Figure 26 plots measured slip displacements against the applied horizontal load for the same test, showing consistent behavior throughout the test. Oscillations in the string pot measurement were attributed to the sensor's resolution threshold.

Figure 27 depicts the shear deformation of the elastomer versus the horizontal load. The results indicated that both measurement techniques consistently captured the shear deformation of the elastomer. The slope of the displacement-load plot, representative of the elastomer's shear modulus, was in agreement between the two sensing techniques.

The DIC system, alongside the primary instrumentation, was also utilized to verify that planes between test components which were assumed not to move during the testing were, in fact, stationary. For example, the masonry plate which was not mechanically attached to the bottom platen was monitored for movement. Figure 28 is a plot of a representative breakaway event for Specimen PF6, focusing solely on the portion where slip of the bottom PTFE occurred. This time-history plot was presented with two vertical axes: the left denoting displacement and the right horizontal load. It included four curves: one for horizontal load, one for relative displacement of the PTFE and the sliding mirror plate, and two for the absolute movement of the masonry plate (one taken by DIC and one by string pot). The relative displacement of the PTFE and sliding mirror plate confirms the observed slip in combination with the observed drop in horizontal load. The masonry plate, however, remained in place, as measured by both DIC and string pot. Figure 29 plots the measured slip displacements against the applied horizontal load for the same dataset. Small oscillations, primarily associated with the resolution of the string pot, were visible in the responses of both DIC and string pots. The string pot and DIC resolutions were approximately 0.001 inch and 0.0001 inch, respectively. At slip, the entire

testing apparatus underwent a loading shock due to the rebalancing of the load among the testing components. Therefore, the slight movements recorded by the DIC were associated with its greater accuracy and an overall movement of the test apparatus relative to the DIC's position on the floor rather than any movement of the masonry plate itself.

Similarly, Figure 30 and Figure 31 show a zoomed-in plot of the relative displacement of the mirror plate and the horizontal load plate at slip. The mirror plates were not mechanically attached to the horizontal load plate. The slight movement in the response measured by both the string pot and the DIC was associated with the horizontal load plate (sandwiched between the two mirror plates in the testing equipment) shifting during slip and not the two mirror plates slipping on the load plate.

Figure 22. Photo of GOM ARAMIS DIC System used for verification testing.

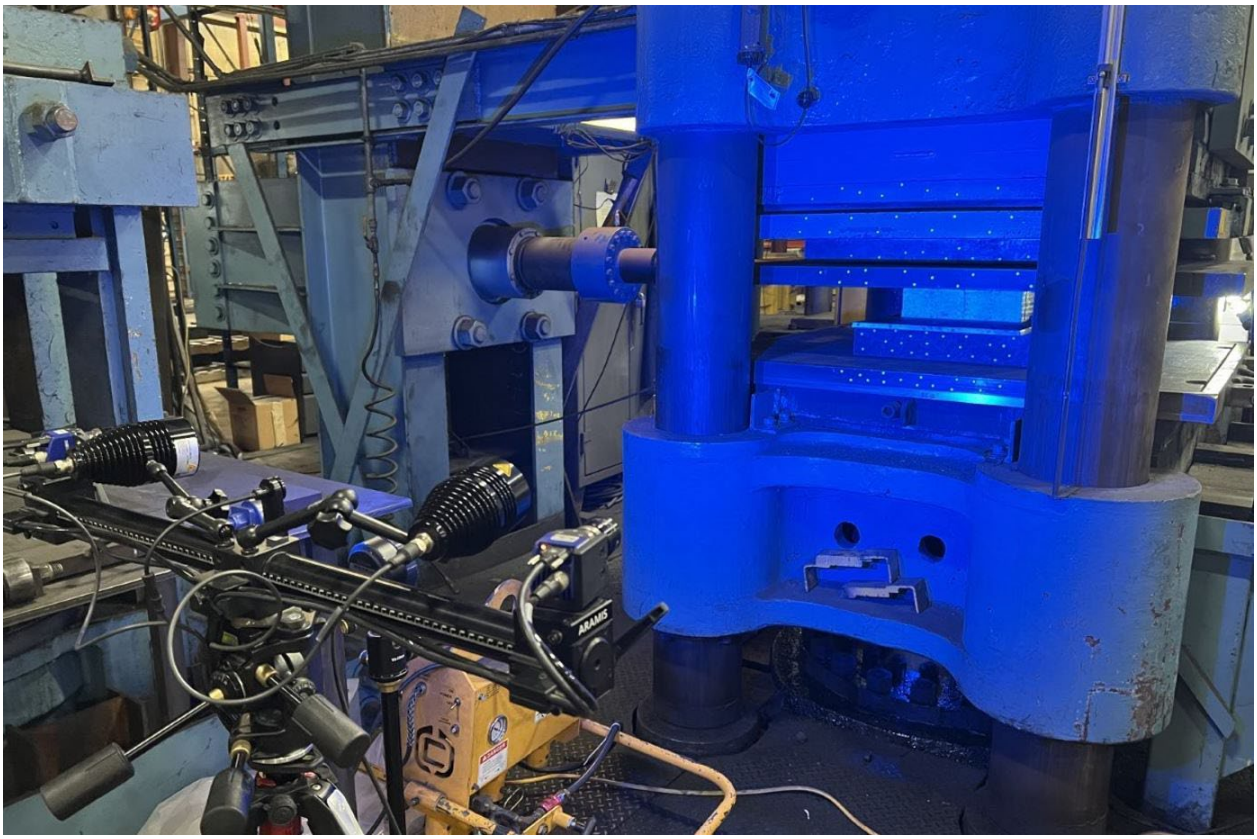

Figure 23. Photo taken from deployed DIC system.

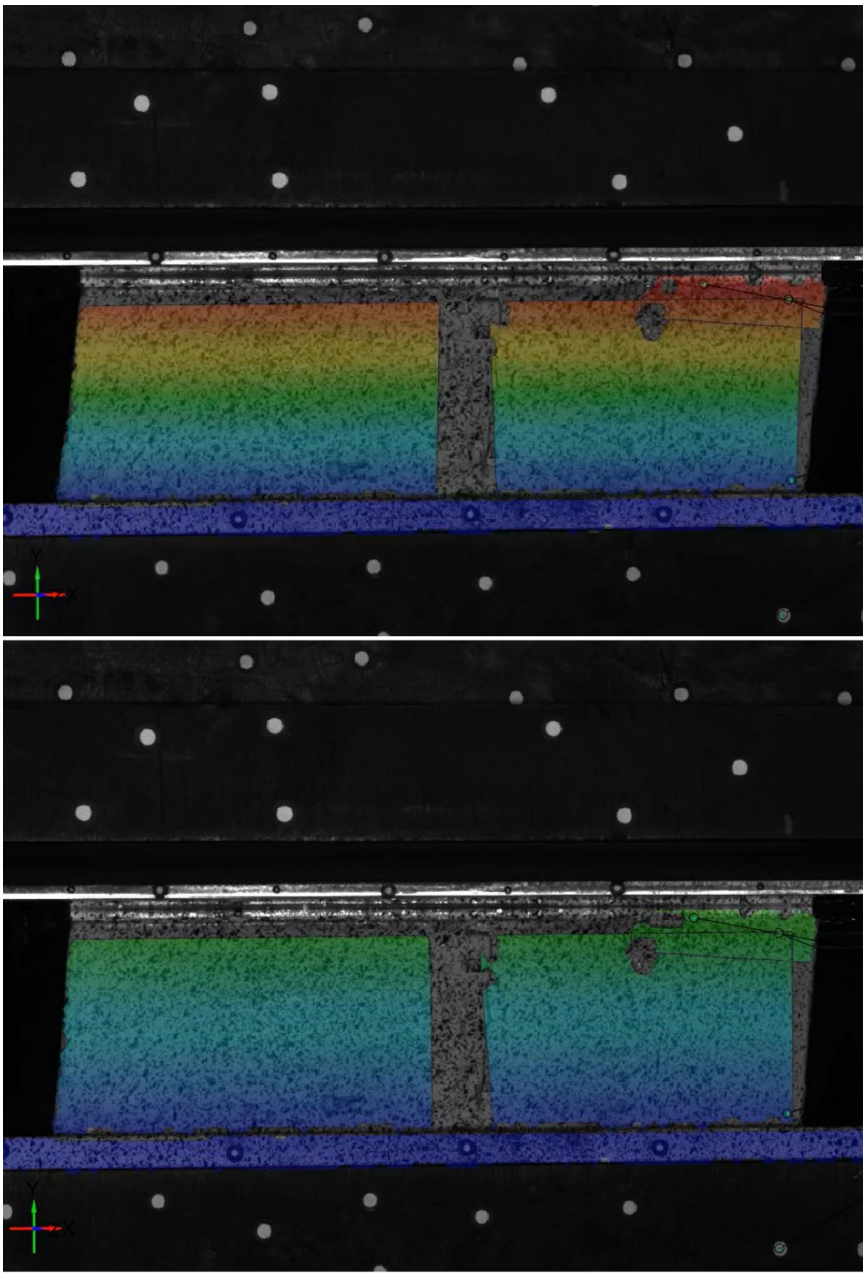

Figure 24. DIC image of slip in the direction of loading for PF6 Specimen just before first slip (top) and after the end of horizontal load (bottom).

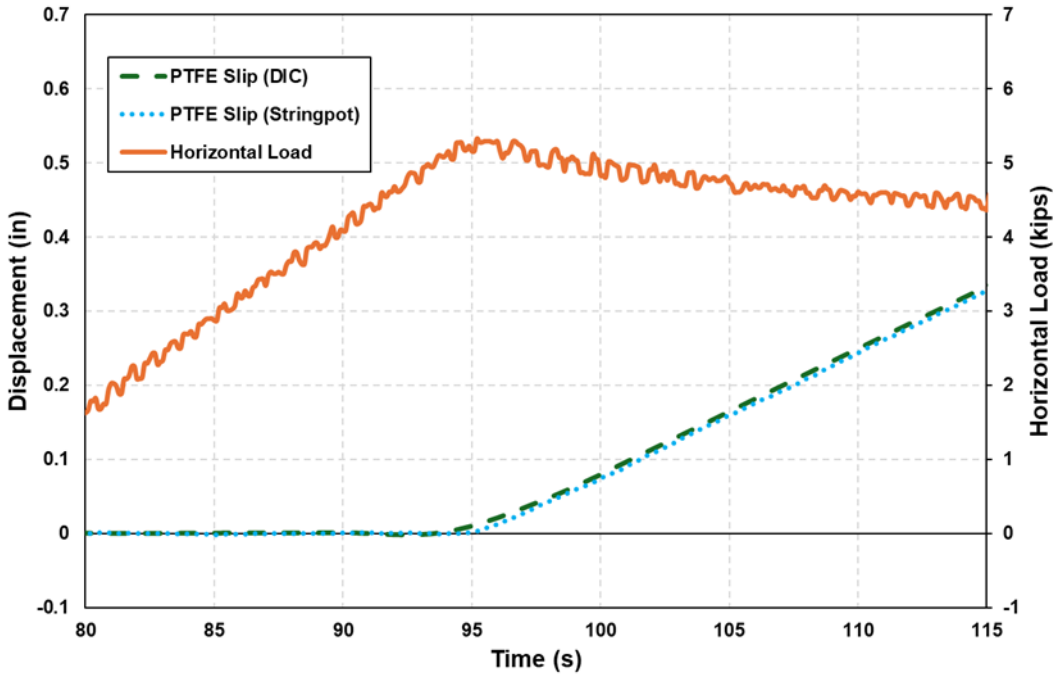

Figure 25. Line chart of bottom PTFE slip plot for Specimen PF6.

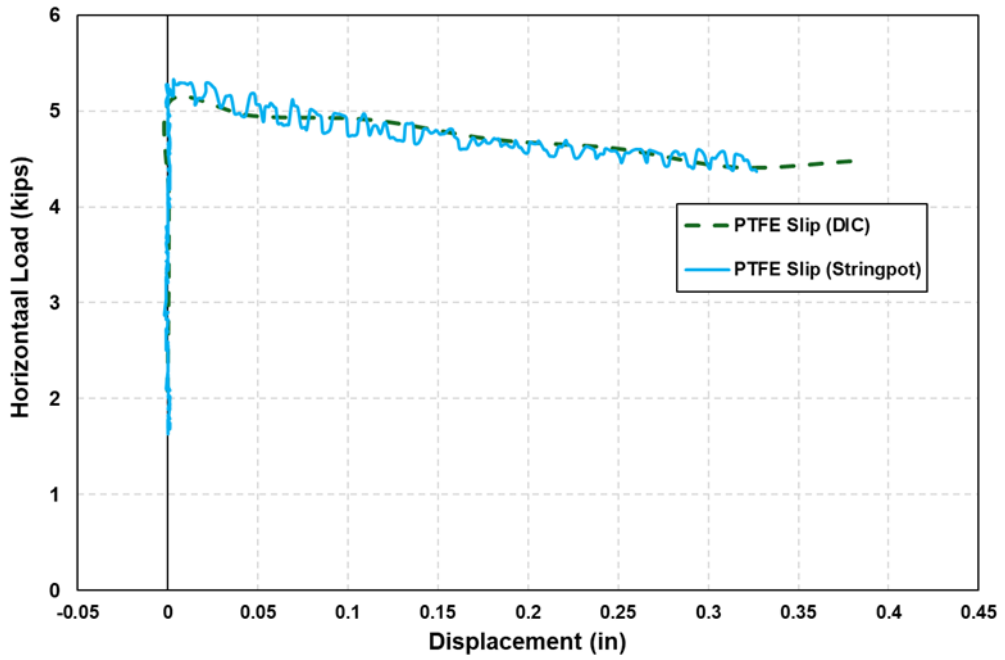

Figure 26. Line chart of load-displacement plot of bottom PTFE slip for Specimen PF6.

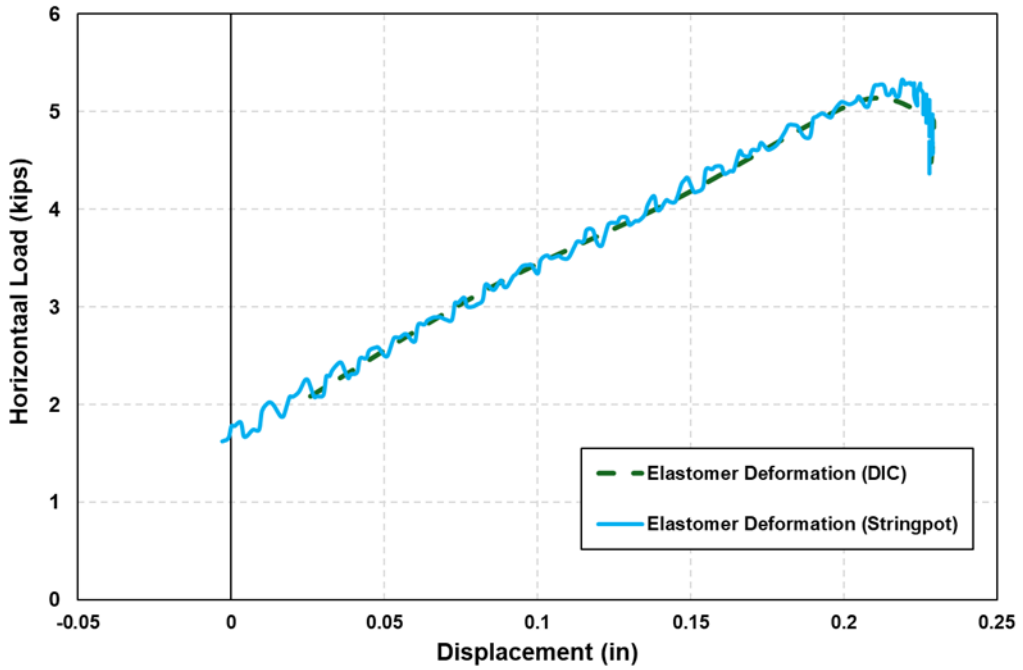

Figure 27. Line chart showing load-displacement plot for shear deformation of elastomer for Specimen PF6.

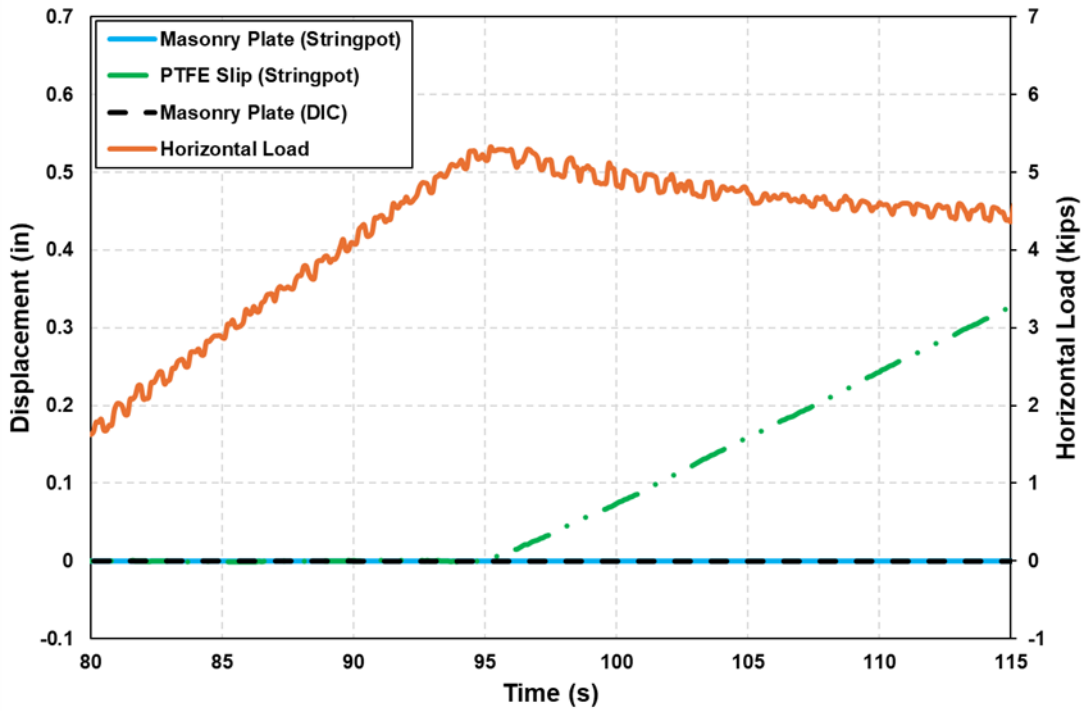

Figure 28. Line chart showing displacement plot of masonry plate (Specimen PF6).

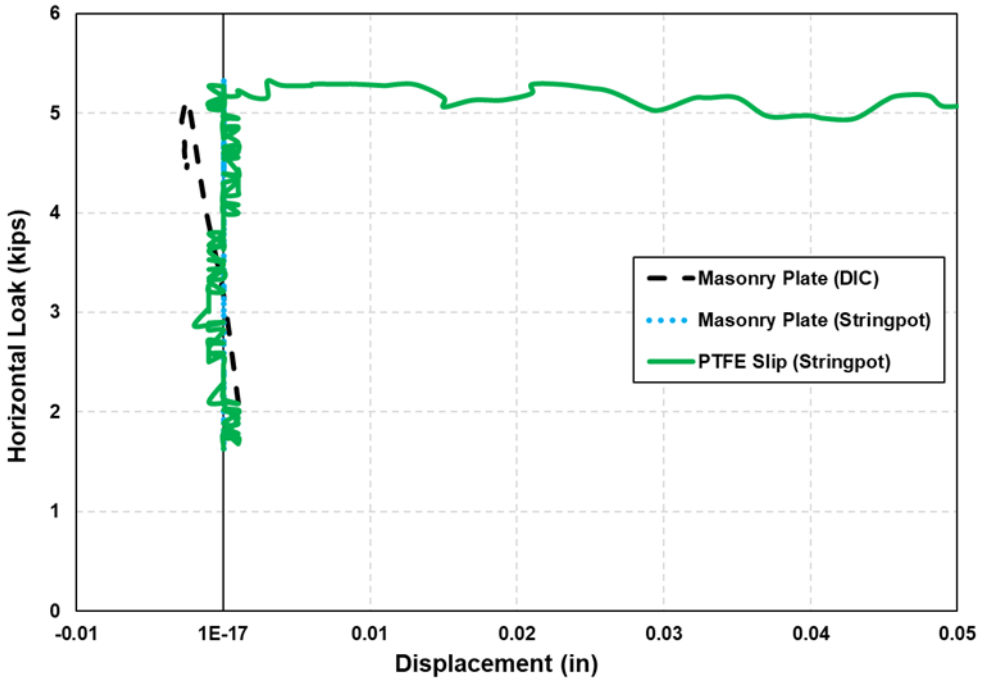

Figure 29. Line chart showing load-displacement plot of masonry plate (Specimen PF6).

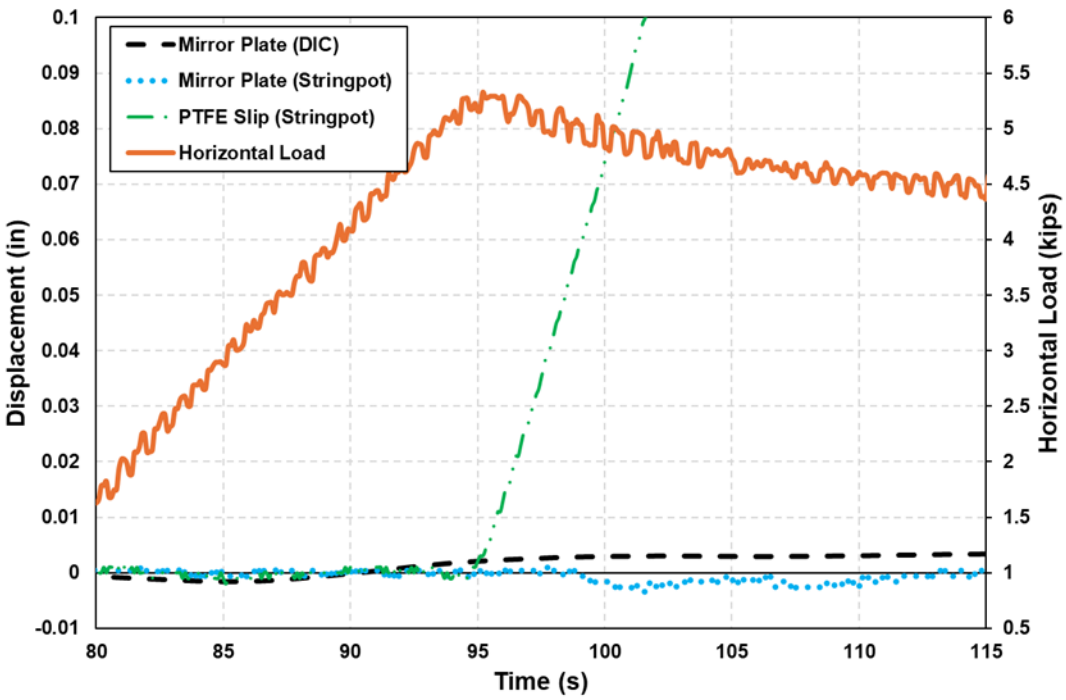

Figure 30. Line chart showing relative displacement of bottom mirror plate and load plate (Specimen PF6).

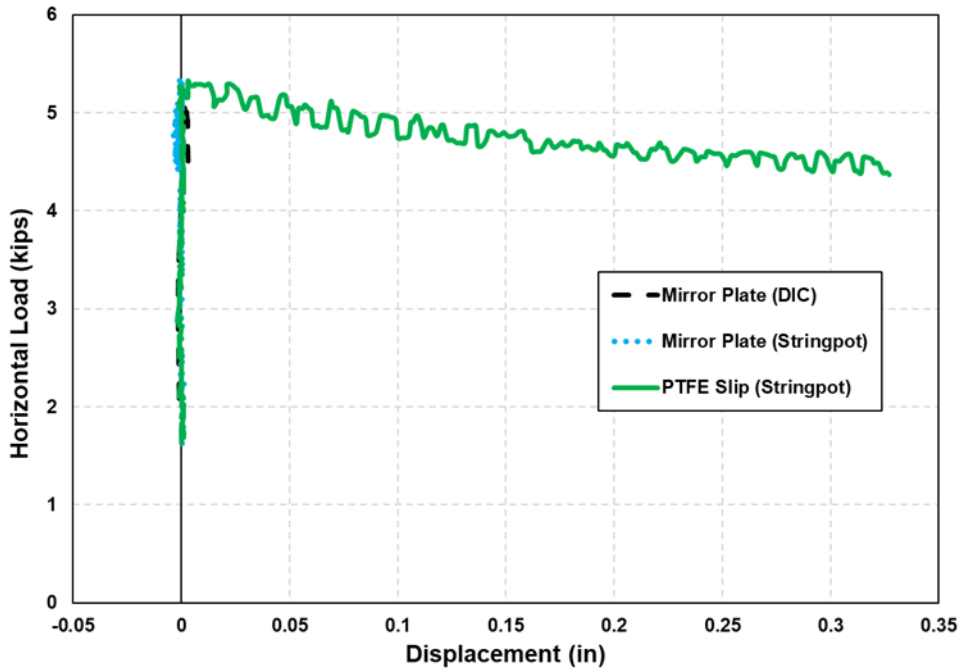

Figure 31. Line chart showing load-displacement plot of relative movement of bottom mirror plate and load plate (Specimen PF6).

Calculation of PTFE Coefficients of Friction

The static friction coefficient of a PTFE surface was calculated using the following formula:

$$\mu_{Lower\ PTFE} = \frac{H_{Lower\ PTFE}}{V} \qquad (Eq.\ 1)$$

Equation 1. Static Coefficient of Friction for a PTFE Surface

where $\mu_{Lower\ PTFE}$ represents the friction coefficient of the bearing with a PTFE surface, located in the lower portion of the test assembly. The terms $H_{Lower\ PTFE}$ and V refer to the horizontal and vertical loads applied to the bearing at the moment of each slip, respectively. V is derived from the total vertical load, while $H_{Lower\ PTFE}$ is the horizontal load transferred to the lower portion of the bearing assembly by the horizontal load plate, adjusted for the effects of the upper portion of the assembly. As previously mentioned, the bottom PTFE often slid simultaneously with or after the top PTFE slipped. Depending on the timing of the slip, one of the following two methods was used to compute the static friction at the lower PTFE:

A) **Top and bottom PTFEs slid simultaneously:** In this scenario, both PTFE surfaces transitioned from static to dynamic mode together. Consequently, the measured load at

the horizontal plate slightly decreased, and there was not a secondary drop as previously illustrated in Figure 18. The static friction coefficient of PTFE surfaces was computed as follows:

$$\mu_{ST-\,Lower\,PTFE} = \mu_{ST-\,Upper\,PTFE} = \frac{H_{LP}}{2V} \qquad (Eq.\,2)$$

Equation 2. Static Coefficient of Friction of PTFE Surface – Two PTFEs Slid Simultaneously

Where $\mu_{ST-Lower\,PTFE}$ and $\mu_{ST-Upper\,PTFE}$ denote the static friction coefficients of the lower and upper PTFE surfaces, respectively. V is calculated from the total vertical load, and H_{LP} is the total horizontal load applied by the horizontal load plate, as measured via an internal load cell.

B) Top PTFE slid before bottom PTFE: In this case, the PTFEs experienced breakaway sequentially. When the bottom PTFE started sliding, the top PTFE had already slipped and was sliding under a constant load value (dynamic friction). Figure 32 shows the time history of the horizontal load exerted by the load plate. The points labeled "A", "B", and "C" indicate the static friction of the top PTFE before slipping, the dynamic friction immediately after slipping, and the static friction of the bottom PTFE before slipping, respectively. The static friction coefficients of PTFE surfaces were calculated as follows:

$$\mu_{ST-\,Upper\,PTFE} = \frac{H_A}{V} \qquad (Eq.\,3)$$

Equation 3. Static Coefficient of Friction of Upper PTFE Surface – Top PTFE

$$\mu_{ST-\,Lower\,PTFE} = \frac{H_C - H_B}{V} \qquad (Eq.\,4)$$

Equation 4. Static Coefficient of Friction of Bottom PTFE Surface – Bottom PTFE

The H_A, H_B, and H_C values are the total horizontal loads applied by the horizontal load plate, measured at instances designated by letters A, B, and C on the horizontal load plot.

The results of thirteen friction tests, as specified in Table 4, are summarized in Table 5. Each test involved multiple repeated cycles of loading performed at varying loading rates. To adopt a conservative approach, the maximum coefficient values associated with the last two cycles of

loading at each rate have been reported in Table 5. Consistent with the results of NCHRP Report 432, a review of the friction coefficient values computed for each rate indicated that the coefficients either increased or remained constant.

Table 5. Summary of static friction coefficient values computed for experimental program tests

Test No.	Specimen No.	PTFE Type	Contact Pressure (psi) [kips]	1st	1 in./min. (12 cycles)	6 in./min. (85 cycles)	2.5 in./min. (3-6 cycles)	1 in./min. (6 cycles)
1	PF1	Unfilled-Flat	800 [86]	6.4%	2.3%	5.9%	5.5%	5.4%
2	PF2	Filled- Flat	800 [86]	7.5%	3.3%	8.1%	-	6.5%
3	PF3	Unfilled-Dimpled	800 [86]	3.1%	0.9%	0.6%	0.6%	0.9%
4	PF4	Filled-Dimpled	800 [86]	4.3%	0.9%	0.9%	1.2%	1.3%
5	PF5	Unfilled-Dimpled	800 [182]	1.9%	0.7%	0.8%	0.9%	0.8%
6	PF6	Unfilled-Dimpled	800 [182]	3.4%	0.9%	0.8%	0.7%	0.8%
7	PF7	Unfilled-Dimpled	800 [324]	5.0%	1.3%	0.6%	0.8%	0.9%
8	PF3	Unfilled-Dimpled	800 [86]	-	-	-	7.6%	7.8%
9	PF3	Unfilled-Dimpled	800 [86]	-	-	-	NA	NA
10	PF3	Unfilled-Dimpled	800 [86]	-	-	-	0.9%	0.9%
11	PF7	Unfilled-Dimpled	200 [81]	-	-	-	1.4%	1.6%
12	PF7	Unfilled-Dimpled	400 [162]	-	-	-	1.4%	1.5%
13	PF7	Unfilled-Dimpled	600 [243]	-	-	-	1.2%	1.1%

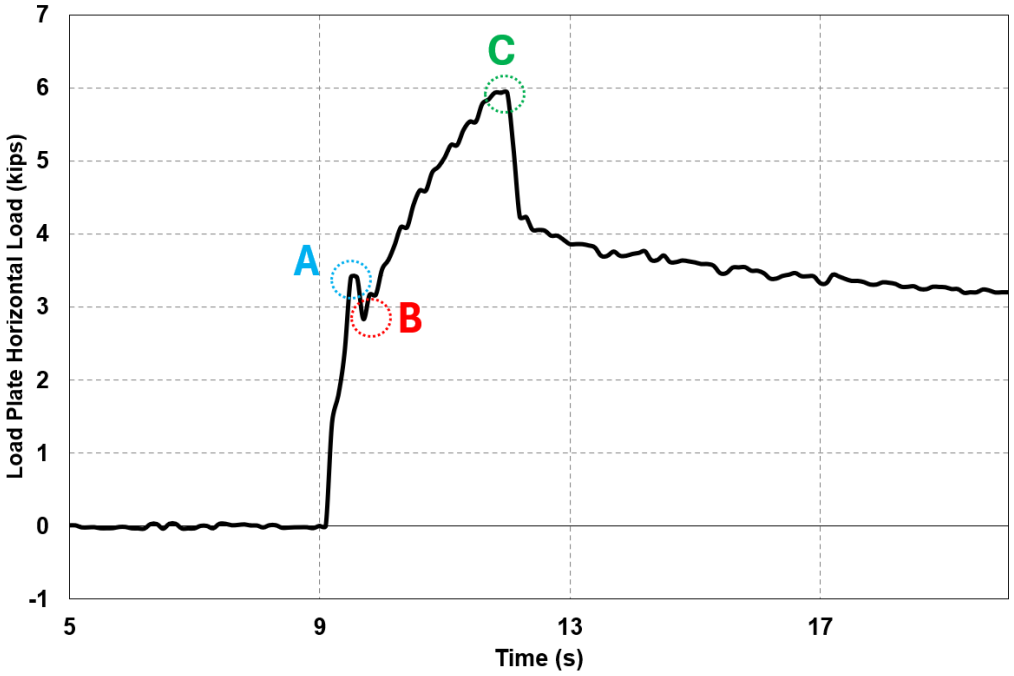

Figure 32. Line chart showing time history plot of total horizontal load in a typical friction test.

Chapter 6. Discussion of Results

The influence of various factors—such as PTFE material type, surface type, size, vertical pressure, loading rate, and surface contamination—on the coefficient of friction for PTFE bearing pads, was assessed through a test matrix defined in the experimental program. Subsequently, a parametric analysis was conducted, and the outcomes are detailed in subsequent sections. In addition, the experimental test results were compared with those obtained by Stanton et al. (1999) under NCHRP Project Report 432, which underpins the AASHTO LRFD BDS design coefficients of friction. The forthcoming sections provide a comparative analysis of pertinent test results with those documented in NCHRP Project Report 432.

Parametric Analysis of the Measured PTFE Coefficients of Friction

The behavior of PTFE bearings under differing applications was investigated. These applications included assessing the influence of various PTFE material types (filled and unfilled), surface types (flat and dimpled), different loading rates, varying pad sizes, increasing levels of surface contamination, changes in temperature, and the impact of contact pressure. Detailed analyses of each parameter were conducted in the subsequent sections, providing a comprehensive understanding of the factors influencing the coefficients of friction for PTFE bearings.

Material Type

To investigate the effects of different PTFE material types on an elastomeric bearing pad, specifically comparing compounds with and without glass fiber content, the study examined the performance of each material using both flat and dimpled surfaces. The computed friction coefficients listed in Table 5 for both flat and dimpled PTFE specimens indicate an increase in the friction coefficient when the material compound containing 15 percent glass fiber was utilized. The increase in the flat surface PTFE was in the range of 1 to 2 percent, while the dimpled surfaces experienced an average increase of 0.5 to 1 percent. This difference is primarily associated with the higher rate of fiber contact (and subsequent increased friction) in the flat surface compared to the lubricated dimpled surface.

Contact Surface Type

To assess the impact of PTFE surface contact type on the performance of an elastomeric bearing pad, two distinct surface configurations were investigated: flat PTFE and lubricated dimpled PTFE. Consistent with NCHRP Report 432 results, the test results, as reported in Table 5, showed a significant difference in the coefficient of friction between the two surface types. Notably, the lubricated dimpled PTFE exhibited a markedly lower coefficient of friction when compared to its flat-surfaced counterpart. This observed difference was attributed to a 25 percent decrease in surface area provided by the dimples on the PTFE surface, as well as a reduced coefficient due to the use of lubrication.

Horizontal Loading Rate

Previous research by Campbell and Kong in 1989, Stanton et al. in 1999 (as part of NCHRP Report 432), and Constantinou et al. in 1999 indicated that the coefficient of friction increases with sliding speed but eventually stabilizes at a constant value. The speed at which this stabilization occurs varies across different materials and surface finishes. For conventional unfilled PTFE and No. 8 mirror polish stainless steel, this critical speed is much higher than any speed likely to be encountered in typical bridge applications. High-speed sliding is primarily of interest in seismic isolation systems. Specifically, NCHRP Report 432 noted that friction values could be 5 to 10 times higher at seismic speeds compared to those associated with thermal expansion. Additionally, it reported that friction could rise to near-static levels if the PTFE surface remains loaded for a period of time without movement. However, this issue generally does not pose a problem in highway structures.

To investigate the effects of loading rate on the friction coefficients, Figure 33 through Figure 34 depict the apparent friction coefficient for the tests conducted on Specimens PF1 through PF4, respectively. To calculate the apparent friction coefficient, the following formula was employed:

$$\mu_{Apparent\_ST-\,Lower\ PTFE} = \frac{H_{LP}}{V} - \mu_{Apparent_{DY}-\,Upper\ PTFE} \qquad (Eq.5)$$

Equation 5. Apparent Coefficient of Friction

Where $\mu_{Apparent\_ST-Lower\ PTFE}$ and $\mu_{\ Apparent\_DY-Upper\ PTFE}$ denote the apparent static friction coefficient in the bottom and apparent dynamic friction coefficient in the top PTFE surfaces, respectively. The V term was calculated using the total vertical load, and the H_{LP} term was the total horizontal load applied by the horizontal load plate (measured via internal load cell). The term 'apparent' coefficient of friction is meant to differentiate the values derived from Equation (5) from those classically obtained through Equations (2) through (4). While Equations (2) through (4) necessitated a manual review of each test cycle, pinpointing instances of PTFE slip, Equation (5) assumed an average for the dynamic friction coefficient of the upper PTFE. This average was then subtracted from the total horizontal and vertical load ratios ($\frac{H_{LP}}{V}$) throughout the entirety of the test. This method provided a more convenient means of assessing the relative changes in the coefficient of friction over prolonged test durations without the extensive computational effort required to identify each instance of slip. Slip coefficient values for the other parametric studies were calculated using the original formulas from Equations (2) through (4).

For Specimens PF1 through PF4, lubricated unfilled dimpled PTFE was employed for the upper PTFE in the test assembly. This selection was beneficial for two primary reasons: First, it resulted in a minimal friction coefficient, ensuring that the lower PTFE was loaded earlier in the application of the horizontal load. Due to its low friction, the upper PTFE began sliding first,

thereby maintaining a constant low load while the bottom PTFE continued to resist slipping. Second, unfilled dimpled PTFE was less affected by loading cycles and loading rates, which allowed those effects to be isolated and evaluated in the bottom PTFE.

Figure 33 represents the apparent friction coefficient values for Specimens PF1 and PF2 (flat unfilled and filled), each with four sets of loading rates (1 in./min., 6 in./min., 2.5 in./min., 1 in./min.). A loading rate of 2.5 in./min. was not initially planned, so the initial test Specimen PF2 was not tested at this loading rate; however, this loading rate was later incorporated in the test plan for all subsequent specimens. Generally, results for PF2 indicated higher friction values when compared to those for PF1, and they both showed an increasing trend of higher friction values when subjected to an increase in the rate of loading.

Except in a few cases (e.g., the first twelve cycles of PF1 or the last five cycles of PF2), the rate of increase in the friction value also followed a linear to logarithmic relationship between the number of cycles and a given loading rate. Regardless of being filled or unfilled, this increasing trend in friction values with increasing number of cycles (especially at higher loading rates) suggests a potential vulnerability of flat PTFE surfaces sustaining low friction properties over time. This observation is consistent with the findings of NCHRP Report 432.

Reasons for this observation could be the heat generated at the interface of the PTFE at higher loading rates and ensuing wear of the PTFE from cyclic loading, all of which could result in micro-level changes to the PTFE surface and higher friction values. PTFE containing glass fibers appears to complicate the wear mechanism, as observed in the nonlinear behavior in Specimen PF2.

The changes in the friction value were not reversible when the loading rate was decreased. In other words, for both specimens, the friction values in the second round of cycles at a 1 in./min. loading rate were always higher than the first round of cycles at the same rate.

Figure 34 represents the apparent coefficient of friction values for Specimens PF3 and PF4 (dimpled unfilled and filled), each with four sets of loading rates (1 in./min., 6 in./min., 2.5 in./min., 1 in./min.). Similar to flat PTFE, the filled dimpled PTFE data indicated higher friction values over unfilled dimpled PTFE data. While the filled dimpled PTFE results showed some influence from exposure to more cycles, this influence on the unfilled dimpled PTFE specimen results was negligible. As expected, the friction values at higher loading rates increased for both types of dimpled PTFE specimens. Similar to the performance of the flat test specimens, changes in friction values were not reversible when the loading rate was decreased.

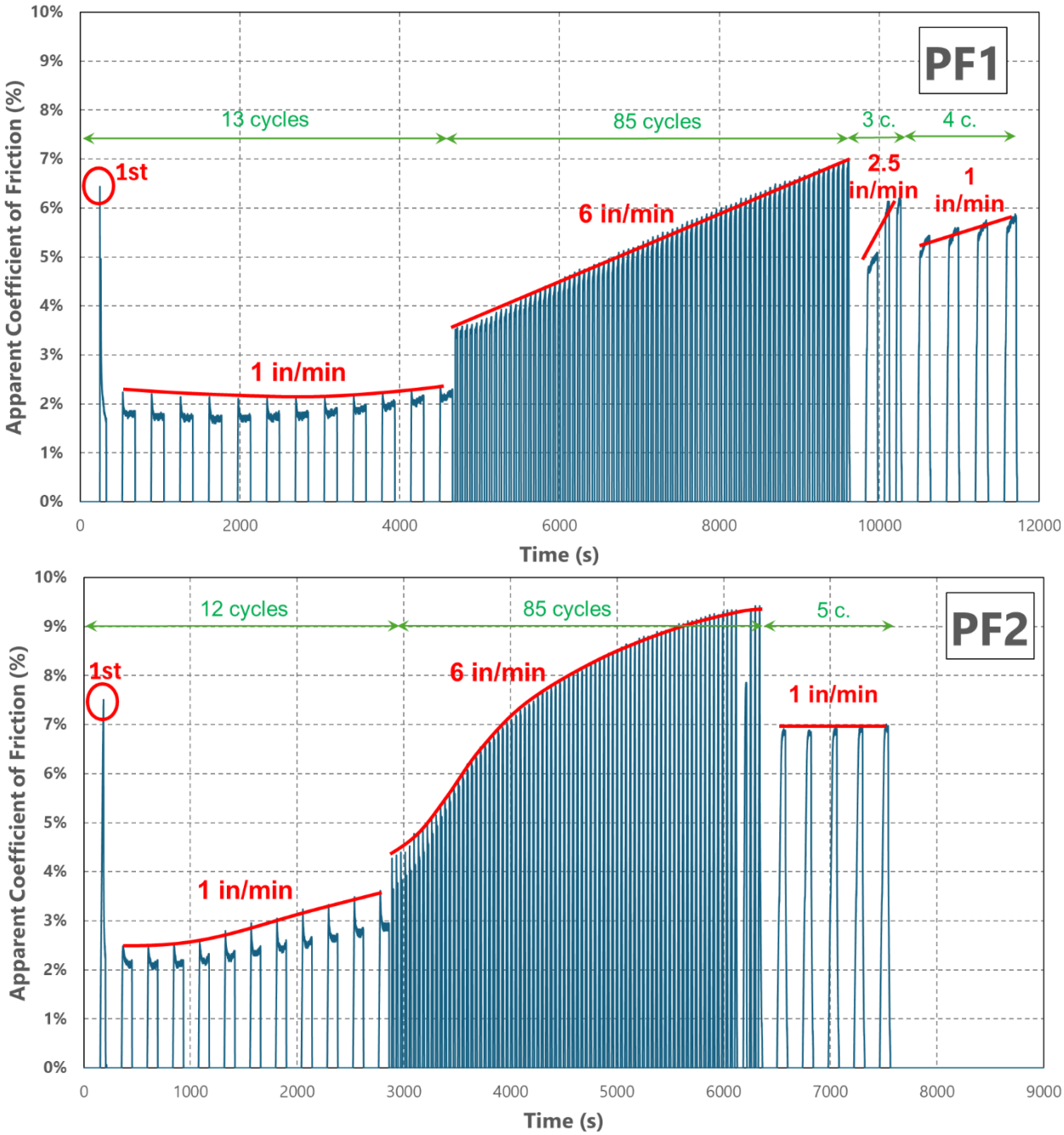

Figure 33. Line charts showing apparent coefficients of friction calculated for Specimens PF1 and PF2 (flat unfilled top, and flat filled bottom).

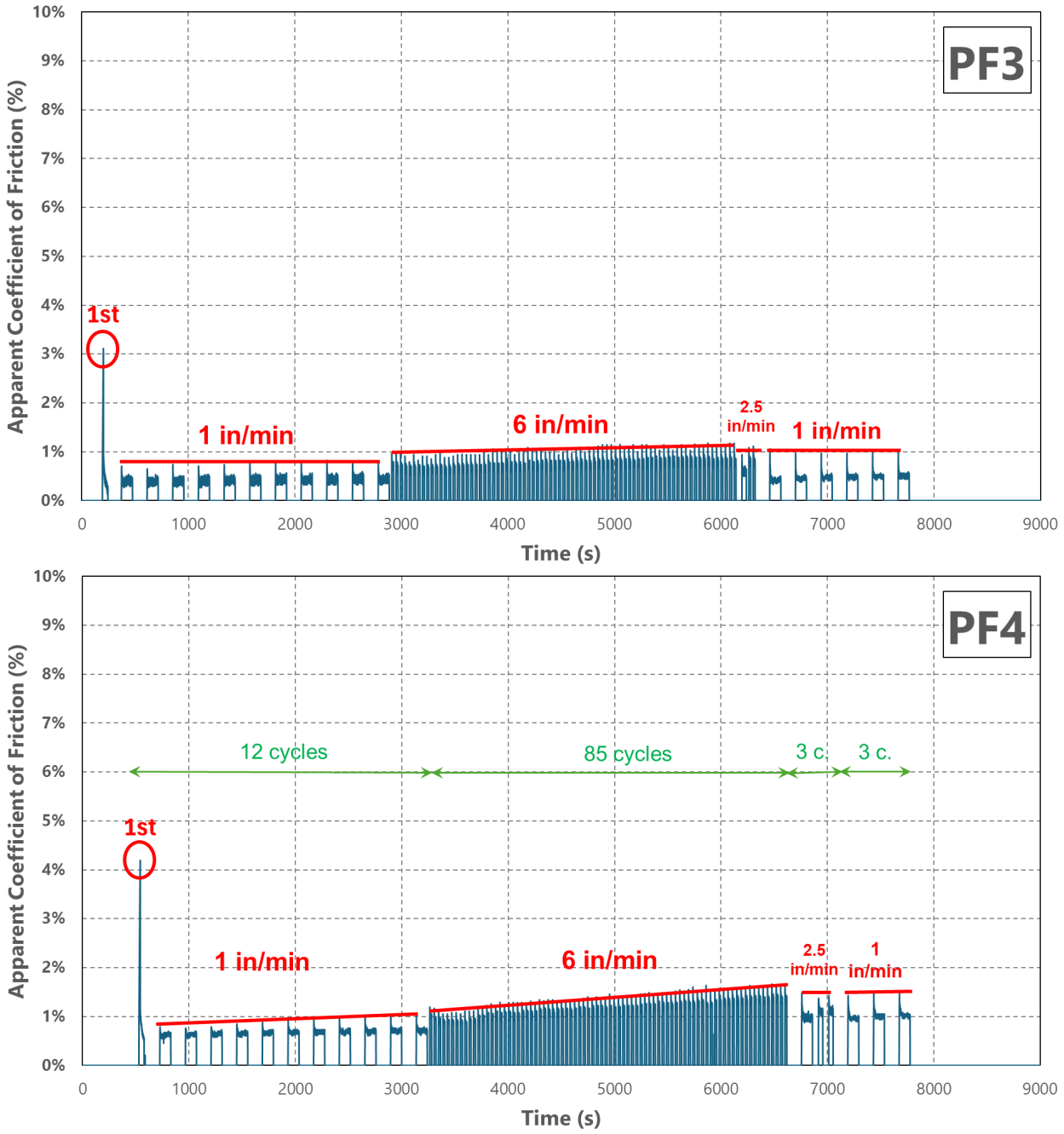

Figure 34. Line charts showing apparent coefficients of friction calculated for Specimens PF3 and PF4 (dimpled unfilled top and dimpled filled bottom).

Temperature

NCHRP Report 432 and AASHTO LRFD BDS (2020) both reported that at lower temperatures, the friction coefficient generally increases. However, for temperatures below -14 deg. F, the coefficient for woven and dry unfilled PTFE seemed to reach a plateau. In contrast, for dimpled

lubricated and filled PTFE, the coefficient of friction continued to increase even when temperatures were as low as -49 deg. F. Nonetheless, it should be noted that the data on low temperature friction and resulting wear remain scant.

For this study, experiments designed to assess the impact of temperature on an elastomeric bearing pad with an unfilled dimpled PTFE sheet were performed. The specimen underwent the standard Phase II loading protocol. The testing procedure involved subjecting the specimen to extreme cold conditions, initially placing it in a freezer at -20 deg. F for 24 hours and subsequently exposing it to dry ice at -80 deg. F for an additional 30 minutes before testing as shown in Figure 35. The temperature of the test specimen was measured at -50 deg. F when placed inside the test setup. After 55 minutes of testing, the specimen's temperature was recorded at +50 deg. F. As indicated in Table 6, the results showed that temperature had minimal influence on the performance of the elastomeric pads with unfilled dimpled PTFE. As illustrated in Figure 36, the load-displacement plot for the cold bearing demonstrated comparable behavior of the same specimen tested at 68 deg. F (room) temperature. The shear deformation in the elastomer, when tested at -13 deg. F, was minimal and comparable to that of the same specimen tested at room temperature of 68 deg. F. Despite the extremely low temperatures, the bearing pad exhibited resilience, suggesting that this specific material composition remains relatively unaffected by temperature variations within the tested range.

Table 6. Effect of temperature on the coefficient of friction

Test No.	Specimen No.	1 in./min.	2.5 in./min.
3	PF3 – room (68°F) temperature	0.9%	0.6%
10	PF3 – cold temperature	0.9%	0.9%

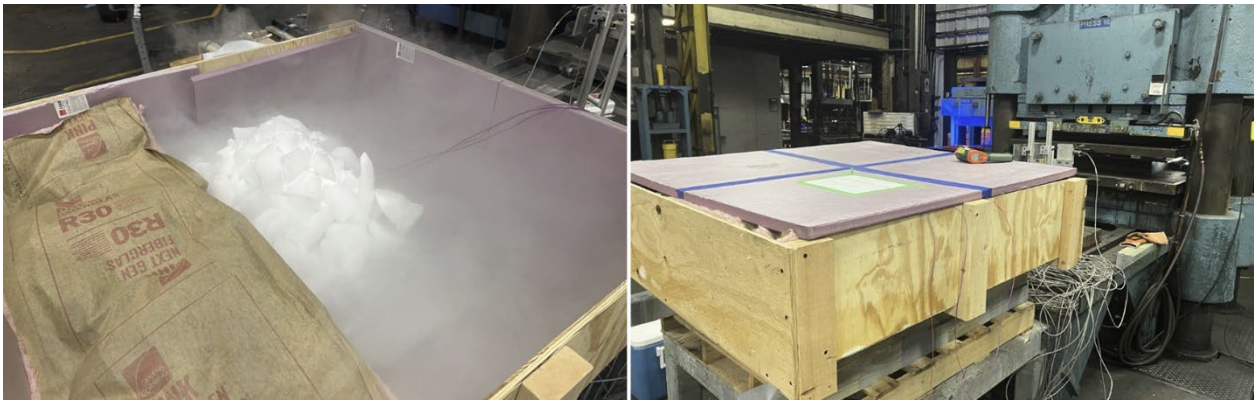

Figure 35. Photos of enclosure for cooling PTFE specimen with dry ice.

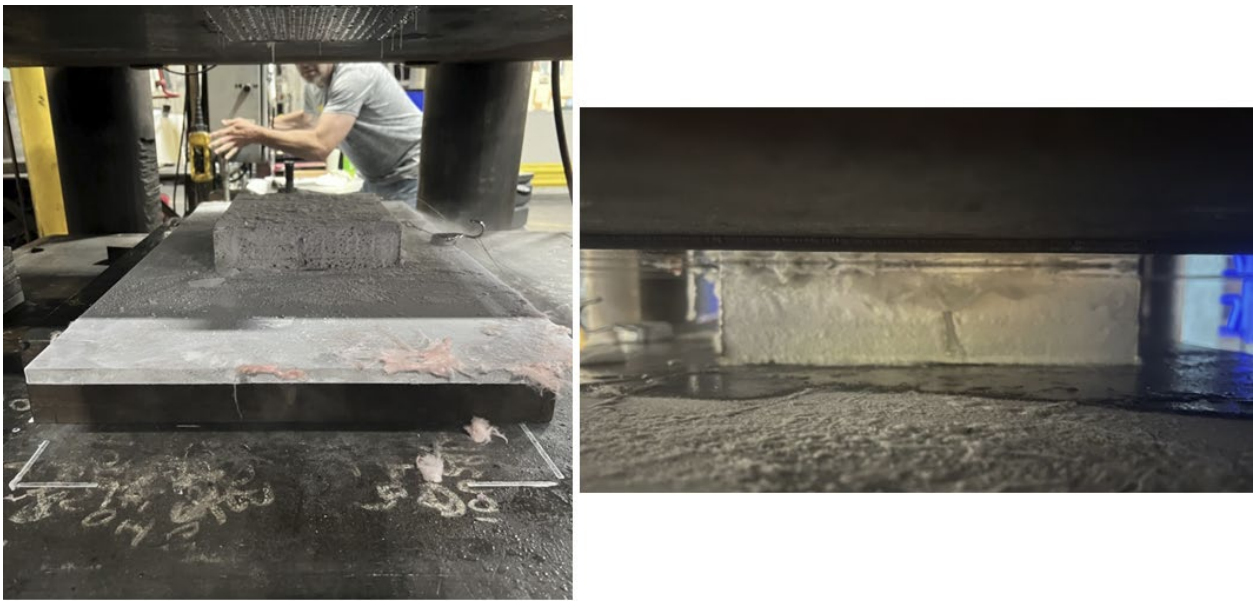

Figure 36. Photos taken of cooled PF3 specimen in the test apparatus prior to testing.

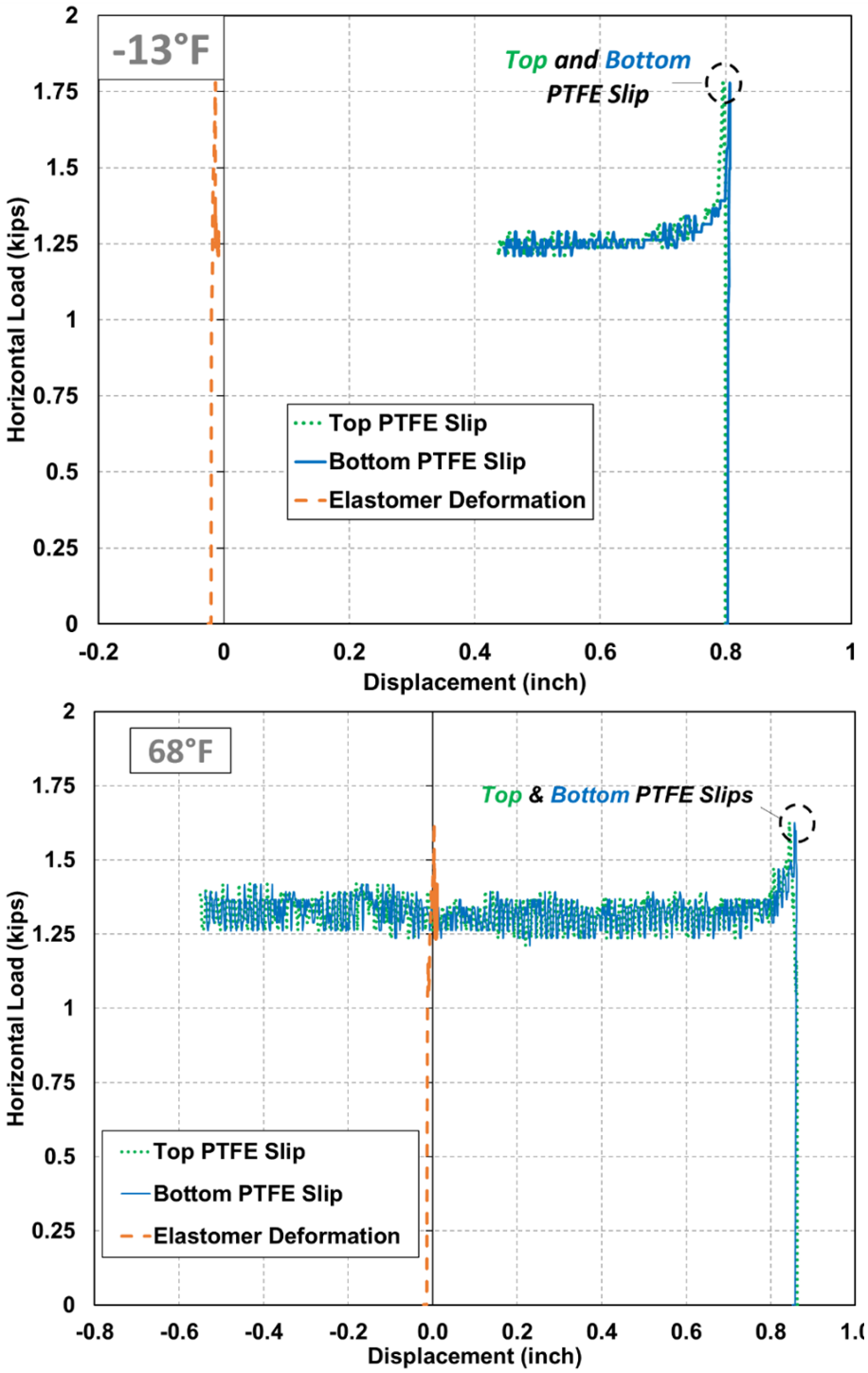

Figure 37. Line charts showing load-displacement plot of horizontal load and relative movements of top and bottom PTFE on PF3 specimen tested at room (68°F) and low temperature (-13°F).

PTFE Size

Previous studies indicated that the size of PTFE specimens had minimal effects on the coefficient of friction (Mazroi et al., 1982; Taylor, 1972; Mokha et al., 1990). To further substantiate this finding, this study explored two primary size effects: contact surface area and elastomer thickness on the performance of PTFE pads. Utilizing a single type of PTFE material with an unfilled dimpled surface, the investigation looked to isolate the effect of each factor.

In addition to Specimen PF3, which measured 9 inch x 12 inch x 1.5 inch, two additional specimens with varying contact surface areas were tested. As shown in Figure 38, these included bearings sized 13 inch x 17.5 inch x 1.5 inch (Specimen PF5) and 18 inch x 22.5 inch x 1.5 inch (Specimen PF7). Additionally, Figure 38 highlights a third bearing size, 13 inch x 17.5 inch x 3 inch (Specimen PF6), which was examined to assess the impact of elastomer thickness. All neoprene elastomers were laminated with internal steel sheets spaced at 1/2-inch intervals. All specimens featured the same unfilled dimpled PTFE configuration.

Figure 39 presents the coefficients of friction for four bearing pad types with different contact surface areas, (Specimens PF3, PF5, PF6, and PF7). The figure reveals that the friction coefficient of the first breakaways for different pads increased with increased surface area. However, the variation in the coefficient of friction between the different surface areas was approximately constant for every loading rate. Except for the first breakaway, the effects of varying surface areas were minimal for a given loading rate.

Figure 40 plots the friction coefficients for Specimens PF5 and PF6 to investigate the impact of elastomer thickness on the performance of dimpled PTFE bearing pads. Figure 41 further presents the load-displacement plot for these specimens. While both specimens shared the same contact surface area, Specimen PF5 had an elastomer thickness of 1.5 inches, whereas Specimen PF6 had a thickness of 3 inches. Notably, the level of shear deformation in the thicker 3-inch elastomer (Specimen PF6) was slightly over twice that of the thinner 1.5-inch thick elastomer (Specimen PF5) at the moment of slip. Although they displayed very close and consistent friction values across various loading rates, their first breakaway values differed markedly. To further validate this finding, an additional dataset was included in the plot, labelled as “Average PFs – 1.5 inch”. This dataset represented the mean friction values from a group of similar unfilled dimpled PTFE specimens, all with 1.5 inches of elastomer but covering a range of contact surface areas (including Specimens PF3, PF5, PF7). When contrasted with the data for Specimen PF6, which had 3 inches of elastomer, more consistent friction values were observed across different loading rates, as well as at the first breakaway. This comparison showed consistent friction values, indicating the apparent independence of friction coefficients from the elastomer thickness.

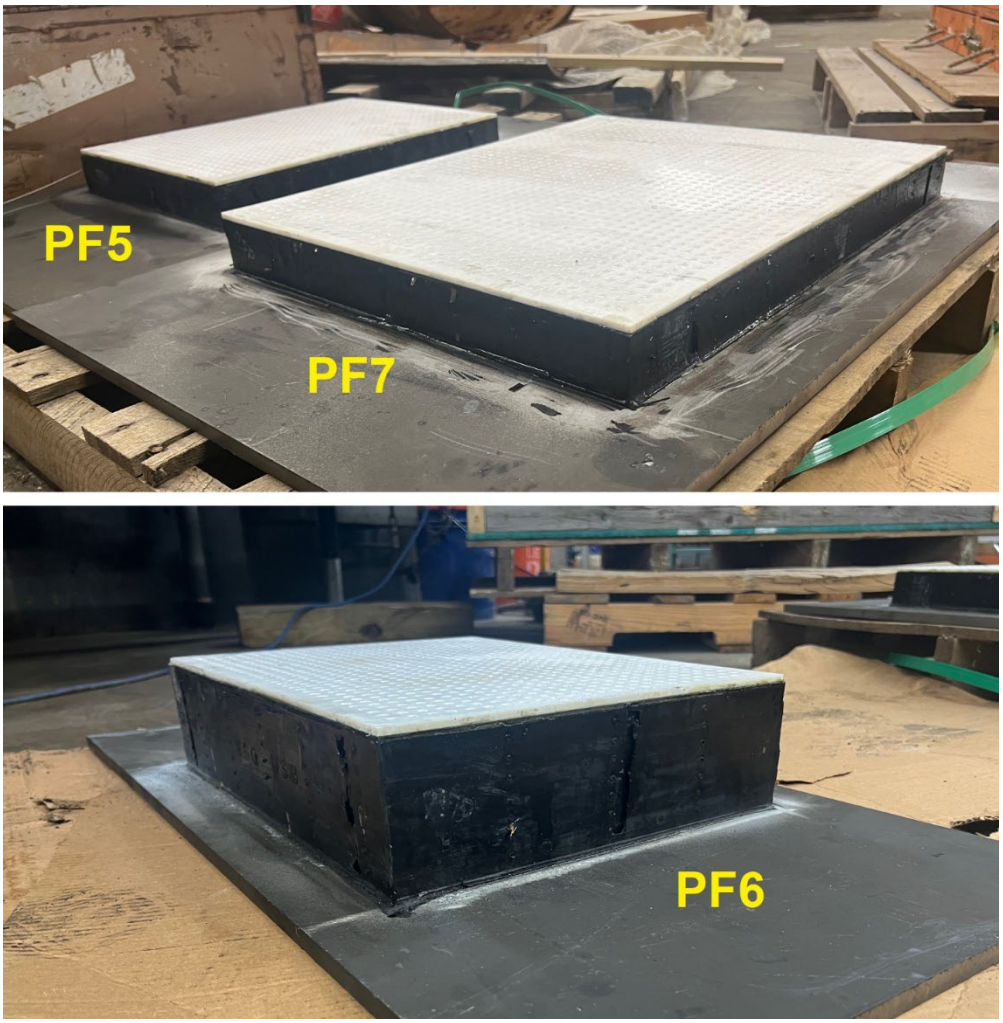

Figure 38. Photos of the additional bearing pad types tested in Phase II.

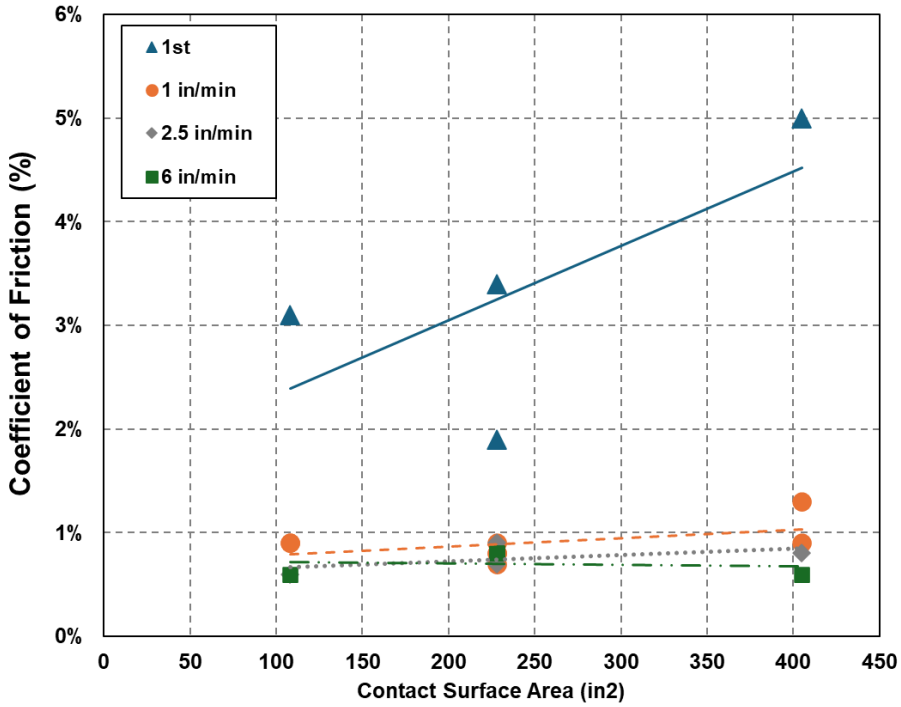

Figure 39. Line chart of summary of friction coefficients for different contact surface areas at different loading rates.

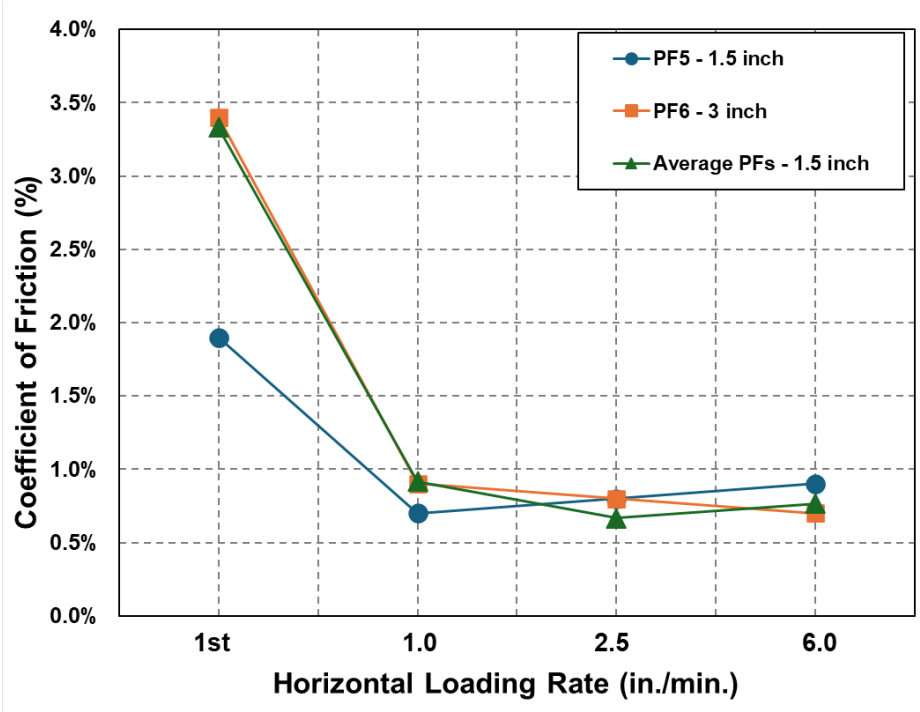

Figure 40. Line chart of summary of friction coefficients for different elastomer thicknesses at different loading rates.

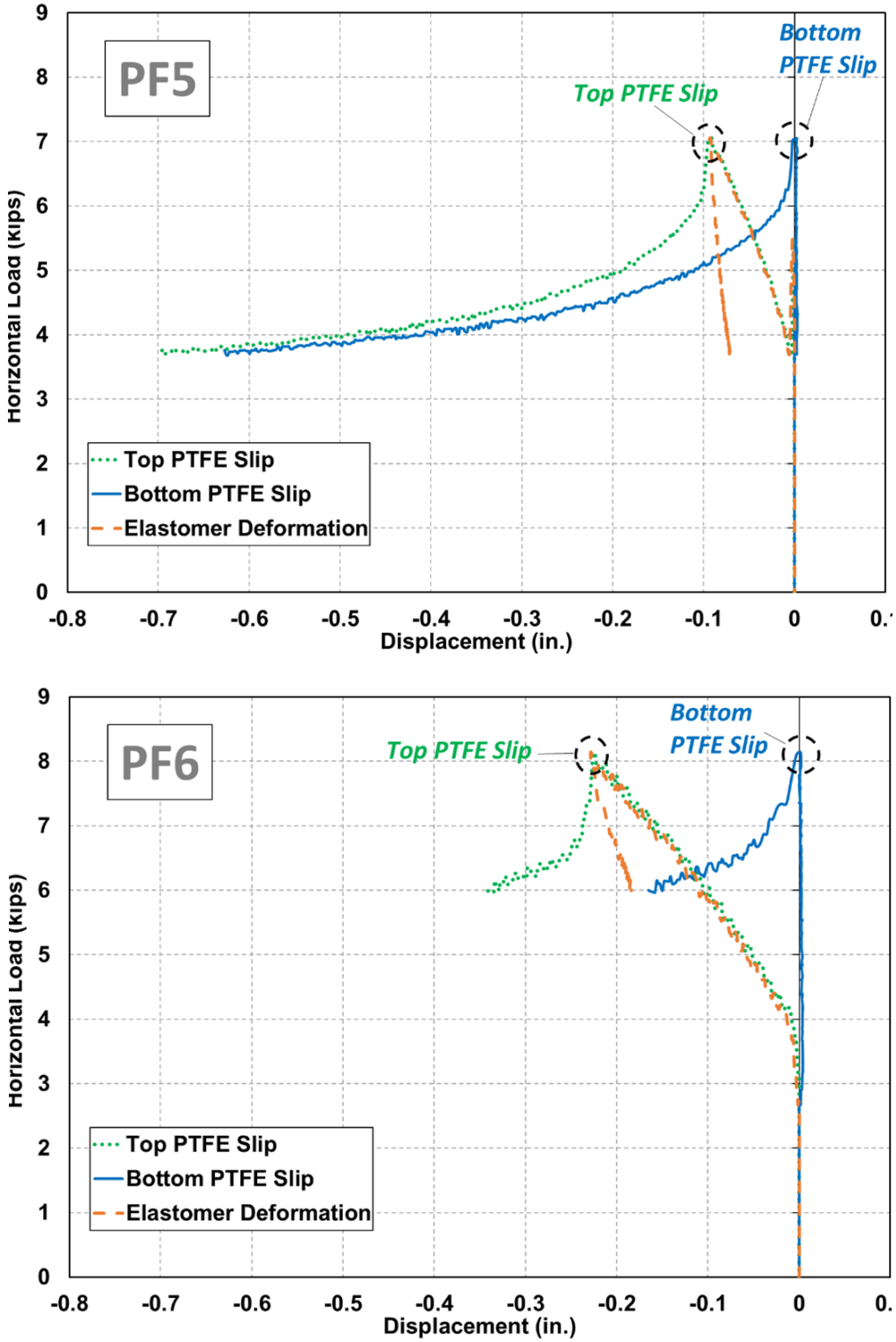

Figure 41. Line charts of load-displacement plot of horizontal load and relative movements of top and bottom PTFEs and elastomer for Specimens PF5 and PF6.

Contact Pressure

Ideally, the coefficient of friction should be independent of the applied vertical and horizontal loads and considered solely a surface-dependent characteristic. However, past literature had indicated that the friction coefficient of PTFE bearing pads could vary depending on the level of vertical force (NCHRP Report 432; Campbell and Kong 1987; Mokha et al., 1990; Mazroi et al. 1982; Taylor 1972). In particular, NCHRP Report 432 posited that the coefficient of friction is approximated to decrease linearly with increasing contact pressure below 3 ksi, and to remain constant at higher pressures. They concluded that there is a level of contact pressure (around 3 ksi) beyond which further increases do not affect the coefficient of friction. The friction values listed in the AASHTO LRFD BDS (2020) are derived from this report.

To examine the effects of vertical contact pressure on the coefficients of friction, a subset of the thirteen friction tests completed at a bearing pressure of 800 psi was also conducted at bearing pressures of 200 psi, 400 psi, and 600 psi. For this purpose, Specimen PF7, having the largest surface area, was chosen to ensure that the vertical ram could apply a sufficiently large load (exceeding the lower range of the vertical hydraulic ram) to the specimen at 200 psi vertical pressure. Figure 42 displays plots of friction coefficients for four different vertical contact pressures at various loading rates. In agreement with prior research, the coefficient of friction was found to decrease almost linearly with increasing bearing pressure at both intermediate and slow loading rates.

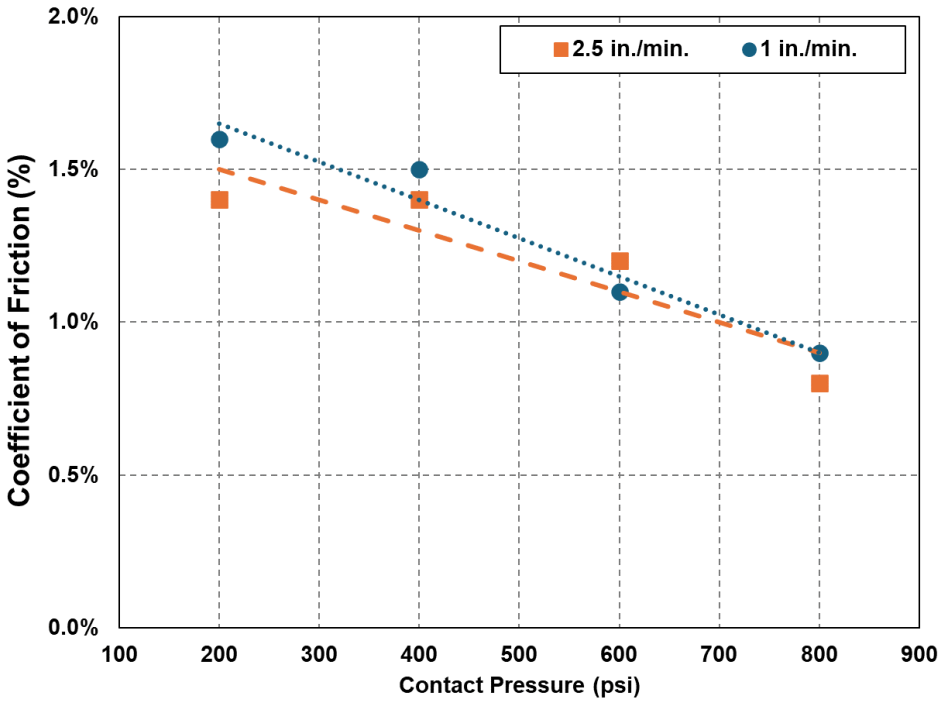

Figure 42. Line chart of summary of friction coefficients for different vertical contact pressures at two loading rates.

Surface Contamination

Utilizing dimpled PTFE pads has been demonstrated to significantly lower the slip coefficient. Nevertheless, questions regarding their longevity and durability have arisen due to potential dirt build-up and the necessity to contain the PTFE within the bearing. Contamination of the sliding interface can contribute to an increased wear rate of PTFE, resulting in a much higher friction coefficient, long-term. Taylor and Stanton (2010) concluded that for lubricated PTFE, the lubrication stops working when contaminated. Furthermore, Campbell et al. (1993) incorporated contaminants into dry and lubricated unfilled PTFE by introducing Portland cement powder. They determined that contaminating the bearings is feasible before assembly, but introducing contaminants after assembly could be difficult, yet not entirely preventable.

To conduct tests on the dimpled PTFE with contamination, the unfilled dimpled PF3 specimen was initially tested without contamination (Phase I) and subsequently contaminated and retested (Phase II). Two degrees of contamination, light and heavy, were applied to the dimpled PTFE specimen. To mimic real-world conditions, contamination with a particle size distribution, depicted in Figure 43 and determined by the document "Evaluating the Particle Size Distribution and Gross Solids Contribution of Stormwater Runoff from Ohio's Roads" published by the FHWA (Winston and Witter 2019), was sprinkled onto the PTFE surface before placing the specimen in the test apparatus. Two distinct tests were carried out to determine the effect of particle quantity on slip performance. The initial test featured a light dusting, with the particle quantity kept under two grams—this amount was chosen based on the mass of street dust on main traffic roads reported by Zhao et al. (2008). In the subsequent test, a heavier dusting of eight grams was used, while also including a few coarse sand aggregates (yet maintaining less than 1 mm maximum size aggregate (MSA)) to enhance the roughness of the sliding surface.

Figure 44 captures the images of the application of two grams of light dust to the bottom PTFE surface before testing Specimen PF3. The dust was so fine that it would not be detectable to the touch, akin to the type of fine dust that often accumulates naturally on objects. Figure 45 presents the load-displacement plots for a single friction test (half-cycle) carried out on the contaminated and clean lubrication specimens. While the uncontaminated top PTFE slipped early at a very low load, the bottom PTFE resisted slipping. As indicated by the orange curve, the elastomer deformed significantly due to the bottom PTFE's resistance to slipping, whereas the same specimen with clean lubrication showed very little deformation. From previous tests on the same specimen with clean lubrication (shown in Figure 45), the slip load was typically around 1-2 kips, whereas the contaminated specimen experienced slip at approximately 8-10 kips, resulting in an average tenfold increase in the friction coefficient (Table 7). Following the slip, the contamination still prevented the specimen from slipping freely. The plot reveals a stepped pattern with subsequent smaller slips, mainly due to the build-up of contamination and resulting resistance until each minor slip occurred. Following the initial breakaway, each 40-micron increment of relative movement between the PTFE and the sliding mirror plate resulted in a build-up of contaminants. This accumulation consequently induced minor slippages,

appearing as stepwise slips depicted in Figure 45. The disturbances in load/displacement caused by these incremental slips of the bottom PTFE were then transferred to the top PTFE, resulting in stepwise slips observed at the top PTFE. In the end, Figure 46 displays examples of the PTFE and its imprints on the sliding mirror plates after the friction test concluded. After cleaning the contaminated lubricant from the mirror plate, both the imprint and physical scratches were visible, though less discernible by touch. The test results demonstrated that even minimal quantities of particle contamination adversely affect the performance of dimpled PTFE elastomeric bearing pads.

In the subsequent contamination test, a heavier dusting that included coarser sand aggregates (less than 1 mm MSA) was applied to the same PF3 specimen. Figure 47 captures the images of the application of eight grams of dust to the bottom PTFE of Specimen PF3 before testing. Once the test began, as illustrated in Figure 48, no slip occurred, and the horizontal load continued to rise, deforming the bearing to at least 75 percent of its elastomer thickness. The test was halted without any slip being recorded at the heavily contaminated bottom PTFE. Figure 49 shows the PTFE and its imprints on the sliding mirror plates post-test. The imprints on the mirror plate clearly showed that no slip occurred at that interface. After the removal of the contaminated lubricant from the mirror plate, the imprint and physical dents became visible and could be felt by touch.

Table 7. Effect of surface contamination on the coefficient of friction

Test No.	Specimen No.	1 in./min.	2.5 in./min.
3	PF3 –no dust	0.9%	0.6%
8	PF3 –light dust	7.8%	7.6%

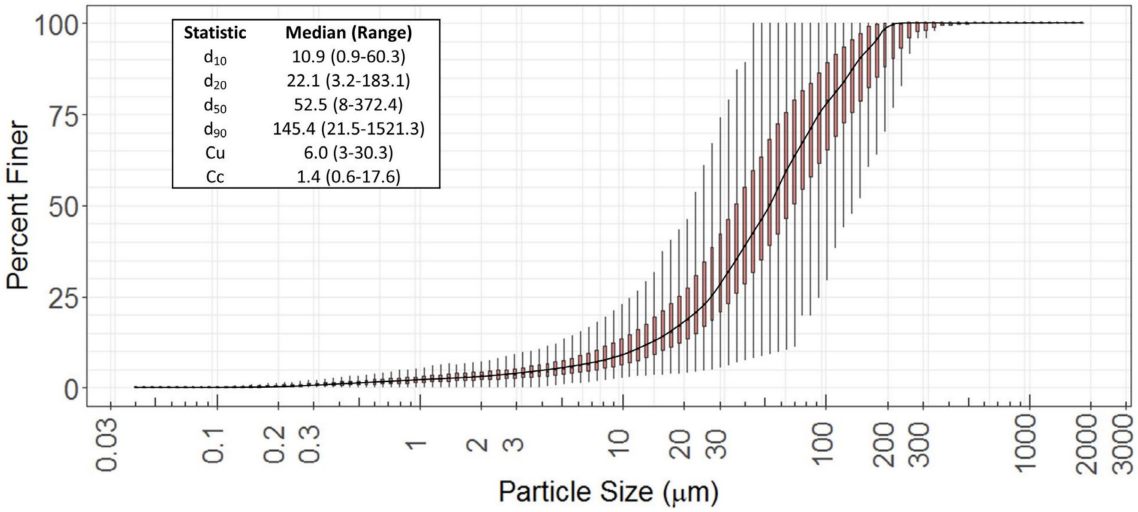

Figure 43. Line chart of aggregate particle size distribution, adopted from FHWA (Winston and Witter 2019).

Figure 44. Pre-test photographs of PF3 specimen sprinkled with a light amount of dust prior to testing.

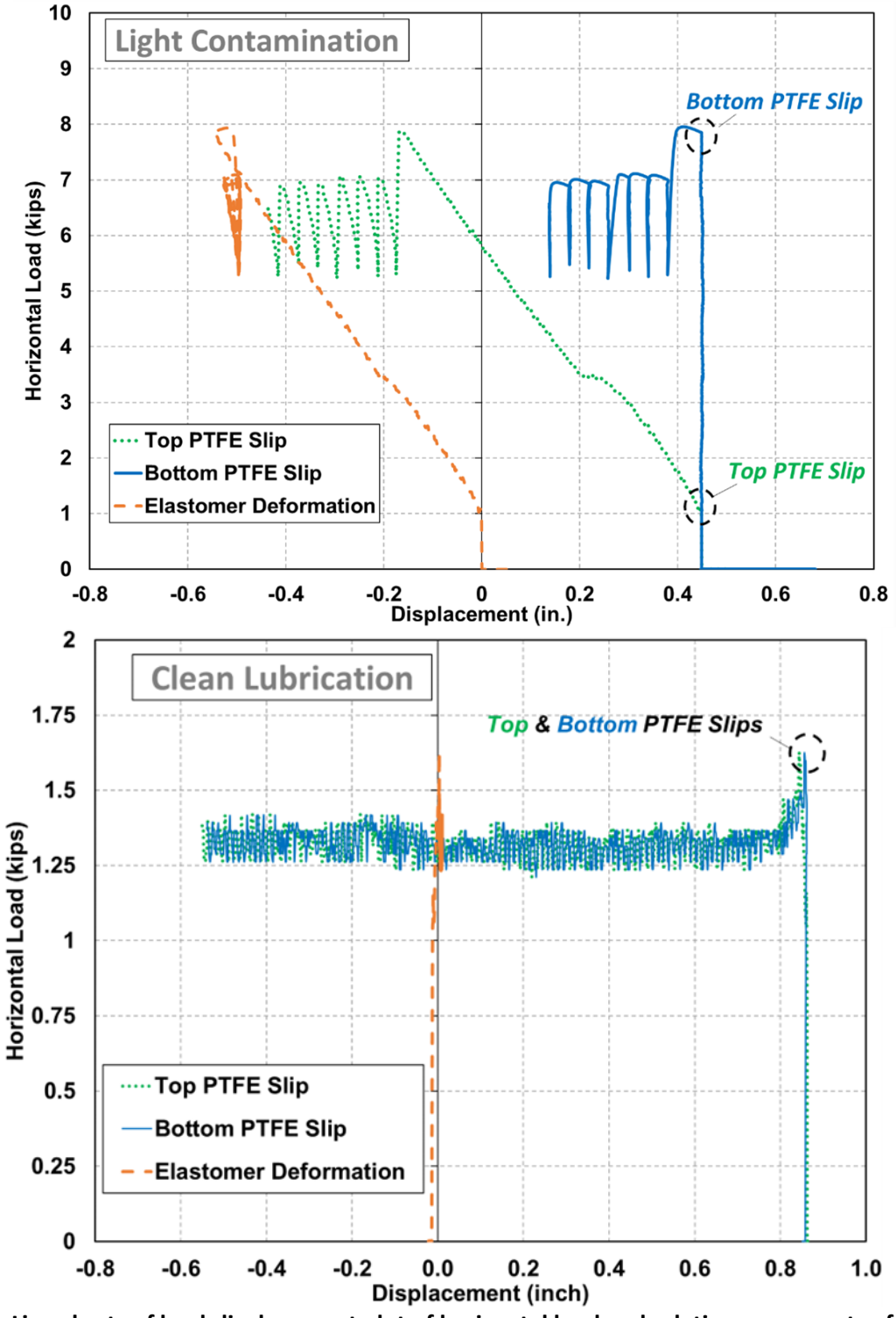

Figure 45. Line charts of load-displacement plot of horizontal load and relative movements of top and bottom PTFEs for Specimen PF3 sprinkled with a light amount of dust and Specimen PF3 with clean lubrication.

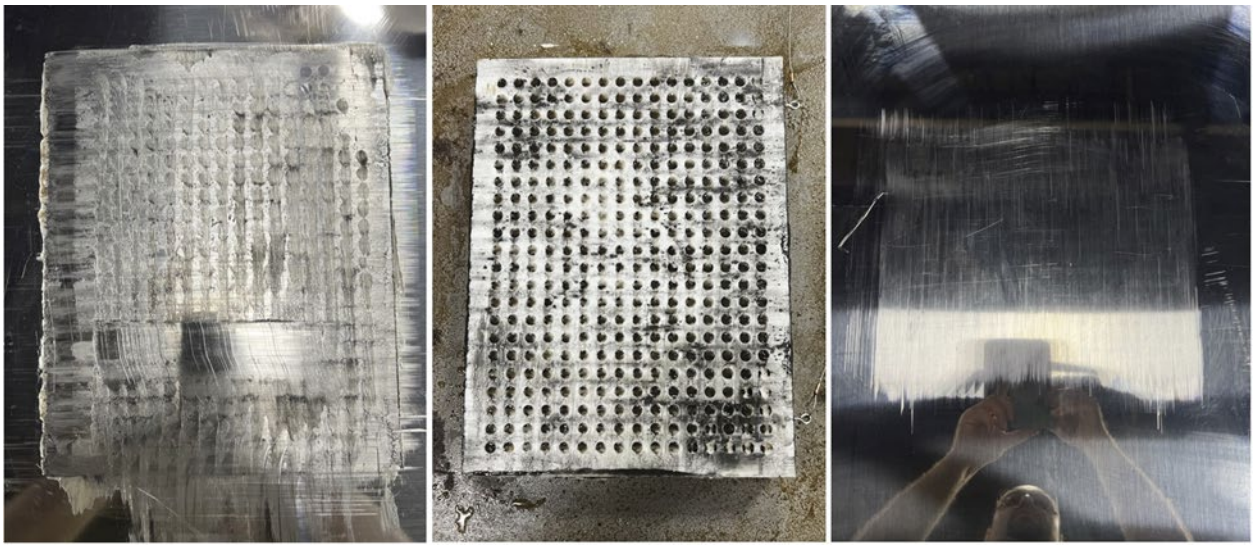

Figure 46. Photos of imprints of lubrication from Specimen PF3 on the mirror plate (left), PTFE (middle) and visible scratches (right) when a light amount of dust contamination was applied.

Figure 47. Pre-test photographs of Specimen PF3 sprinkled with a heavy level of dust prior to testing.

Figure 48. Photo of deflected Specimen PF3 sprinkled with a heavy level of dust. The elastomer is coated in white, and the top portion of the photo shows the reflection of the elastomer on the mirror plate.

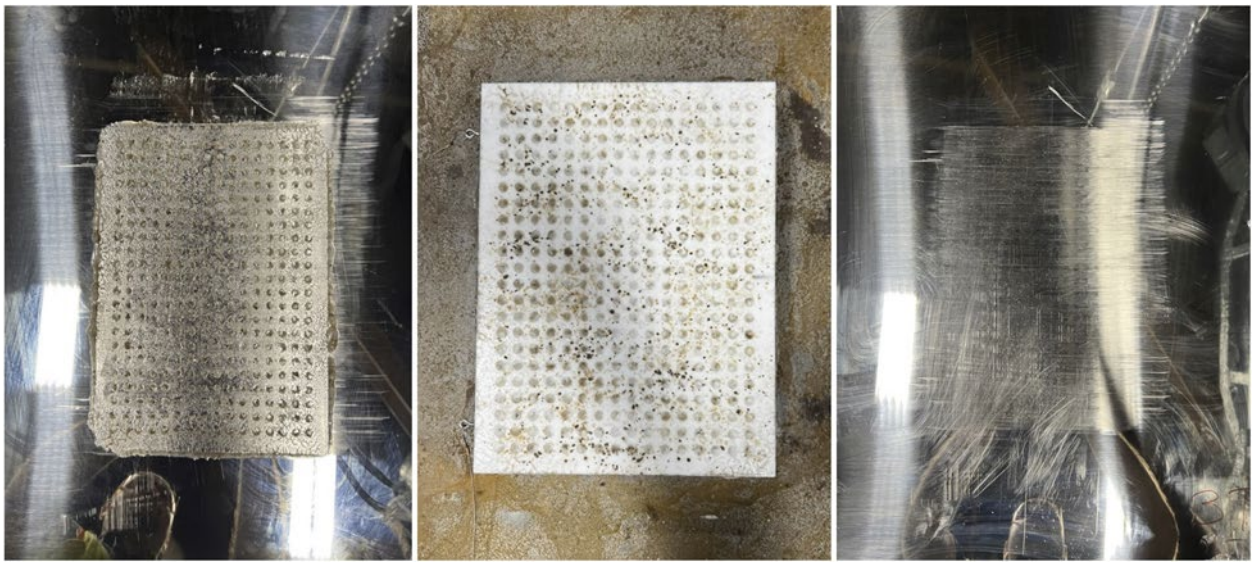

Figure 49. Photos of imprints from lubrication of Specimen PF3 on the mirror plate (left), PTFE (middle) and observable scratches (right) from the application of a heavy level of dust contamination.

Comparison of Results with NCHRP Report 432

The research by Stanton and Campbell (1999) for NCHRP Project 10-20 (Report 432) established the foundational AASHTO LRFD design coefficients of friction for various PTFE types. They conducted ninety-nine tests on 3-inch diameter PTFE specimens involving filled, unfilled, and woven types. This study examined the effects of multiple factors, such as temperatures (ranging

from 68 deg. F to -48 deg. F), rapid sliding speeds (2.5 and 25 in./min.), high contact pressures (from 500 psi to 6000 psi), and rough mating surfaces (mirror and annealed). Results for dimpled lubricated PTFE in the NCHRP report were drawn from an earlier study by Campbell and Kong (1989), which utilized an identical test setup and specimen size, and investigated similar attributes. This section compares experimental test results (labeled "NCHRP") with the current experimental findings (labeled "WJE").

Specimens

In the NCHRP study, PTFE specimens measured 3 inches in diameter (with a 7.1 square inch surface area) and varied in thickness depending on the type (thickness of 0.25 inch for dimpled and 0.125 inch for flat PTFE). These PTFE specimens were recessed 0.08 inches into a steel backing plate with no elastomeric pad bonded during the tests. Dimpled PTFE specimens had a dimple diameter of 0.3 inches and depth of 0.08 inches, with a dimpled-to-total surface area ratio of about 22 percent. Specimens were preloaded for twelve hours prior to testing.

Specimens in the current study were rectangular, with a surface area of 108 square inches and thicknesses of 0.125 inch for dimpled and 0.1875 inches for flat PTFE. Each PTFE specimen was bonded to a steel plate, then vulcanized to an elastomeric bearing. In the case of dimpled PTFE, the dimpled-to-total surface area ratio was about 25 percent. Recommended by AASHTO LRFD BCS (2017), specimens were preloaded for one hour prior to testing.

Comparison of Results

Table 8 lists the first breakaway and subsequent coefficients of friction at an 800 psi contact surface pressure and a room temperature of 68 deg. F. Due to the NCHRP results being primarily graphical and not tabular, the values in Table 8 are subject to some estimation error. Results pertinent to the current study's test range were selected from the extensive testing in the NCHRP report and are displayed in Table 8, interpolated for 800 psi. A loading rate of 2.5 in./min., the lowest used by NCHRP, was compared to the range of 1 to 6 in./min. in the WJE study.

In alignment with findings from NCHRP Report 432, unfilled dimpled lubricated PTFE and filled flat PTFE presented the lowest and highest coefficients of friction, respectively. The friction coefficients for unfilled flat and filled dimpled PTFE fell in between, comparable to the extremes presented by the other two PTFE types.

Each of the NCHRP tests was conducted at only one loading rate. Conversely, the WJE tests incorporated a range of rates within a single set, where changes in the loading rate had noticeable residual effects, especially in flat specimens. Three sets of friction coefficients were determined for WJE tests: the initial breakaway, the maximum of the first four cycles post-breakaway, and the maximum coefficient of friction (excluding the first breakaway), typically occurring at the end of 98 cycles when the rate decreased from 6 to 2.5 in./min., as depicted in Figure 33 and Figure 34. Similarly, NCHRP tests extracted three sets of coefficients: the initial

breakaway, the maximum of the first four cycles post-breakaway, and the peak coefficient of friction (excluding the first breakaway), usually observed in the mid-to-end range of 300-500 cycles.

Upon review, the coefficients of friction for unfilled flat PTFE determined by WJE were found to be primarily in line with those reported by NCHRP. The increased values noted by NCHRP were mainly ascribed to the higher loading rates at which their tests were conducted. For instance, the measured first breakaway and the maximum of the first four cycles were 6.4 percent and 2.3 percent at a loading rate of 1 in./min., respectively, in the current WJE tests, while comparable results from NCHRP stood at 8 percent and 3.7 percent at 2.5 in./min. As anticipated, WJE's highest coefficient of friction at 6 in./min. was 5.9 percent which surpassed the peak value of 5.6 percent reported by NCHRP at 2.5 in./min. after 300 cycles. Despite errors inherent in adapting and extrapolating data from the NCHRP report to align with WJE's test configuration, such as contact pressure and specimen size, consistency between the results was maintained. Furthermore, both NCHRP and WJE findings revealed an upward trend in the coefficient of friction with the number of cycles, particularly as the loading rate increased, surpassing the initial breakaway, as illustrated in Figure 50 (adopted from NCHRP) and Figure 33 (WJE).

In the case of filled flat PTFE with 15 percent fiberglass, NCHRP's reported values were nearly 2.4 times that of the values reported in the current tests. For example, NCHRP's highest value at 2.5 in./min. after 500 cycles (19 percent) was approximately 2.3 times WJE’s maximum value (8.1 percent) at 6 in./min. after 98 cycles. The comparison depicted in Figure 51 demonstrated that both sets of data exhibited the same trend concerning the first breakaway and the subsequent four cycles, as well as the maximum values. Nonetheless, this significant variance between WJE and NCHRP coefficients of friction cannot be solely attributed to the increased loading rate utilized by NCHRP; other factors, such as variations in material type, loading configuration, PTFE finish, and specimen size and configuration, could also have played a role. Notably, the preloading duration, or dwell time, along with the specimen configuration—particularly whether it included an elastomer—appeared to play a crucial role in the variance noted.

An increase in the initial coefficient of friction was recorded when loads on the PTFE were sustained for several hours prior to the initiation of sliding (Campbell and Kong 1987; 1989). This increase was noted to escalate rapidly until approximately 24 hours of continuous loading, at which point it plateaued. Hence, the duration of load application prior to sliding was determined to be a variable influencing the coefficient of friction. The difference in preloading times, with NCHRP imposing a 12-hour period compared to WJE's 1-hour duration, is likely to have contributed to some level of discrepancy between the two sets of test results. Furthermore, NCHRP tests involved PTFE specimens bonded to steel without use of an elastomeric pad, whereas the WJE tests incorporated specimens with bonded elastomers. As previously mentioned, the elastomer's flexibility could in some way serve to reduce the

coefficient of friction when compared to the unyielding behavior of PTFE directly adhered to steel.

Furthermore, the NCHRP findings, highlighted in Figure 52, indicated that the coefficient of friction continued to increase with the number of cycles, exceeding the first breakaway—a trend not typically observed with other PTFE types like dimpled specimens. This pattern was also seen in the WJE tests (see Figure 33), where the behavior of flat filled PTFE changed non-linearly with both the loading rate and the number of cycles, surpassing the initial breakaway values.

Regarding dimpled lubricated PTFE, the values in the NCHRP report, which were derived from Campbell and Kong (1989)'s work, depicted a lower initial breakaway than what was observed in the WJE test results (Figure 53). This disparity could partially be explained by the effects of specimen size, the distribution of the dimples, and the type and amount of lubricant applied. Nevertheless, the subsequent coefficients of friction were found to be within the same range and followed the predicted pattern, with the NCHRP values slightly higher than those reported by WJE, predominantly due to the difference in loading rates.

Neither NCHRP nor Campbell and Kong (1989) provided test results for filled dimpled PTFE specimens, therefore no comparison could be made.

Table 8. Comparative analysis of current study results with those from NCHRP Report 432

PTFE Type	WJE First Breakaway	WJE 1 in./min. (first 4 cycles)	WJE 6 in./min. (max – 98 cycles)	NCHRP First Breakaway	NCHRP 2.5 in./min. (first 4 cycles)	NCHRP 2.5 in./min. (max: 300-500 cycle)
Unfilled-Flat	6.4%	2.3%	5.9%	8%	3.7%	5.6%
Filled (15%)-Flat	7.5%	3.3%	8.1%	18%	8.0%	19.0%
Unfilled-Dimpled	3.1%	0.9%	0.9%	1.8%	1.2%	1.4%
Filled-Dimpled	4.3%	0.9%	1.3%	-	-	-

Source: NCHRP Report 432; Campbell and Kong (1989).

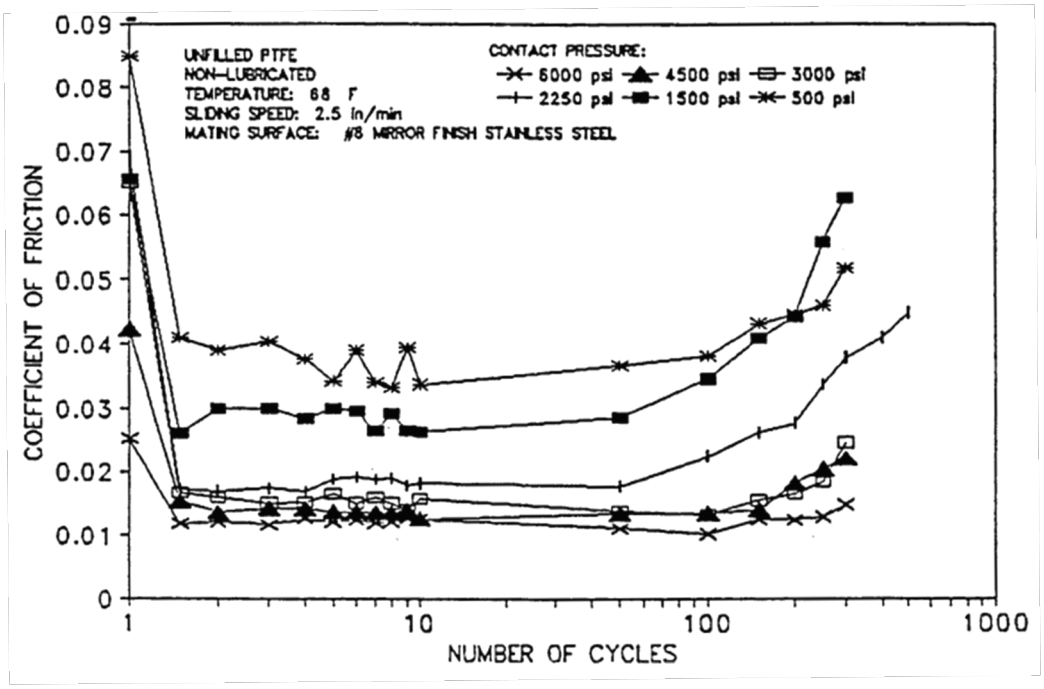

Figure 50. Line chart of coefficient of friction versus number of cycles for unfilled PTFE tested at 68°F and a sliding speed of 2.5 in./min. (NCHRP Report 432: Figure C-7).

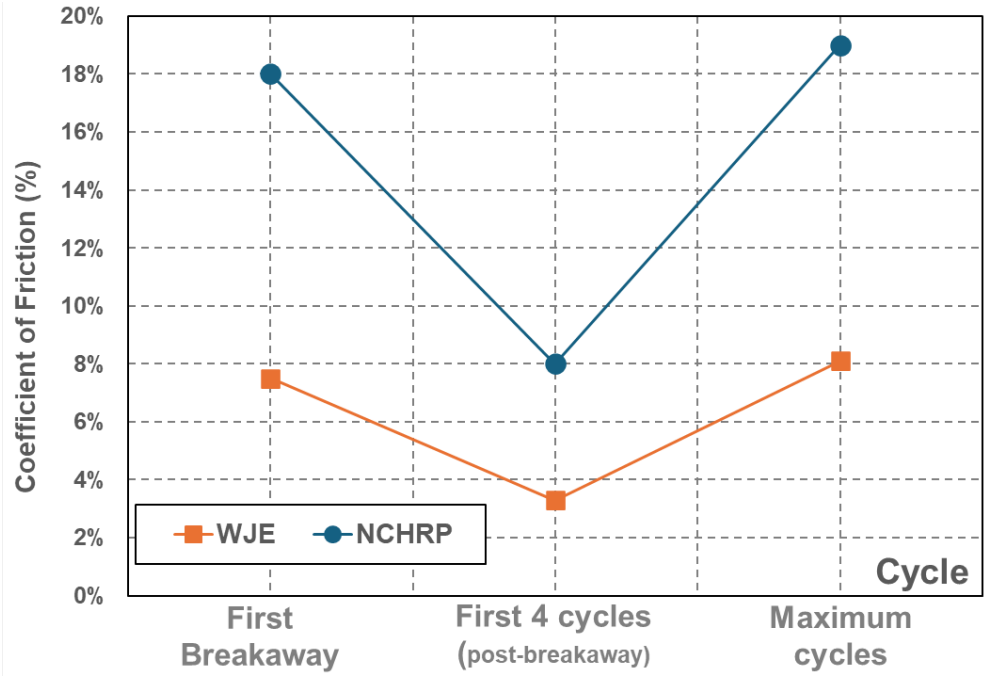

Figure 51. Line chart of comparative analysis of filled flat PTFE results with those from NCHRP Report 432.

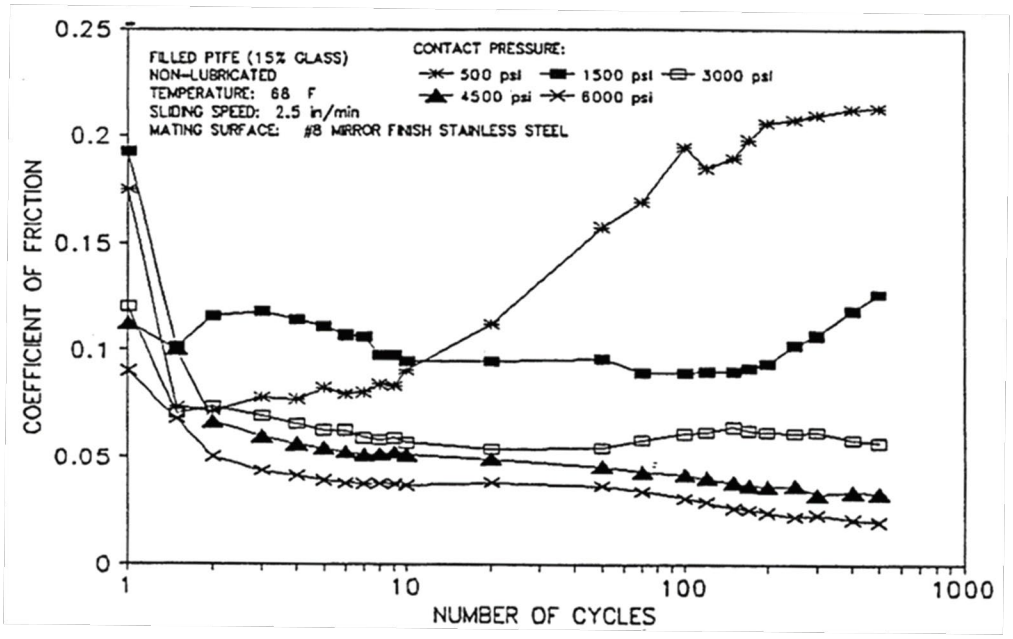

Figure 52. Line chart of coefficient of friction versus number of cycles for filled PTFE (15% glass fiber) tested at 68°F and a sliding speed of 2.5 in./min. (NCHRP Report 432: Figure C-10).

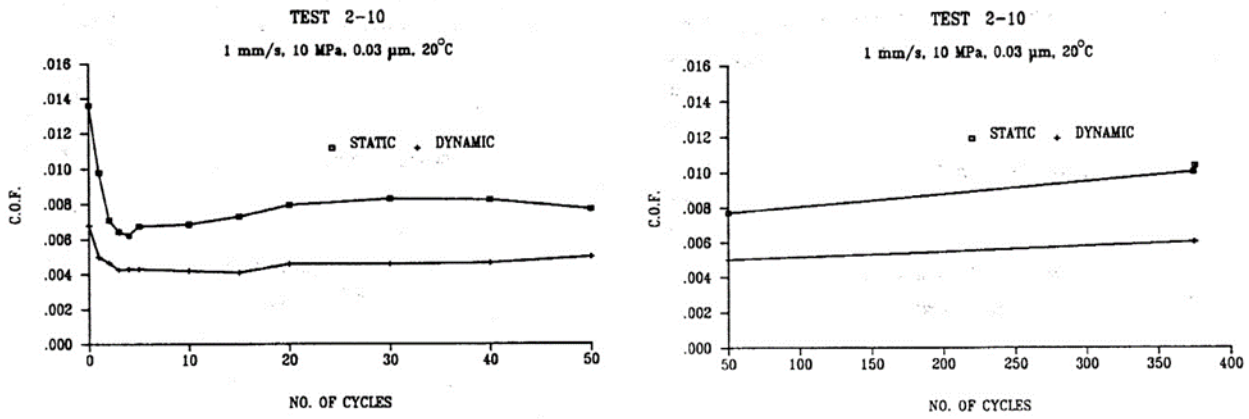

Figure 53. Line chart of coefficient of friction versus number of cycles for unfilled lubricated PTFE tested at 68°F and a sliding speed of 2.5 in./min. (Campbell and Kong (1989): Appendix A).

Chapter 7. Design and Construction Recommendations

This section offers recommendations for the adoption of design coefficients of friction, which have been determined through the evaluation of results from the current experimental program, as well as through the review of outcomes from pivotal past studies. The impact of surface contamination will also be addressed, with the provision of mitigation strategies for the construction and maintenance of PTFE bearings. Additionally, the need for further studies to thoroughly understand the performance of such bearings under varying conditions will be discussed.

Proposed Updated Design Coefficients of Friction

The analysis and comparison of results from the four primary tested PTFE specimens with those from NCHRP Report 432 revealed good agreement for unfilled flat and dimpled PTFEs. However, the comparison also showed a substantial difference—up to twice the coefficient—for flat filled PTFE specimens in the WJE tests.

NCHRP published two tables: one summarizing the test outcomes, and another proposing design values that were later adopted by AASHTO LRFD BDS (2020). The values in the summarized test results were predominantly taken as the maximum measured over the test duration, excluding the initial breakaway. This approach was applied on all test results except for unfilled PTFE, where a factor of two was applied to account for observed discrepancies between repeated tests.

It was recognized by NCHRP that the friction coefficient for the initial breakaway is consistently higher in the first cycle of movement than in subsequent cycles. Thus, the design friction coefficient was conservatively estimated to be lower than the measurement of the initial breakaway cycle. This approach was rationalized since the initial breakaway value, if used for design, would lead to higher design loads, and is unlikely to occur because the first sliding movement is anticipated during construction, before the bridge carries its full load. Furthermore, they noted that experimental evidence indicated a rise in the coefficient of friction towards its initial breakaway value if it remained loaded without movement for some time, although it never quite reaches the original breakaway value.

However, intermittent slip-stick movement is quite likely for bridge bearings, with the increased coefficient invariably larger than their later cyclic test outcomes. To accommodate such variability, the following criteria were utilized to derive design coefficients of friction as the greater of:

- The maximum measured coefficient during the first two cycles, excluding breakaway, with an allowance of 0 to 2 percent for discrepancies between laboratory and field conditions.
- Half the value of the initial breakaway.

The allowance of 0 to 2 percent compensated for the differences between laboratory and field conditions, particularly significant for materials like dimpled lubricated PTFE, prone to contamination. The design values were proposed based on a loading speed of 2.5 in./min., according to NCHRP. They posited that using half the initial breakaway value ensures that even if full breakaway friction occurs under full load, the built-in safety factors in the design would prevent bridge component failure, although higher-than-normal service level stresses might be experienced.

NCHRP observed a notable increase in the coefficient of friction at low temperatures; however, test results at these conditions, particularly at lower stress levels, were scarce. Some reported values for design were based on a theoretical model, and they recommended further testing to accurately establish these design values.

NCHRP further established certain criteria as the quality measures of new PTFE specimens during construction. Quality measures for PTFE specimens were defined as the acceptable coefficient of friction based on the maximum coefficient measured during 100 cycles of cyclic slip following the first complete cycle. This coefficient should not exceed the design coefficient of friction specified in the design standards. The initial static breakaway coefficient for the first cycle must not be greater than twice the rated coefficient.

It is well-established that the coefficient of friction for PTFE escalates with sliding speed. NCHRP utilized 2.5 and 25 in./min. for their primary testing speeds and the results at 2.5 in./min. were adopted by AASHTO as their design values. Referencing work by Campbell and Kong (1987; 1989), 2.5 in./min. was deemed representative of the speeds experienced by bridge bearings. Another reference indicated that the coefficient of friction rises with speed up to approximately 2400 in./min. before stabilizing (Campbell and Kong 1989). Compared to thermal movements (0.0007 in./min. for a reinforced concrete bridge deck and 0.005 in./min. for an unsurfaced steel box structure), which are negligible, traffic effects on bridges generates significantly higher sliding speeds, such as 47 in./min. for steel railway bridges and 165 in./min. for steel/concrete composite bridges. These speeds suggest that only static friction should be considered for design. However, field measurements showed that under earthquake conditions, bearings might experience speeds as high as 900 in./min., well below the 2400 in./min. threshold where friction plateaus. Given the date of these references (primarily between 1950 and 1960), potential inaccuracies in field measurements, and traffic pattern changes, further field measurements are required to ascertain actual sliding speeds for different bridge types.

Table 9 listed the coefficients of friction at 800 psi vertical pressure based on the design values from AASHTO LRFD BDS (2020), MoDOT EPG (2024), the results from NCHRP, and the WJE results table. For the MoDOT design values, the values for flat PTFE, sourced from the TR202204 Request for Proposal document (Request for Proposal TR202204), were not found elsewhere. It was noted in this document that the values for dimpled PTFE were derived from the AASHTO LRFD BDS design coefficients of friction. In the associated columns for NCHRP in

Table 9, the initial four columns originated from Table 8, and the last column represented their suggested values for coefficients of friction using only their test data. The values in the “Suggested Value” had not yet utilized the design criteria previously mentioned to propose the design value, which is referred to in a separate column under "AASHTO LRFD". The section pertaining to the WJE study uses three columns reproduced from Table 8. The final column lists the calculated design values using the aforementioned design criteria. It should be noted that all calculations involved a certain degree of estimation error due to manual extraction of data from the printed plots. Ultimately, the last column, referred to as “Proposed Updated Design” corresponds to the adoption of updated design coefficients of friction.

Unfilled Flat PTFE

For unfilled flat PTFE, discrepancies were observed in the test results from NCHRP; thus, the NCHRP design criteria were not used to derive the final design value. The coefficient of friction, based on the NCHRP test data, was calculated to be twice the friction value at the 100th cycle, resulting in a friction coefficient of 7.4 percent. This value was used in the AASHTO LRFD BDS design value without additional safety factors. Estimating the design value based on WJE test results using the abovementioned design criteria, the larger value was chosen between a) half of the breakaway, which was 3.2 percent, and b) the maximum of the first four cycles subsequent to the first breakaway plus an allowance of 0-2 percent. With a midpoint variability of 1 percent—considering flat PTFE is less prone to contamination—the proposed value would be 3.3 percent. Consequently, the larger value 3.3 percent was used. However, if a more conservative approach is adopted then the average of two components—the first four cycles at 1 in./min. and the maximum at 98 cycles and 6 in/min. (adding 2 percent to account for the highest rate of contamination effects), yields a proposed design value of 6.1 percent.

As indicated in Table 9, using the abovementioned design criteria, the coefficient of friction based on WJE's results suggests a range between 3.3 percent and 6.1 percent, which is below the initial breakaway. This range is below the value suggested by AASHTO LRFD BDS (2020) and MoDOT EPG (2024). Due to the consistency in results between NCHRP and WJE discussed in the previous sections, the recommended design coefficient of friction for unfilled flat PTFE is 6 percent.

Filled Flat PTFE

In the case of flat filled PTFE, a review of the results suggested that NCHRP did not completely adhere to the established criteria for deriving design values, primarily because the coefficients of friction exceeded the first breakaway value. Figure 52 showed that for 500 psi, the coefficient of friction continually increased with the number of cycles. NCHRP seemed to utilize the maximum coefficient of friction as the representative value in their test results table. The interpolated value for 800 psi was approximately 18.6 percent, later adjusted by 1 percent to account for contamination effects.

If a similar approach for WJE's test results is followed by taking the maximum measured coefficient of friction—even at the higher rate of 6 in/min—and adding 2 percent for contamination effects, a friction coefficient of 10.1 percent is calculated. This results in a range of coefficients of between 7.5 percent for first breakaway and the measured 10.1 percent value. Given the unresolved discrepancies between the WJE and NCHRP results, further testing is deemed necessary before an additional reduction below 10.1 percent is recommended. Thus, the proposed design friction coefficient for filled flat PTFE is 10 percent.

Unfilled Dimpled PTFE

For the dimpled unfilled lubricated specimens, the NCHRP recommended design value used the larger of a) half the initial breakaway, recorded at 0.9 percent, and b) the maximum of the first four cycles following the initial breakaway with an additional allowance of 0-2 percent for uncertainties. When a 2 percent increase for contamination effects was included, a design value of 3.2 percent was calculated (greater than the 0.9 percent). However, AASHTO apparently increased that value to 3.4 percent at a contact pressure of 800 psi. A note in the TR202204 Request for Proposal document indicated that MoDOT's reported value for unfilled dimpled PTFE, which was 3.4 percent at 800 psi, were based on the AASHTO LRFD BDS design friction coefficient.

Applying the NCHRP design criteria to the WJE test results using the greater of a) half the initial breakaway, at 1.6 percent (rounded up), and b) the maximum of the first four cycles following the initial breakaway plus 0-2 percent for uncertainties, produced a design value for unfilled dimpled PTFE of 2.9 percent. This value is below the initial breakaway value of 3.1 percent as well as the AASHTO LRFD BDS design value. Considering the consistency between the findings previously discussed, and acknowledging that the coefficient of friction was not significantly affected by either the number of cycles or the loading rate, a design value for unfilled dimpled PTFE of 3 percent is proposed.

Filled Dimpled PTFE

Neither NCHRP nor Campbell and Kong (1989) provided test results for filled dimpled PTFE, hence no design values were proposed by either entity. Nonetheless, it was important to consider the impact of fiberglass in the dimpled PTFE, which could not simply be inferred from the values for unfilled dimpled PTFE. This is particularly pertinent if lubricant gradually erodes, exposing dry dimpled PTFE to the mirror plate, where the presence of fiberglass could increase the coefficient of friction similarly to the difference observed between flat filled and unfilled PTFE.

To estimate the design value for filled dimpled PTFE based on WJE test results, the larger of a) half the initial breakaway, at 2.2 percent, and b) the maximum of the first four cycles following the initial breakaway plus 0-2 percent for uncertainties, was selected. Using 2 percent as the added uncertainty for contamination effects, yielded a coefficient of friction value of 2.9 percent. Adopting a more conservative approach by considering the maximum coefficient of

friction measured at 6 inches per minute, the design values increases to 3.3 percent. Both results fall below the initial breakaway value of 4.3 percent and is nearly equal to the AASHTO LRFD BDS design value of 3.4 percent for unfilled dimpled PTFE. Based on a noticeable reduction in slip resistance over the current AASHTO design value of 7.4 percent, a design value for filled dimpled PTFE of 4 percent is proposed, although further analysis is deemed necessary to explore the slight dependency of the friction coefficient on the number of cycles.

Various Contact Pressures

In Chapter 6, it was demonstrated that the coefficient of friction increases as vertical contact pressure decreases. Figure 54 illustrates the relationship between the coefficient of friction (calculated at 2.5 in./min) and contact pressure, using data from both NCHRP (AASHTO's design values) and WJE's experimental tests across various PTFE types. Depending on the trend observed for each PTFE type, either linear or polynomial curves were fitted to the datasets. For dimpled lubricated PTFE specimens, two curves were developed: one from NCHRP's report and another from WJE's current experimental tests. To interpolate the design coefficient of friction values, the curve from the WJE datasets with a steeper slope was used, resulting in a slightly higher coefficient of friction as a conservative safety factor. Table 10 summarizes the interpolated design coefficient of friction ranging from 200 psi to 1000 psi. Due to the uncertainty associated with deriving the coefficients of friction through interpolation, the updated design values have been rounded to the nearest percent integer.

Contamination

For dimpled PTFE, the proposed design coefficients of friction for both unfilled and filled types accounted for a 2 percent increase in slip resistance due to contamination. However, current test results and those by Long (1969) indicated that even light dust contamination could cause an 8-10 fold increase, amounting to a 10 percent or higher rise in friction values. A heavier level of contamination even prevented PTFE from sliding altogether. If such variability is considered in the design values, they would rise substantially, defeating the purpose of using PTFE to reduce friction and the load transferred from the superstructure to the substructure. Therefore, it is important to ensure that the design, construction, and maintenance of such bearings recognize the effects of contamination on bearing performance and substructure loading.

Table 9. Proposed updated design coefficients of friction at 800 psi vertical pressure

PTFE Types	**NCHRP** First Breakaway	**NCHRP** 2.5 in./min. (first 4 cycles)	**NCHRP** 2.5 in./min. (max.)	**NCHRP** Suggested Value	**AASHTO LRFD**	**MoDOT** First Breakaway	**MoDOT** Sub. Breakaway	**WJE** First Breakaway	**WJE** 1 in./min. (first 4 cycles)	**WJE** 6 in./min. (max – 98 cycles)	**WJE** AASHTO's Design Criteria	**Proposed Updated Design**
Unfilled- Flat	8.0%	3.7%	5.6%	7.4%	7.4%	12.0%	6.0%	6.4%	2.3%	5.9%	3.3%-6.1%	**6%**
Filled (15%)- Flat	18.0%	8.0%	19.0%	18.6%	19.8%	-	-	7.5%	3.3%	8.1%	7.5%-10.1%	**10%**
Unfilled- Dimpled	1.8%	1.2%	1.4%	0.9%	3.4%	3.4%	3.4%	3.1%	0.9%	0.9%	2.9%	**3%**
Filled- Dimpled	-	-	-	-	7.4%	-	-	4.3%	0.9%	1.3%	2.9%-3.3%	**4%**

Table 10. Proposed updated design coefficients of friction at various vertical pressures

PTFE Types	**Proposed Updated Design**				
	200 psi	**400 psi**	**600 psi**	**800 psi**	**1000 psi**
Unfilled- Flat	7%	7%	6%	6%	6%
Filled (15%)- Flat	20%	16%	13%	10 %	8%
Unfilled- Dimpled	4%	3%	3%	3%	3%
Filled- Dimpled	5%	4%	4%	4%	4%

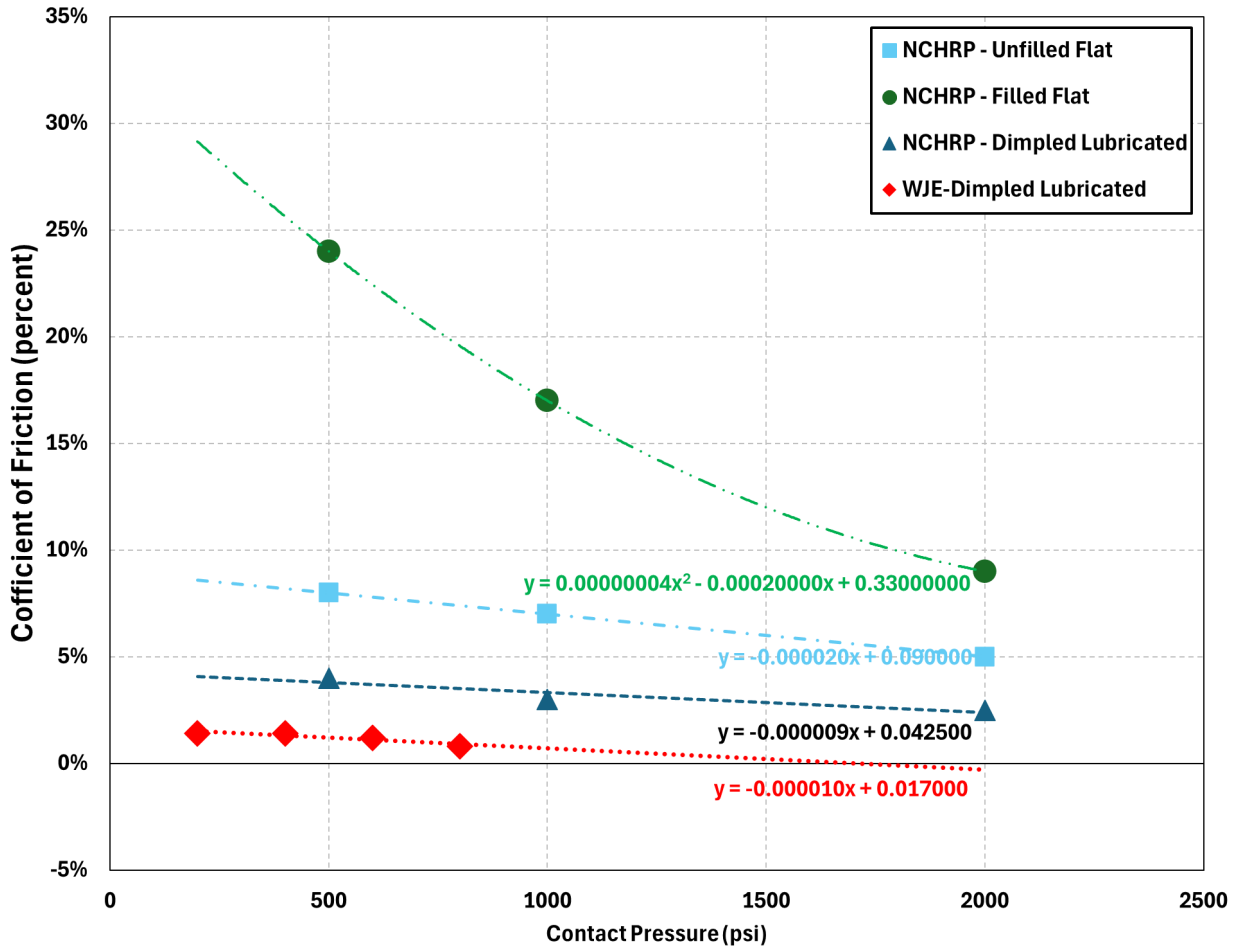

Figure 54. Line chart of summary of friction coefficients for different vertical contact pressures at 2.5 in./min. loading rates based on results from WJE tests as well as NCHRP/AASHTO design values.

Construction Methods to Prevent Surface Contamination

No specific mandate by any DOT was found that requires the protection of PTFE elastomeric bearing pads from surface contamination. Industry consensus holds that the contact surface of PTFE and stainless steel is shielded from contaminants by the pressure applied on the bearing. Various departments of transportation often include standard details for PTFE elastomeric bearing pads in their specifications. The details include side retainers, which are primarily designed for wind/earthquake load transfer, which could add some protection from accumulating dust. These protective measures, whether intentionally or inadvertently aimed at safeguarding the PTFE surface, can act as proactive steps to enhance the longevity and performance of PTFE elastomeric bearing pads; however, previous research quantifying the effectiveness of different PTFE protection details was not found. In our literature review, no additional protective measures for the PTFE and stainless-steel contact surfaces were identified.

Based on this research, the performance of PTFE elastomeric bearing pads depends on the cleanliness of the PTFE and stainless-steel contact surfaces. Incorporating a side retainer or a similar enclosure system into the PTFE elastomeric bearing may help prolong its service life. There are also various other methods to protect these surfaces, such as a protective shroud, a designed enclosure system, or the geometry of the surrounding abutment/pier. In a 1986 publication from Germany, as an example, airborne contamination of the lubricant was mitigated by equipping the bearing with skirts or bellows, as depicted in Figure 55 (Kauschke and Baigent 1986). Each of these protective methods could be beneficial in preventing the infiltration of contaminants to the contact surface, but additional long-term studies have not been conducted to evaluate their effectiveness.

The results from testing light contamination levels (two grams) on the PTFE bearing clearly demonstrated its susceptibility to performance degradation. The application of heavier contamination (eight grams) further confirmed this vulnerability. Although this study classified eight grams (over 9 inch×12 inch) of dust as heavy contamination, in real-world conditions where a bearing undergoes millions of movement cycles over its lifecycle spanning 25-50 years, the accumulation of dust could be considerably greater. Despite optimal construction quality and appropriate protective measures, the infiltration of dust over the course of the bridge/bearing lifecycle is inevitable. Our preliminary observations have identified several potential sources through which dust could infiltrate the interface of PTFE:

a. Airborne dust could gradually mix with the exposed lubricant on the mirror plate and eventually penetrate the interface.
b. In bearings subjected to low vertical pressures, dust may infiltrate the interface during thermal movements, particularly when vertical loads are temporarily alleviated by moving live loads across the bridge.
c. Large, short-duration fluctuations in vertical loads, often accompanying significant lateral deformations of the bearings, can facilitate further dust infiltration.
d. While dimples in the PTFE are designed to restore lubrication, this lubrication can gradually wash away, altering the behavior of lubricated PTFE to mimic that of non-lubricated PTFE.
e. Poor-quality construction, especially during the placement of girders over bearings, can significantly increase the rate of contamination on PTFE.

Lubrication is typically applied to PTFE bearings during the installation of the girders, which emphasizes the importance of maintaining clean PTFE surfaces and girder underside mirror plates during construction. This aspect may be ignored by contractors, particularly amid the challenges of setting girders during construction. From the time lubricant is applied to the PTFE surface until the girder is fully seated on the bearing, contamination can easily be introduced, especially as construction activities tend to raise dust levels in the environment. The time taken to place girders is a crucial period for maintaining PTFE cleanliness. Without proper supervision and erection procedures identifying the need for cleanliness, ensuring PTFE surfaces remain uncontaminated remains problematic.

An additional concern arises in service if the steel surface adjacent to the PTFE becomes contaminated before the PTFE elastomeric pad starts to slip. Over time, the cyclical slipping of the PTFE elastomeric can incorporate this contamination into the lubricant.

Over time, cyclic loading is likely to reduce the depth of the dimples, thereby wearing away the lubricant. According to AASHTO LRFD BDS, if the dimples lack lubricant, they tend to flatten out, transforming the surface to resemble that of unfilled PTFE.

Moreover, a recurring issue with contaminants entering the area of a PTFE elastomeric bearing is due to the location of bridge joints typically above the bearings. A bridge joint allows water and debris to infiltrate the areas where PTFE elastomeric bearing pads are positioned below. Figure 56 shows a bearing under a bridge joint exposed to water infiltration and debris accumulation. Regular inspection and cleaning of the adjacent surfaces near the PTFE material should be performed to prevent dust and debris buildup. Integrating preventive maintenance protocols into infrastructure management practices is crucial to ensure the longevity and optimal performance of PTFE bearing systems in various operational environments.

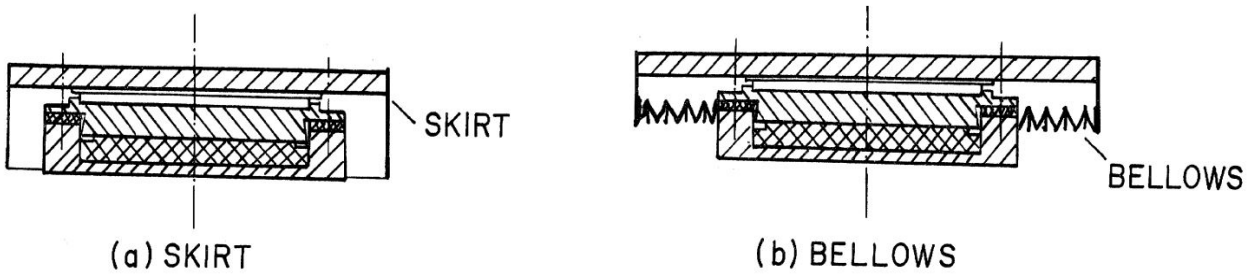

Figure 55. Image of drawings of protection of sliding surfaces (Kauschke and Baigent 1986).

Figure 56. Photo of a pot bearing below a bridge joint with moist concrete that identifies water infiltration occurred (orange arrows) and debris accumulation (blue arrow). An elastomeric bearing may be placed in a similar environment.

Additional Proposed Research

Dependence on multiple parameters for the performance of PTFE bearing pads was demonstrated, with some significant parameters investigated in this study. Despite a limited test program, an evaluation was conducted to determine the impact of these parameters on PTFE bearing performance. This section outlines a summary of further research that could help further define these effects on slip coefficients.

Loading Cycles

It was established that the coefficient of friction is generally correlated with the total accumulated movement, equating to the number of cycles, particularly for flat PTFE specimens. For lubricated dimpled PTFE specimens, a lesser dependence was noted in laboratory tests; however, extended testing with higher load cycles is warranted to verify this observation. Material examinations using microscopy are also necessary to comprehend PTFE wear over extended cycling and travel histories. Prior to experimental trials, additional numerical analysis should be conducted to further define the relationship between the coefficient of friction and total sliding length/cycles.

Despite the results showing considerably lower friction values for lubricated unfilled dimpled PTFE surfaces with minimal cycle dependence, a thorough investigation is advised to evaluate

the sensitivity and reliability under varied conditions of these surfaces as they affect the coefficient of friction, such as inconsistent lubrication and exposure to repetitive cycles.

Due to the correlation between the number of cycles (travel length) and sliding speed on the coefficient of friction, future tests should examine different scenarios involving varying travel lengths and speeds.

Loading Rate

Previous literature studies have determined an increase in the coefficient of friction with speed until approximately 2400 in./min. before plateauing. Traffic on bridges, significantly faster than thermal movements, can generate higher sliding speeds. These speeds suggest that only static friction should be considered for design. Additional field measurements are needed to confirm actual sliding speeds for various bridge types and loading situations, including temperature, traffic, and seismic impacts. Once suitable loading rates are determined, further laboratory testing can be used to assess each PTFE material type's performance under these rates.

Temperature

Temperature effects on PTFE bearing performance may be a factor; however, to what extent has not been fully determined. The NCHRP Report 432's extensive experimental work on low-temperature impacts was beneficial yet acknowledged the limitations of their data. Current low-temperature design provisions are based on extrapolated test results and theoretical models. More experiments are needed to solidify design data for low temperatures and decide if low-temperature certification or quality control tests are necessary for ensuring satisfactory performance in extreme conditions.

Although the current study incorporated low-temperature testing, it is important to examine the behavior of larger PTFE bearings at reduced temperatures within controlled environments that simulate bridge applications.

Surface Contamination

Contamination has a significant effect on bearing performance, especially for dimpled PTFE. Additional laboratory studies to develop and assess the effectiveness of protective enclosures are needed. Long-term trials are also needed to evaluate such enclosures in preventing dust ingress into bearing contact surfaces. The effects of deicing chemicals and their influence on lubricated dimpled PTFEs should also be studied.

Contact Pressure

The recognized decrease in the coefficient of friction with increased contact pressure prompts the need to test a broader pressure range alongside other variables to discern PTFE performance under varying pressures.

Other Attributes

Factors not addressed in this study—eccentric loading, creep, surface roughness, PTFE attachment to the backing plate/elastomer, and wear—all influence PTFE bearing performance. Addressing these through additional experimental work could be valuable in establishing design parameters for PTFE bearings.

Further laboratory experiments paralleling NCHRP's setup are recommended to eliminate the influences of preloading and elastomeric flexibility, thereby isolating and accurately comparing these effects on PTFE material types.

Chapter 8. Summary and Recommendations

WJE was retained to conduct an experimental program to investigate and verify key PTFE bearing performance criteria so that adjustments in PTFE bearing design procedures could be made, if needed, to improve the efficiency in designing substructure elements. The purposes of this investigation were to obtain data to assist MoDOT with establishing design values for their standard Type N PTFE bearings when distributing forces for substructure design. The secondary objective was to assess whether the dimpled lubricated PTFE bearing pads are an effective alternate over the flat PTFE, and if affirmative, what should be added to the specifications to address the concerns with contamination.

In this study, seven standard Type N PTFE bearing specimens, commonly utilized by MoDOT, were tested. These included four different PTFE types: unfilled flat, filled flat, unfilled dimpled, and filled dimpled. A testing matrix featuring thirteen tests, each involving sixteen to over a hundred cycles, was executed using an apparatus that allowed simultaneous application of vertical and horizontal loads to a test pad. This experimental program was conducted in two phases: the first aimed to isolate the effects of PTFE material type (filled or unfilled) and surface type (flat or dimpled), while the second phase focused on additional parameters such as size, contact pressure, loading rate, and surface contamination.

The experimental results, in terms of the coefficient of friction, were then compared with findings from the NCHRP Project 10-20 (Report 432), which later informed the bearing design coefficients of friction in the AASHTO LRFD BDS. Consequently, updated coefficients of friction were proposed for the PTFE types included in this investigation. Furthermore, strategies for design, field construction, and maintenance were discussed to mitigate surface contamination impacts on lubricated dimpled PTFE.

The following provide a summary of conclusions and recommendations concerning the coefficient of friction in the design of PTFE bearings for MoDOT bridges:

- Dimpled, lubricated PTFE consistently showed lower friction coefficients than flat surfaces, typically ranging from half to one-third of those of flat PTFE.
- Fifteen percent glass fiber-filled PTFE displayed slightly higher friction coefficients, approximately 1-2 percent more than unfilled surfaces.
- Coefficients of friction for unfilled lubricated PTFE remained stable across temperature changes from 68 deg. F to -13 deg. F, suggesting further studies at elevated temperatures may be necessary.
- The coefficient of friction decreased almost linearly with increased bearing pressure at all tested loading rates.
- Both flat and dimpled PTFE specimens showed increased friction with higher loading rates. Once elevated, friction values did not reduce even when loading rates decreased, indicating irreversible changes to the PTFE surfaces. Additional field measurements are needed to confirm actual sliding speeds for various bridge types and loading situations.

- First breakaway coefficients of friction increased with larger surface areas, though subsequent impacts remained minimal. Apart from the first breakaway, where variable results were observed, consistent friction values were observed, indicating independence from the elastomer thickness.
- Surface contamination significantly raised friction coefficients, with light dust levels increasing friction tenfold and heavier levels preventing sliding.
- Despite preventive measures, real-world conditions demonstrate that dust accumulation occurs, highlighting the necessity of regular maintenance and protective strategies to ensure the longevity and functionality of PTFE bearings.
- Experimental results aligned with NCHRP Report 432, but some discrepancies suggested other factors like material type, elastomer influence, and preloading could be the reasons for the discrepancies between the results. Further laboratory experiments paralleling the NCHRP investigation are recommended to better understand these variables.
- Based on the current study, updated design coefficients of friction were proposed for contact pressures ranging from 200 psi to 1,000 psi. In particular, the updated design coefficients of friction under 800 psi design contact pressure were proposed as listed in the following table. These proposed design coefficients considered some effects of surface contamination and loading cycles.

Table 11. Updated design coefficient of friction for PTFE specimens tested under 800 psi contact pressure under room temperature (68°F)

PTFE Type	Updated Design Coefficient of Friction
Unfilled- Flat	6%
Filled (15% glass fiber)- Flat	10%
Unfilled- Dimpled	3%
Filled (15% glass fiber)- Dimpled	4%

References

AASHTO LRFD BCS. (2017). “LRFD Bridge Construction Specifications (BCS)”, 4th ed., Washington, DC.

AASHTO LRFD BDS. (2020). “LRFD Bridge Design Specifications (BDS)”, 9th ed., Washington, DC.

Ala, N., Power, E. H., and Azizinamini, A. (2015). “Experimental Evaluation of High-Performance Sliding Surfaces for Bridge Bearings.” J. Bridge Eng., 2016, 21(2): 04015034

Nejad, S., and McGormley, J. C. (2022). “Evaluation of Elastomeric Bearing Pad Performance for the State of Louisiana.” The Louisiana Department of Transportation and Development (LADOTD), Baton Rouge, LA, in press.

Nejad, S., Santosuosso, B., and Lauer, S. (2022). “Field Investigation and Laboratory Assessment of PTFE Bearing Pads Retrieved from SR 62 over Pigeon Creek.” The Indiana Department of Transportation (INDOT), Indianapolis, IN, in press.

Campbell, T. I., and Kong, W. L. (1987). “TFE sliding surfaces in bridge bearings.” Rep. ME-87-06, Ontario Ministry of Transportation and Communications, Downsview, ON, Canada.

Campbell, T. I., and Kong, W. L. (1989). “Laboratory Study of Friction in TFE Sliding Surfaces for Bridge Bearings.” Rep. MAT-89-04, Ontario Ministry of Transportation and Communications, Downsview, ON, Canada.

Campbell, T.I., Fatemi, M.J. and Manning, D.G. (1993). "Friction in Bridge Bearings with Contaminated TFE Slide Surface." ASCE Jo. Str. Eng. 119(11) pp. 3169-3177.

Constantinou, M.C., Mokha, A., and A. Reinhorn. (1990). “Teflon bearings in base isolation II: Modeling.” Journal of Structural Engineering 116(2):455–474.

Dorafshan, S., Johnson, K.R., Maquire, M., Halling, M. W., Barr, P. J., and Culmo, M. (2019). “Friction Coefficients for Slide-In Bridge Construction Using PTFE and Steel Sliding Bearings.” J. Bridge Eng., 2019, 24(6): 04019045.

FHWA. InfoBridge website https://infobridge.fhwa.dot.gov/Home. Federal Highway Administration, U.S. Department of Transportation, Washington, DC. 1995.

Indiana Design Manual (2013). “Chapter 409: Abutment, Bent, Pier, and Bearing.” Indiana Department of Transportation, Indianapolis, IN.

Kauschke, W. and Baigent M. (1986) "Improvements in the Long-Term Durability of Bearings in Bridges.", Joint Sealing and Bearing Systems for Concrete Structures, ACI Publication SP-94, Vol.2.

LaFave, J., Fahnestock, L., Foutch, D., Steelman, J., Revell, J., Filipov, E., and Hajjar, J. (2013). “Experimental Investigation of the Seismic Response of Bridge Bearings.” Research Report No. FHWA-ICT-13-002, Illinois Center for Transportation, Urbana, IL.

Long, J. E., (1969). "The Performance of PTFE in Bridge Bearings," Civil Engineering and Public Works Review, Vol. 64, pp 459-462.

Mazroi, A., Wang, L.R.L., and Murray, T.M. (1982). "Effective Coefficient of Friction of Bridge Bearings.", Research Report, Fears Structural Engineering Laboratory, School of Civil Engineering and Environmental Science, University of Oklahoma, Norman, Oklahoma, 103 pp.

Maryland Structural Details Manual (2024). “Chapter 409: Abutment, Bent, Pier, and Bearing.” Maryland Department of Transportation State Highway Administration (MDOT SHA), Baltimore, MD.

Missouri Engineering Policy Guide (EPG) (2024), State of Missouri Department of Transportation, Jefferson City, MO.

Missouri Standard Specifications for Highway Construction (2022), State of Missouri Department of Transportation, Jefferson City, MO.

Mokha, A. S., Constantinou, M. C., and Reinhorn, A. M. (1990). “Teflon bearings in base isolation. I: Testing.” J. Struct. Eng., 10.1061/(ASCE) 0733-9445(1990)116:2(438), 438–454.

Stanton, J. F., and Campbell, T. I. (1999). “High-load multi-rotational bridge bearings: Appendix C: Friction and wear of PTFE sliding surfaces.” NCHRP Rep. 432, Transportation Research Board, National Research Council, Washington, DC.

Taylor, M.E. (1972). "PTFE in Highway Bridge Bearings.", Report No. TRRL-LR-491, Transport and Road Research Laboratory, Crowthorne, England, 62 pp.

Taylor, J. C., and Stanton, J. F. (2010). “SPR#0092-08-13: Friction Coefficients for Stainless Steel (PTFE) Teflon Bearings.” Report No. WHRP 10-01, Wisconsin Highway Research Program, Madison, WI.

TR202204 Request for Proposal document (2022). “TR202204: Design Coefficients of Friction for MoDOT PTFE Bearings.” State of Missouri Department of Transportation, Jefferson City, MO.

Winston, R. J, and Witer, J. D. (2019). “Evaluating the particle size distribution and gross solids contribution of stormwater runoff from Ohio’s roads” Ohio DOT/FHWA Report No. 2019-9, Columbus, OH.

Zhao, H., Yin, C., Chen, M., and Wang, W. (2008). “Runoff pollution impacts of polycyclic aromatic hydrocarbons in street dusts from a stream network town.” Water Science & Technology Water Supply 58(11):2069-76.